DETERMINING THE INTRAMOLECULAR MECHANISMS DRIVING ALTERED CONTRACTION IN THE MYOSIN MUTATIONS E525K AND V606M

Kalen Robeson

A dissertation

submitted in partial fulfillment

of the requirements for the degree of

DOCTOR OF PHILOSOPHY

University of Washington

2025

Reading Committee:

Michael Regnier, Co-Chair

Jennifer Davis, Co-Chair

David L. Mack

Program Authorized to Offer Degree:

Bioengineering

University of Washington

Abstract

Determining the Intramolecular Mechanisms Driving Altered Contraction in the Myosin Mutations E525K And V606M

Kalen Robeson

Chairs of the Supervisory Committee:

Michael Regnier

Departments of Bioengineering and Neurobiology & Biophysics

Jennifer Davis

Departments of Laboratory Medicine & Pathology and Bioengineering

Force generation in the heart relies on the interaction of myosin and actin filaments, a tightly regulated process where subtle changes can lead to heart disease. Mutations in β-cardiac myosin impact the number of available myosin molecules, their binding to actin, and their ATP utilization rate. Understanding how this family of mutations alter heart contraction requires investigation of myosin at the single molecule, the sub-cellular, and the physiological level. This study investigates the mechanism of altered myosin function in two β-myosin mutations (E525K and V606M). The first project, presented in Chapter 2, uses molecular dynamics simulations of E525K and V606M myosin to highlight a regulatory role for the loop 2 structure in crossbridge binding. The second project, presented in chapter 3, involves a deep investigation of the E525K mutation using stem cell derived cardiomyocyte. Cells and tissues with the E525K mutation showed decreased force

generation, consistent with dilated cardiomyopathy; however, single myofibril preparations demonstrated that myofibrils containing E525K myosin can generate more force than wild type under some conditions. These findings underscore the importance of multi-scale studies of myosin mutations. While single-molecule biochemical assays are informative, they may not always reflect the complete picture. As cardiac medicine moves towards personalized treatment, in-depth understanding of how specific myosin mutations alter chemomechanics is vital for designing tailored drugs for cardiomyopathy.

Table of Contents

List of Figures

List of Supplemental Figures

Frequent Acronym Glossary

Calcium-induced calcium release	CICR
Cardiomyocyte	CM
Cardiac myosin	β-myosin (gene name *MYH7*)
Dilated cardiomyopathy	DCM
eGFP	enhanced Green Fluorescent Protein
Excitation contraction coupling	EC coupling
Hypertrophic cardiomyopathy	HCM
Human induced pluripotent stem cell	hiPSC
Molecular Dynamics	MD
Myosin Binding Protein C	MyBPC
Principal component analysis	PCA
Negative logarithm of the calcium ion concentration	pCa
Ryanodine receptors	RyR
Sarcoplasmic reticulum	SR
Tension Time Integral	TTI
Wild Type	WT

Acknowledgements

I would first like to thank both of my advisors, Michael Regnier and Jennifer Davis, for their mentorship, coaching, and unwavering support throughout this project. Mike, the lab and community you have built for science is truly a wonderful space, and it has helped me grow into the scientist I am today. Jen, your passion and willingness to jump into the details of any scientific question have nurtured my own passion for science—thanks for being my coach through all of this. It has been an honor to work with both of you and to be a part of the communities you have established in your labs.

I would also like to thank the other members of my supervisory committee: David Mack, Rong Tian, and Lisa Maves. Every time we gathered for a committee meeting or a milestone exam, I was struck by the intellectual inspirations that each of you are. I feel lucky to have had the opportunity to engage with and learn from each of you. I would especially like to thank David for his constant willingness to meet one-on-one and his enthusiasm towards mentorship and science.

All science is a collaboration, and each member of both the Davis and Regnier Labs has contributed to my work. I would particularly like to thank Kristi Kooiker, Tim McMillen, Matt Childers, Kerry Kao, and Darrian Bugg for their direct help and mentorship with the work presented in this thesis. To my friends in the lab—Abby, Bella, Kerry, Ross, and Anthony—you make coming into work a pleasure. Your excitement when experiments worked and your support when they did not are a large part of why I am here today and why I made it through this PhD. I would also like to thank each of the undergraduates I have worked with and mentored, this project would not have been possible without your help. I would particularly like to thank Kieran Fruebis and Rachelle Soriano, your banter and enthusiasm for science got me through the final two summers of this PhD.

Finally, I would like to thank my friends and family. To my mother, Beth Robeson, thank you for your hands-on approach towards education and for constantly engaging with me. I remember when you taught me to read, and it was that level of commitment to my education that brought me here. To my father, Brad Robeson, thank you for reminding me to take breaks and helping me to be creative. All the figures and diagrams in this thesis were made using skills I learned looking over your shoulder. To my friends in Ohio (Aaran, Nick, and Alec), each of you has listened to me and helped me through the highest and lowest points of this long project. To my girlfriend, Olivia, thank you for being my teammate and for helping me through the final mile of this PhD. Working with you at coffee shops on Sundays made finishing this thesis not only possible but fun.

Dedication

I would like to dedicate this thesis to my two grandfathers James F. Robeson PhD and Ray E. Jacobsen DVM. Both of my grandfathers were the first members of their family to attend college, and they taught me to learn as much as I can because it isn't heavy to carry around.

Thesis Aim Overview

Cardiac muscle contraction is driven by the precise interplay between myosin and actin, a process intricately regulated by the chemomechanical properties of myosin molecules. Diverse myosin isoforms exhibit unique characteristics, enzymatic activities, and binding affinities, enabling specialized functions across various cells and tissues. However, mutations in the MYH7 gene, which encodes β-myosin heavy chain, are a leading cause of cardiomyopathy, a condition marked by impaired cardiac function. This thesis investigates how two specific cardiomyopathy-linked mutations, E525K and V606M, alter myosin function and subsequent cardiac contractility. To achieve this, we employed a multi-scale approach, combining molecular dynamics (MD) modeling with stem cell biology techniques to study myosin function from the single molecule to the whole tissue level.

Single-molecule simulations were used to explore how the E525K and V606M β-cardiac myosin mutations affect myosin protein folding. Subsequently, electrostatic modeling elucidated how these mutations alter the interaction between myosin and actin. The E525K mutation was then further characterized at a mechanical level using human induced pluripotent stem cell (hiPSC)-derived cardiomyocytes (hiPSC-CMs). Mechanical measurements were conducted to assess how this mutation impacts contraction at the single myofibril, single cell, and whole tissue levels. The findings of this investigation are summarized in the aims below.

Aim 1: Determine the Structural Dynamics of Myosin Loop 2 and its Role in Actomyosin Interactions.

Motivation: The flexible loop 2 region of myosin is critical for regulating its interaction with actin and facilitating cross-bridge formation. Despite its importance, high-resolution structural information for this region is limited, hindering a complete understanding of its function. This aim

utilized computational approaches to model loop 2 structure and evaluate its contribution to electrostatic interactions with actin.

Specific Goal: We employed molecular dynamics (MD) simulations to model the conformational state space of loop 2 in both wild-type and mutant (E525K or V606M) myosin. The *DelphiForce* program was then used to model electrostatic interactions between myosin and actin, determining how these cardiomyopathy-associated mutations alter these interactions. Our results indicate that both mutations induce changes in the conformational state of loop 2, leading to an increased affinity for actin.

Aim 2: Investigate the Functional Consequences of the E525K Mutation on Cardiac Muscle Contractility.

Motivation: The E525K mutation in β-cardiac myosin is a clinically significant mutation associated with dilated cardiomyopathy. Understanding how this mutation disrupts cardiac contractility is essential for developing targeted therapeutic strategies. This aim investigated the effects of the E525K mutation on force generation, contraction mechanics, and calcium handling in human stem cell-derived cardiomyocytes.

Specific Goal: The effects of the E525K mutation were assayed in hiPSC-CMs by measuring sarcomere shortening in isolated cells, force generation in engineered heart tissues (EHTs), and contractility in isolated myofibrils. This work advances our understanding of how the E525K mutation alters myosin function within a loaded and contracting sarcomere. Furthermore, these findings have implications for the development and application of novel myosin-targeted drugs for cardiomyopathy treatment.

Chapter 1 — Introduction and Background:

Cardiovascular Disease

The average human heart will beat around three billion times in a lifetime. While the size of that number is impressive the dynamic nature of heart contraction is perhaps even more striking. This pacemaker of our lives not only works without ceasing but has an astonishing ability to adapt to different situations and to overcome physiological changes. When an organism is threatened or the body undergoes a hemorrhage sympathetic stimulation drives functional changes in the heart increasing the hearts ability to contract and to relax—this allows a healthy human's heartrate to vary from 60 to 200 beats per minute (Katz 2010; Mohrman and Heller 2013). On the other hand, chronic changes in cardiac demand due to physiological fluctuations such as hypertension lead to remodeling of the heart where the contractile cells in the heart grow larger in response to increased demand for force (Katz 2010). This beautiful and complex regulation of cardiac output represents a fascinating system in which to study how perturbations to the system are compensated for and how the buildup of perturbations can eventually overcome or hijack the hearts adaptability leading to heart failure.

Heart failure occurs when the heart can no longer pump sufficient blood to meet the physiological demands of the body. This can be caused by the heart failing to pump strongly enough (systolic failure) or failing to relax fully and fill with blood (diastolic failure). Clinically these changes in heart function are monitored using echocardiography and can be seen as changes a patients ejection fraction (EF)—or the fraction of blood that is pumped out of the ventricles during systolic contraction. Patients suffering from heart failure with an EF of 40% or less are diagnosed with heart failure with reduced ejection fraction (HFrEF) while patients suffering from heart failure with an EF of 50% or more are diagnosed with heart failure with preserved ejection fraction (HFpEF). Patients with EF between 41% and 49% are diagnosed with mild HFrEF (Heidenreich et al. 2022). Physiologically the manifestation of heart failure is seen as shortness of breath,

fatigue and weakness, as well as swelling of the belly/abdomen and lower extremities (Heidenreich et al. 2022). As the heart loses its ability to pump blood through the body the lack of oxygen and nutrients reaching tissues increase leads to the fatigue and shortness of breath. The swelling of the lower body is caused by a buildup of blood in the compliant venous system.

While many cases of heart failure are acquired due to lifestyle and environmental factors heart disease can also be genetic (Ahmad, Seidman, and Seidman 2005). Gene mutation can also lead to disease (Iyama and Wilson 2013; Xu et al. 2015). The genetic mutations that underly inherited heart disease can be in many different proteins but one of the key players in this process is the molecular motor myosin. Myosin is an ATPase enzyme which is responsible for the generation of force in all musicals including the heart. Mutations in myosin can cause heart disease by changing the structure and therefore function of myosin. The following section will introduce the myosin motor, its links to disease, and the important regulators of this protein.

Myosin—A Motor to Power the Heart

Myosin is the molecular motor responsible for force generation in the heart, but myosin molecules can be found in all types of muscle and non-muscle myosins carry out yet more functions in many different cell types. Each of these types of myosin molecules are tuned to task. For example myosin molecules found in a fast twitch muscle fiber must have a faster ATPase activity and shorter duty ratio (time spent bound to actin) than myosins found in slow twitch muscle fibers (Geeves and Holmes 2005). This tuning allows a fast myosin to avoid creating drag during in a quickly contracting muscle twitch. The tuning of myosin is achieved through changes in the rate constants of the myosin crossbridge cycle depicted in (**Figure 1-1 A**). A deep understand of these rates and how they can be changed is not only interesting from a biological and biophysical perspective but important for our understanding of disease and drug interactions. Mutations in myosin that cause cardiomyopathy are known to change these rates. Novel myosin activator or

inhibitor drugs change these rates in ways that are not yet fully understood (Auguin et al. 2024; Kooiker et al. 2023). The work presented here aims to investigate model myosin mutations and understand how the rates of the crossbridge cycle are changed.

The myosin crossbridge cycle is divided into six states depicted in **Figure 1-1 A** and (Childers and Regnier 2024). By moving through these six states myosin molecules harness the energy from ATP hydrolysis to fuel the power stroke and drive muscle contraction. All known myosin molecules move through the same chemo-mechanical crossbridge cycle, but by changing the transition rates between these crossbridge cycle states different myosin molecules can carry out specific functions (Sweeney and Houdusse 2010). How then do different myosin molecules change these rates. As in all biological systems structure and function are tightly interwoven. It is the structure of myosin (**Figure 1-1 B**) that changes these rates, and it is these variable rates that allow myosin molecules to be tuned to specific tasks. The next sections will discuss the structural domains of myosin and then the biochemistry and physiological significance of the crossbridge states.

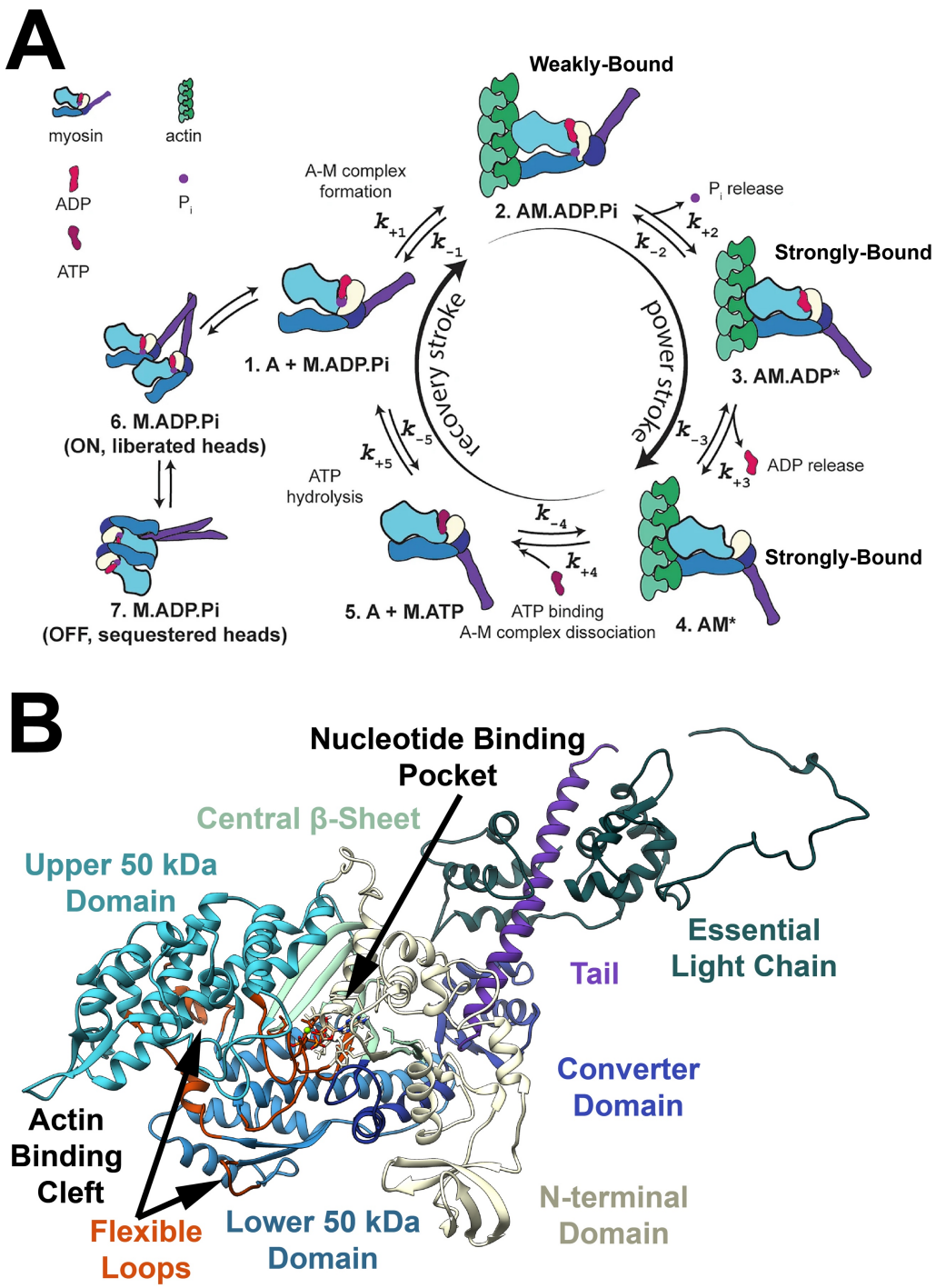

Figure 1-1 The myosin crossbridge cycle and subdomains of the myosin S1 head.

(A) Schematic depiction the six-state myosin crossbridge cycle and the interacting heads motif bases of the ON/OFF state of myosin. Adapted from Dr. Matt Childers (Childers and Regnier 2024). (B) Ribbon diagram of pre-powerstroke human β-myosin S1. Key subdomains of the myosin motor domain are indicated.

The Domains of Myosin

Here are summarized the main domains of the Myosin head molecule (visualized in **Figure 1-1 B**). Also summarized are the main regulatory or structural function that each of these domains play during myosin function and the crossbridge cycle.

The upper 50 kDa domain and Lower 50 kDa domain:

These two domains form the core of the motor domain, housing the ATP-binding site. This motor caries out a storm of activity during muscle contraction. The upper 50 kDa domain is primarily involved in nucleotide binding, while the lower 50 kDa domain contributes to actin interaction. Together, they create the catalytic pocket where ATP hydrolysis occurs. The interactions between these domains change based on the bound nucleotide, causing conformational changes that are essential for the power stroke as well as the transition from a weakly-bound state to a strongly-bound-state (**Figure 1-1 A**).

The actin-binding cleft:

This cleft, located on the surface of the motor domain, is where myosin interacts with actin filaments. The precise interactions within this cleft are critical for the formation of the actomyosin complex, which is necessary for force generation. During initial weak binding between myosin and actin the cleft is open and myosin binds to actin mostly via the lower 50 kDa domain. As the actomyosin complex transitions to a strongly-bound-state the upper 50 kDa domain binds to actin and the cleft between the two domains closes (Klein et al. 2008). Changes in the conformation of this cleft, allow for progression though the chemomechanical cycle (phosphate release) and the power stroke (**Figure 1-1**).

The flexible Loops:

Though often overlooked in schematics and hard to resolve using crystallography the flexible loops of myosin are critical domains that regulate the function of the motor. These loops are crucial for the communication between the ATP-binding site and the actin-binding cleft. Specifically, loop 2 and loop 3 play a significant role in electrostatic interactions between myosin and actin. Loop 4 is known to play a role repositioning tropomyosin on actin during muscle activation and relaxation (Doran, Rynkiewicz, Pavadai, et al. 2023). These loops may also play important allosteric roles that regulate the changes that the myosin head undergoes during the power stroke—for example the closing of the actin binding cleft during transition from a weakly bound actomyosin complex to a strongly bound actomyosin complex (Clobes and Guilford 2014; Yengo and Sweeney 2004).

The central beta sheet:

This is a core structural element within the motor domain, providing a stable framework for the other functional domains. It acts as a structural support and helps to transmit conformational changes throughout the myosin head. More specifically, the central beta-sheet is a key structural component of the myosin head, and it is found between the two 50 kDa domains. This part of myosin is structurally linked with many of the other myosin subdomains and provides a nexus of for structural communication within the myosin head. It can be thought of as a physical bridge, linking the actin binding surface, to the nucleotide binding pocket, and helps to coordinate product release in response to actin binding and cleft closure (Walklate, Ujfalusi, and Geeves 2016). This linkage is crucial for the coordinated action of myosin. Importantly this structure is near the nucleotide binding pocket and mutations in this regain can impact the binding/release kinetics of ATP/ADP (Lee et al. 2024).

The N-terminal domain & the converter domain:

The N-terminal domain contributes to the overall structure of the myosin head and participates in nucleotide binding. It works in conjunction with the upper 50 KDa domain to create the nucleotide binding pocket. The converter domain acts as a lever, amplifying the small conformational changes in the motor domain into larger movements of the lever arm. It is critical for the generation of the power stroke, translating the chemical energy of ATP hydrolysis into mechanical work. Interestingly two recently developed myosin modulating drugs bind to these regions of myosin and modulate myosin function (Auguin et al. 2024).

The essential and regulatory light chain:

While not technically part of the myosin molecule, these proteins are critical regulators of myosin function. The essential light chain (ELC) protein binds to the lever arm, stabilizing its structure and contributing to the efficiency of the power stroke. It helps regulate the movement of the lever arm and therefore regulates the force of the muscle contraction (Hernandez et al. 2007). The regulatory light chain (RLC) can modulate the recruitment of myosin. Phosphorylation of RLC, primarily by myosin light chain kinase (MLCK), modulates the kinetics of cross-bridge binding and the rate of force development (Gordon, Homsher, and Regnier 2000; Zaleta-Rivera et al. 2019).

The Myosin Crossbridge Cycle

The myosin crossbridge cycle is the fundamental unit of muscle contraction responsible for driving the sliding filament theory and is therefore crucial for heart function. Myosin is an ATP driven molecular motor and through its interaction with actin is the protein responsible for force generation in all muscles. The key players in this molecular force generation are myosin comprising the thick filament, actin comprising the thin filament, and ATP delivering chemical energy. The interaction of these players is regulated by tropomyosin and the troponin complex which decorate the actin thin filament allowing or blocking myosin from interacting with actin. Through years of structural biology and biochemical analysis the 6-state crossbridge cycle has been developed as a model for how myosin interacts with actin (**Figure 1-1 A**). The following section will discuss each step in this cycle and delve into the regulatory importance of each of these chemomechanical steps. The chemical makeup of each state is indicated in bold.

Actomyosin Complex Formation: **A + M.ADP.Pi**

To bind actin and begin a force generating powerstroke, ADP and inorganic phosphate (Pi) must be bound myosin. This “pre-powerstroke” conformation of myosin first interacts with actin to form a weakly bound complex. The initiation of this interaction is thought to be driven by the Lower 50 kDa Domain of myosin (Klebl et al. 2025; Yengo and Sweeney 2004). Specifically, the helix loop helix (HLH) motif on the lower 50 kDa domain as well as loop 2 and loop 3 (**Figure 1-1 B**) are known to initiate interaction with actin. Of particular interest here are the positive charges on Loop 2 that form interactions with the negative charges on the N-terminus of actin.

Phosphate Release: **AM.ADP.Pi**

Once in the weakly bound state, myosin can form stronger interactions with actin and release Pi. The myosin cleft separating the Upper and Lower 50 kDa Domains closes allowing the upper 50 kDa domain to interact with actin forming a strongly bound state. This transition in

the myosin cleft is coupled to movement of the myosin lever arm, creating strain in the complex that can be measured as force. These changes in myosin structure are association with the release of Pi, which is highly dependent on actin binding and is usually the rate limiting step of the cycle under no or low resistive loads (Geeves and Holmes 2005; Sweeney and Houdusse 2010).

ADP Release: **AM.ADP**

The next step in the crossbridge cycle is ADP release. This rate is strain dependent and is often limiting during force generation. During experimental load or due to afterload in the beating heart, ADP release slows increasing the duty ratio of myosin (Moss and Fitzsimons 2002; Sweeney and Houdusse 2010). This is an excellent example of how changes in the various rates of the crossbridge cycle regulate the function of myosin and contribute to the physiological flexibility of heart contraction. The fact that ADP release slows in response to afterload directly contributes to increased cardiac output in response to physiologic demand and is one mechanism behind the Frank Starling effect (Katz 2010).

ATP Binding and Actomyosin Complex Dissociation: **AM**

Once ADP is released myosin and actin remain in a strongly bound “rigor” complex. Myosin cannot detach from actin in the absence of ATP because it is the binding of a new ATP molecule that allows for conformational changes in myosin and the dissociation of the actomyosin complex. Indeed, the stiffness observed in recently deceased animals known as rigor mortis is caused by this exact phenomenon and muscle stiffness can be used to estimate time of death (Shrestha, Kanchan, and Krishan 2024).

ATP Hydrolysis: **A + M.ATP**

Once a new ATP molecule binds to a free head, the catalytic domain of myosin hydrolyzes it to ADP.Pi. Energy from this hydrolysis is used to reset the myosin lever arm and prepare the myosin molecule to begin the crossbridge cycle again. The period of cyclic movement of myosin through these 5 states is known as the “myosin cycling rate,” and is the myosin ATPase activity. However, the rate at which a pool of myosins utilizes ATP is also controlled through recruitment of myosin molecules out of an OFF state.

The “OFF” Myosin State: **M.ADP.Pi**

Myosin in the ADP.Pi bound “pre-powerstroke” state has the capacity to enter an ATP sparing/energy conserving state where its ATPase activity is reduced by an order of magnitude. This “OFF” state of myosin is biochemically defined as an order of magnitude decrease in myosin ATPase rate. The conformation of the two myosin heads and their arrangement relative to the myosin backbone are hypothesized to contribute to the reduced ATPase activity (Mohran et al. 2024; Spudich 2015). The transition of myosin heads between “ON” and “OFF” states is termed myosin recruitment and plays a critical role in modulating muscle contractility (Campbell, Janssen, and Campbell 2018).

The Duty Ratio:

The duty ratio of myosin refers to the proportion of time a myosin head spends strongly attached to an actin filament during its complete cycle of activity (Geeves and Holmes 2005; Sweeney and Houdusse 2010). There is a great deal of variation depending on the specific myosin type: skeletal and cardiac muscle myosin typically have a very low duty ratio. This means they spend most of their time detached, allowing for rapid cycling and generation of forceful contractions needed for muscle movement (Chin et al. 1998; Sweeney and Houdusse 2010). Non-muscle myosins, like those involved in intracellular transport, have a much higher duty ratio, potentially exceeding 70%. This allows for a more processive movement, where the myosin head

stays attached and "walks" along the actin filament for longer distances (Sweeney and Houdusse 2010; Yengo and Sweeney 2004:2). The parts of the myosin crossbridge cycle that contribute to the duty ratio are the strong binding states to actin. By understanding the duty ratio of different myosin types or different myosin mutations insight can be gained into how different myosin types/mutations contribute to variation in cellular and organ level function.

Regulation of Contraction

The regulation of contraction in cardiac muscle, and in striated muscle in general, is exerted primarily through the effect of calcium (Ca^{2+}) on thin filament regulatory elements. The concentration of Ca^{2+} in muscle cells is thus tightly regulated allowing for excitation contraction coupling (Bers 2002). Structural and biochemical studies have established that tropomyosin (Tm) blocks the myosin binding sites on actin during resting conditions in muscle (Gordon et al. 2000). Upon membrane depolarization Ca^{2+} is allowed into the cell and the sarcomere. Ca^{2+} binds to troponin (Tn) which in turn frees Tm, allowing it to become mobile, thus uncovering the myosin binding sites on actin and allowing for crossbridge formation. This process of thin filament activation is regulated at two levels. The amount of Ca^{2+} released or rate of calcium release can be altered, or the sensitivity/binding kinetics of the Tn Ca^{2+} interaction can be altered (Geeves, Lehrer, and Lehman 2019; Gordon et al. 2000). In addition to this regulation at the thin filament level muscle contraction can also be regulated at the thick filament or myosin level. This regulation of myosin is carried out at three levels first myosin must be recruited off the thick filament backbone, next myosin must be activated through electrostatic interactions with actin to bind and form a crossbridge between the thick and thin filaments, finally the cycling rate or ATPase activity of myosin can regulate the rate/extent of force generation (Childers and Regnier 2024; Gordon et al. 2000). The next sections will explain in detail how regulation of the thick and thin filament is modulated and how this modulation can change in the context of cardiac stress or cardiac disease.

Thin Filament Regulation of Contraction

Regulation of the cardiac thin filament is the primary way that contraction is controlled in cardiomyocytes. This regulation is achieved through various calcium dependent mechanisms. In response to depolarization calcium enters the cell triggering calcium-induced calcium release. This elevates intracellular (and intra-sarcomere) calcium levels and is followed by activation of

the troponin complex. This activation allows tropomyosin to shift away from blocking the myosin binding sites on actin. The sensitivity of this activation can be adjusted through phosphorylation. Finally, the intracellular calcium concentration is reduced by transport into the sarcoplasmic reticulum (SR) and out of the cell. Coordination at each stage of this process regulates force generation in the heart and will be discussed in the following section.

Calcium induced calcium release

Calcium-induced calcium release (CICR) is the fundamental mechanism by which cardiac myocytes achieve rapid and substantial increases in intracellular calcium concentration, for excitation-contraction coupling. At rest (diastole) the intracellular calcium concentration is very low (~1 nM or a pCa of 9.0). During an action potential, L-type calcium channels in the sarcolemma open, allowing a small influx of extracellular calcium. This "trigger calcium" binds to ryanodine receptors (RyRs) located on the sarcoplasmic reticulum (SR), the cell's internal calcium store. This binding induces a conformational change in RyRs, causing them to open and release a much larger bolus of calcium from the SR into the cytosol (Bers 2002). The magnitude of this SR calcium release is proportional to the amount of trigger calcium and the SR calcium load, ensuring that the force of contraction is tightly coupled to the electrical excitation of the cell. The concentration of calcium during contraction can increase orders of magnitude up to ~6 uM or a pCa of 5.2 (Bers 2002). It is worth noting however that this still only represents a submaximal stimulation, in isolated myofibrils or skinned tissue constructs increasing calcium continues to increase force beyond what is archived by systolic calcium concentrations. Maximum force generation is (and maximum thin filament activation) is only achieved by calcium concentrations on the order of 100 uM or a pCa of 4.0 (Gordon et al. 2000).

The CICR process is tightly regulated to prevent excessive calcium release and maintain cellular homeostasis. Key regulatory proteins, such as calsequestrin and triadin, within the SR lumen modulate RyR activity and calcium release. Additionally, the balance between calcium

influx through L-type channels and calcium reuptake by SERCA pumps determines the SR calcium load and, consequently, the magnitude of CICR. SERCA itself is regulated by phospholamban (PLN), which inhibits SRCA activity its unphosphorylated state. Phosphorylation of PLN reduces inhibition of SERCA and accelerates calcium reuptake in response to sympathetic stimulation (Hagemann and Xiao 2002). Dysregulation of CICR, due to genetic mutations or pathological conditions, can lead to abnormal calcium handling, resulting in arrhythmias, heart failure, and other cardiac pathologies (Eisner et al. 2017).

The Troponin Complex: The Calcium-Sensitive Switch

The troponin complex, a key regulator of cardiac muscle contraction, comprises three subunits: cardiac troponin C (cTnC), cardiac troponin I (cTnI), and cardiac troponin T (cTnT). cTnC acts as the calcium sensor, possessing two high-affinity calcium-binding sites that are typically occupied—even at low calcium concentrations—and one low-affinity sites that binds calcium during systole as the intracellular calcium concentration rises (Gordon et al. 2000). When this low-affinity site is occupied, a conformational change in cTnC is triggered. This conformational shift propagates through the complex, influencing the position of cTnI. cTnI, the inhibitory subunit, normally binds to actin, preventing myosin from interacting. When calcium binds to cTnC, cTnI's affinity for actin decreases, allowing myosin to bind and initiate contraction. cTnT, the tropomyosin-binding subunit, anchors the troponin complex to tropomyosin, ensuring the coordinated movement of tropomyosin in response to calcium binding (Tobacman 1996). Variations in cTnT isoforms, along with post-translational modifications, can subtly modulate calcium sensitivity and contractile properties (Gordon et al. 2000).

Tropomyosin: The Steric Gatekeeper

Tropomyosin, a coiled-coil protein, wraps around the actin filament, forming a continuous strand that sterically blocks myosin-binding sites on actin in the relaxed state. This steric

hindrance prevents the formation of cross-bridges and maintains the muscle in a relaxed state. The calcium-induced conformational changes in the troponin complex, particularly the shift in cTnI, cause tropomyosin to move away from the myosin-binding sites (Tobacman 1996). This movement uncovers the binding sites, allowing myosin heads to interact with actin and initiate the cross-bridge cycle.

Phosphorylation: Fine-Tuning Calcium Sensitivity

Phosphorylation of thin filament proteins, especially cTnI, plays a crucial role in modulating calcium sensitivity. Protein kinase A (PKA) is a key enzyme that phosphorylates cTnI at specific serine and threonine residues on its N-terminal extension. Phosphorylation of cTnI reduces the affinity of cTnC for Ca^{2+} at site II (the primary Ca^{2+} binding site), decreasing the calcium sensitivity of the myofilaments (Gordon et al. 2000; Tobacman 1996). This effect accelerates relaxation and contributes to the lusitropic (relaxation-enhancing) effects of beta-adrenergic stimulation. This is a critical mechanism for rapidly adjusting cardiac function in response to physiological demands. The degree of cTnI phosphorylation can vary depending on the balance of kinase and phosphatase activities, allowing for fine-tuned control of calcium sensitivity.

PLN and SERCA: Regulators of Calcium Availability

While not direct components of the thin filament, phospholamban (PLN) and sarcoplasmic reticulum Ca2+ ATPase (SERCA) significantly influence calcium availability, indirectly impacting thin filament activation. SERCA, located in the sarcoplasmic reticulum (SR), is responsible for pumping calcium back into the SR during diastole, lowering cytosolic calcium levels and promoting relaxation. PLN, when dephosphorylated, inhibits SERCA activity, slowing calcium reuptake. PKA-mediated phosphorylation of PLN relieves this inhibition, enhancing SERCA activity and accelerating calcium removal (Hagemann and Xiao 2002). This modulation of SERCA

activity directly affects the amount of calcium available to bind to cTnC, thereby influencing the extent of thin filament activation and the rate of relaxation (Bers 2002).

Summary

Thin filament regulation in cardiac muscle is a finely tuned process involving a complex interplay of protein interactions and post-translational modifications. Understanding these intricate mechanisms is crucial for elucidating cardiac physiology and developing therapeutic strategies for heart diseases.

Thick Filament Regulation of Contraction

While thin filament regulation is the primary way that contraction is controlled via excitation contraction coupling the thick filament has intrinsic levels of regulation as well. Thick filament regulation refers to the mechanisms that control the activity of myosin that are intrinsic to the myosin molecule itself. These regulatory mechanisms determine when and how myosin finds its binding site on actin and how it interacts with itself and actin to regulate and produce muscle contraction. Thick filament regulation takes place at three levels recruitment, activation, and cycling (**Figure 1-2**). These levels of regulation are summarized in the following section, but briefly: (1) Recruitment of myosin refers to the transition of myosin heads from on OFF state where they interact with the myosin backbone to an ON state where they are free to interact with actin. (2) Activation refers to the electrostatic interaction between myosin and actin that leads to the formation of a crossbridge between the thick and thin filaments. (3) The cycling of myosin or the rate at which myosin moves through the chemomechanical cycle is the final level of thick filament regulation.

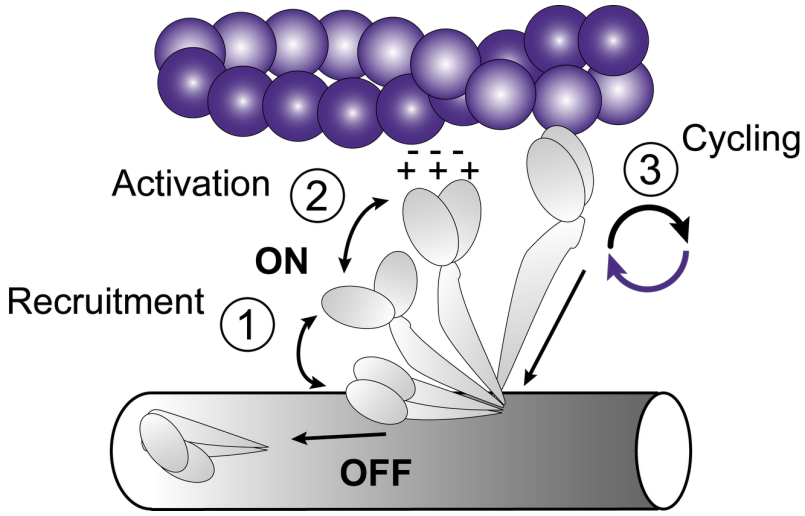

Figure 1-2: Mechanisms of Thick Filament Regulation

Regulation of the thick filament takes place at three levels. (1) Recruitment of myosin of the thick filament backbone—a transition from the OFF state to the ON state. (2) Activation of myosin and the formation of the actomyosin crossbridge. This is an electrostatic interaction and a cooperative process where myosin molecules help each other bind. (3) Myosin cycling rate or ATPase rate.

Myosin Recruitment: The Biochemically Defined Super Relaxed State & The Structurally Defined Interacting Heads Motif

Myosin heads exist in an equilibrium where some heads are free to interact with actin while others are sequestered forming interactions with themselves and the myosin backbone. The process of getting myosins off the backbone and ready to interact with actin is known as myosin recruitment and is studied both through biochemistry and structural biology. The normal enzymatic activity or ATPase activity of myosin S1 heads in isolation is often measured using a fluorescent ATP analog (mantATP). Myosin molecules (or myofibrils, myofilaments, myocytes etc.) are mixed with mantATP and—after homeostasis is achieved—mixed with an excess of normal or "dark" ATP. The decay in fluorescence can then be measured as an analog for myosin ATPase rate (Hooijman, Stewart, and Cooke 2011; Toepfer et al. 2020). These results are often fit with a double exponential describing two rates of decay, one fast rate and one slow rate. When β-cardiac myosin is assayed this way a fast ATPase rate of ~0.02-0.05 s^{-1} and a slow ATPase rate of ~0.002-0.005 s^{-1} are observed (Mohran et al. 2024). These two different biochemical rates are defined as the

slow super-relaxed (SRX) state and the fast disordered-relaxed (DRX) state of myosin. The SRX state represents a significant reduction in the basal ATPase activity of myosin, effectively conserving cellular energy when muscle contraction is not actively required (Toepfer et al. 2020). The SRX state is thought to be a crucial regulatory mechanism, allowing muscle fibers to remain in a quiescent state with minimal ATP consumption. This is essential for maintaining cellular energy homeostasis and preventing unnecessary ATP depletion. This state also acts as a reserve pool available to increasing the contractile strength of individual muscle cells. Importantly the disruption of the homeostasis between these two states is thought to be a key etiology in many cases of hypertrophic and dilated cardiomyopathy (Barrick and Greenberg 2021; Duno-Miranda et al. 2024; Toepfer et al. 2020).

Structurally, the interacting heads motif (IHM) is a key feature correlated with the SRX state. The IHM describes a conformation where the two myosin heads fold back and interact with each other and the myosin tail domain (as seen in **Figure 1-2**). This interaction is conserved across different organism and is believed to stabilize the myosin molecule in a low-energy conformation (Lee et al. 2018). It has been hypothesized that the IHM contributes directly to the reduced ATPase activity characteristic of the SRX.

However, it is important to remember that the SRX state is defined biochemically while the IHM state is defined structurally. More research is needed to fully understand the relationship between these states. While the IHM is often correlated with the SRX, emerging evidence suggests that the SRX state may not be exclusively dependent on the IHM conformation (Mohran et al. 2024). Other factors, such as interactions with accessory proteins within the sarcomere and subtle variations in myosin tail conformation, may also play a role in modulating myosin's ATPase activity and contributing to the SRX state. This indicates a more nuanced regulatory landscape than initially proposed. Understanding the interplay between the biochemically defined SRX and the structurally defined IHM is crucial for elucidating the mechanisms of myosin recruitment and their implications in muscle physiology and pathology. Further investigation is needed to fully

characterize the structural determinants of the SRX state and how they are modulated by various regulatory factors—some of which are discussed next.

Regulators of Myosin Recruitment

Many different chemical, structural, and physical forces and modulate the recruitment of myosin and are therefore force generation. A few of these are relevant to the work presented here and will be discussed. Strain and/or load on the thick filament destabilizes the folded back state of myosin allowing for increased recruitment of myosin heads off the myosin backbone under loaded conditions (Campbell et al. 2018; Wang et al. 2024). This represents a major limitation of many studies that have investigated the importance of the OFF state of myosin.

Myosin-binding protein C (MyBP-C) exhibits properties of thick filament regulation. This protein is not found in the whole thick filament; it is restricted to the C-zone or central zone. This protein is particularly interesting because it interacts with both myosin and actin meaning it can play roles in both regulation of the thin filament and the thick filament (Ackermann and Kontrogianni-Konstantopoulos 2011; Mun et al. 2014). Exactly how this protein regulates myosin recruitment is an active area of research, this investigation includes defining the regulation that MyBP-C carries out in the C-zone but also in other regions of the sarcomere thick filament. That being said, a lot is already known about this regulatory protein. Phosphorylation of MyBP-C—by PKA—alters its interactions with actin and myosin, affecting the availability of myosin heads for cross-bridge formation (Ackermann and Kontrogianni-Konstantopoulos 2011). This can influence the number of available actin-binding sites along with the relative position of the thick and thin filaments and thus the extent of myosin recruitment.

Finally, recently published results have shown that calcium can directly interact with myosin and may be another regulatory of myosin recruitment. X-ray diffraction measurements were used to show that increased calcium alone (in the presence of an inhibitor of thin filament activation) can destabilize the interacting heads motif (IHM) state (Ma et al. 2022). It is not clear

by what mechanism calcium affects thick filament activation and recruitment. However, this effect may be an import way that myofilaments respond to increased calcium and initiate contraction.

Myosin Activation

Once recruited of the backbone myosin must form an electrostatic interaction with actin to generate force. This formation of the actomyosin crossbridge is known as myosin activation. This binding requires the actin binding surface of myosin to find its binding site on actin. The importance of the actomyosin interaction has been established for decades (Regnier, Morris, and Homsher 1995) but the exact portions of myosin and actin that interact to form a weakly bound crossbridge have only been identified in crystal structures over the last decade or so (Doran, Rynkiewicz, Rasicci, et al. 2023; Klebl et al. 2025). From these structures it can clearly be seen that actin binding surface of myosin is made up of the helix-loop-helix (HLH) motif on the lower 50 kDa domain along with two flexible loops on either side of the HLH motif, loop 2 and loop 3. These flexible loops are of particular interest since their dynamic (flexible) nature means they could play regulatory roles moving their charged residues closer to or away from actin to facility or inhibit interaction respectively. This actin binding surface of myosin is primarily positively charged and the myosin binding site on actin is dominated by negative charges. Indeed loop 2 was originally described as “the lysine rich loop” (Gordon et al. 2000) highlighting the importance of the positively charged residues in this loop. In a recently published structure of the weakly bound actomyosin complex the positively charged residues in loop 2 can be seen interacting with negatively charged residues on the N-terminus of actin (Klebl et al. 2025). This dynamic “handshake” between a flexible loop and a flexible tail is potentially important, but no assay has yet managed to observe the dynamics of this interaction.

Myosin activin is regulated by more than just the binding surface of myosin. Myosin heads do not exist in isolation, through their tails they are connected in pairs and to the larger thick filament. Because of this the activation/binding of a single myosin head moves other myosin

heads closer to the thin filament. Additionally, recent research has shown that as myosin transitions from the weakly bound state to the strongly bound state it can push tropomyosin further away from the actin binding site (Doran, Rynkiewicz, Pavadai, et al. 2023:4). Since tropomyosin molecules are connected in series this could be another mechanism by which myosin activation is potentiated. This means that the activation of a myosin molecules is a highly cooperative event (Wagoner and Dill 2021). This degree of cooperativity can be measure as the slope of the force pCa relationship known as the Hill coefficient (Mijailovich et al. 2012). It is also worth noting that myosin activation—the binding of myosin to actin—can directly influence the timing and extent of thin filament activation. Finally, the regulatory light chain (RLC) can modulate the activation of myosin. Phosphorylation of RLC, primarily by myosin light chain kinase (MLCK), can modulate the kinetics of cross-bridge binding and the rate of force development (Gordon et al. 2000; Zaleta-Rivera et al. 2019).

Myosin Cycling

The myosin molecule moves though the chemomechanical cycle or crossbridge cycle to generate force. Yet different myosin molecules move through this cycle at different rates (Sweeney and Houdusse 2010) these changes in rate allow different myosin molecules to carry out different functions. The steps of the myosin cycle were reviewed in detail in a previous section, here the regulatory importance of changes in the myosin ATPase/cycling rate will be discussed.

The ATPase rate of isolated myosin in the absence of actin and under no load is limited by the rate of phosphate release (Yengo and Sweeney 2004). However, in the presence of actin and under load the rate limiting step in the myosin cycle changes. At the heart of this phenomenon lies the ability of myosin to adjust its activity in response to varying resistive forces. Under conditions of high load, such as during strenuous muscle contraction or when transporting heavy cargo, the release of ADP from the myosin head is significantly slowed (Doran, Rynkiewicz, Rasicci, et al. 2023; Sweeney and Houdusse 2010). This prolongation of the strong-binding state

to actin is crucial for maintaining force generation, ensuring that the necessary tension is sustained to overcome the encountered resistance. Conversely, when the load is minimal, ADP release occurs more rapidly, facilitating a faster cycling rate and enabling swift movement. This dynamic adjustment allows myosin to adapt its performance to the specific demands of the task, optimizing efficiency and preventing energy waste.

Cardiomyopathy

The research presented here focuses on cardiomyopathy the most common form of heart disease worldwide (Mozaffarian et al. 2016). Cardiomyopathy can manifest as an acquired disease brought on by hypertension, smoking, alcohol abuse, or many other causes. In these acquired cases of heart failure, the heart fails to compensate for the physiological demand or abuse. Cardiomyopathy can also be an inherited disease brought on by genetic mutation. In the inherited case there is a maladaptive response in the heart due to changes in muscle/heart contraction caused by mutation. These mutations are found in the proteins that are responsible for force generation in the heart or those that regulate the generation of force in the heart. All cardiomyopathies are therefore diseases of contraction or relaxation—they alter the way in which force is generated in the heart—but the way in which this force generation is altered changes the disease phenotype. Inherited cardiomyopathy is a particularly interesting system to study the progression of myopathy since the disease causing mutations are generally expressed very early in development or adolescence (Ahmad et al. 2005). Cardiomyopathy is generally broken down into two subgroups hypertrophic cardiomyopathy (HCM) characterized by concentric growthy or thickening of the cardiac muscle (Maron and Maron 2013), and dilated cardiomyopathy (DCM) characterized by eccentric growth or a thinning of the cardiac muscle (Schultheiss et al. 2019). Both of these forms of cardiomyopathy are a disease of the heart muscle that leads to decreased cardiac output and eventually heart failure (Saeed et al. 2023). The underlying principals governing the way in which cardiac muscle grows are an active area of research but response to force and mechanotransduction are key regulators (Lyon et al. 2015). An increase in the force generated by a cardiac muscle twitch over time—the tension time integral (TTI)—is associated with HCM while a decrease in the TTI is associated with dilated growth (Davis et al. 2016; Powers et al. 2020). Since this set of diseases are driven by contraction, they are best understood through the proteins that generate and regulate force in the heart.

On the surface it should then be simple to study a given mutation in each protein, determine if it leads to hypo- or hyper-contraction and then predict if that mutation will cause DCM or HCM respectively. In practice however there are many different steps of force generation and each of them can lead to increases or decreases in force. Any given mutation may impact one, none, or many of these elements of force generation. Currently the standard of care for all genetic cardiomyopathies is not adjusted for a patients genotype (Maron and Maron 2013; Schultheiss et al. 2019). The work presented here aims to address this issue. By investigating deeply how mutations lead to changes in contraction we hope to inform drug development and eventually patient care. The next sections will discuss HCM and DCM highlighting the proteins involved in force generation in the heart as well as the regulation of force generation in the heart. But what protein mutations have been identified in patients? Sarcomeric proteins known to be mutated in HCM and/or DCM are visualized in **Figure 1-3**.

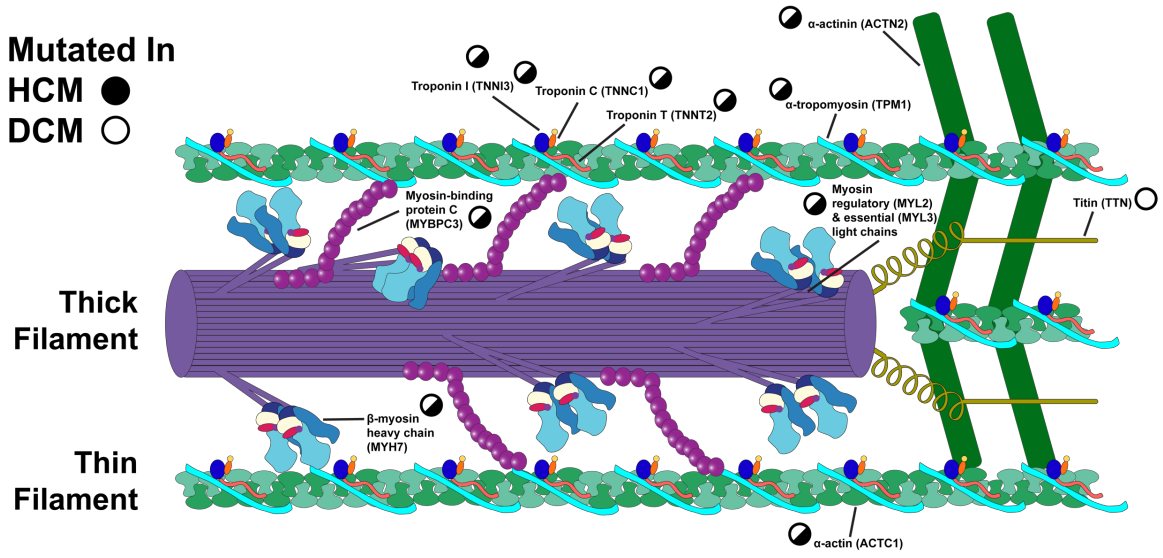

Figure 1-3: Genetic mutations in sarcomeric proteins known to cause cardiomyopathy.

A depiction of the half sarcomere. Key structural, regulatory, and mechanical proteins are highlighted. Almost all the proteins which make up the cardiac sarcomere are implicated in hypertrophic cardiomyopathy (HCM), dilated cardiomyopathy (DCM), or both. Figure adapted from: Schultheiss et al. 2019 Dilated Cardiomyopathy. Nature Reviews Disease Primers; Maron et al. Hypertrophic Cardiomyopathy. Lancet; and Childers et al. 2024 Atomistic Simulations of Sarcomere Proteins. Methods in Molecular Biology.

Hypertrophic Cardiomyopathy

The muscle growth associated with hypertrophic cardiomyopathy (HCM) leads to diastolic dysfunction or an inability of the heart to relax and fill with blood between each contraction. The myocardial thickening or concentric growth seen in HCM means that the ventricles of the heart lose volume as the muscle hypertrophies. Notably there is little to no hyperplasia present in this disease, the increase in heart size and weight is due primarily to the growth of individual cardiomyocytes and not the proliferation of cardiomyocytes. This growth is dominated by the addition of sarcomeres in parallel leading to wider rather than longer cardiomyocytes (lower aspect ratio). Notably cardiomyocytes do not fuse together—unlike skeletal muscle myotubes (Quinn et al. 2017). In extreme cases of HCM the myocardium of the ventricular and septal walls can become so thick that blood outflow through the pulmonary and aortic arteries can be blocked (Maron and Maron 2013). Finally HCM is also associated with sudden cardiac death, while this is the most visible and unpredictable symptom of HCM it is relatively rare and occurs in less than 5% of HCM cases (Stroumpoulis, Pantazopoulos, and Xanthos 2010). Almost all mutations known to cause HCM are found in cardiac sarcomeric proteins responsible for force generation in the heart (**Figure 1-3**). A summary of these proteins follows arranged by prevalence in the HCM population percentages represent the percent of HCM cases with a positive causal mutation.

Sarcomere mutations and HCM

β-myosin heavy chain (MYH7) ~35% of HCM cases: Myosin is the molecular motor of force generation in the heart and the β isoform of myosin (encoded by the *MYH7* gene) is the dominant isoform expressed in the adult human ventricle (Katz 2010). It therefore makes sense that mutations in *MYH7* would account for a large percentage of HCM cases. Notably most of these mutations are associated with an increase in contractility and ATPase activity of the myosin molecule (Adhikari et al. 2019; Vander Roest et al. 2021; Wang et al. 2024). Though it should be noted that an increase in ATPase activity is not equivalent to a hypercontractile phenotype.

Myosin-binding protein C (MYBPC3) ~35% of HCM cases: This protein has both structural and regulatory roles in the sarcomere and is responsible for at least as many if not more cases of HCM than MYH7. Fully half of MYBPC3 mutations leading to HCM are caused by truncations, highlighting the structural importance of this protein (Tudurachi et al. 2023). This protein forms strong interactions with the myosin thick filament through its C-terminal domain while its N-terminal domain can form interactions with myosin heads and the thin filament. Through these interactions it regulates the interaction of myosin and actin. Interestingly most disease HCM linked mutations in *MYBPC3* are truncation mutations leading to haploinsufficiency. This, combined with the understanding that hypercontraction is associated with HCM, has led to the hypothesis that the MYBPC3 protein may act as a "break" that slows contraction in the C-zone of the thick filament (Pioner et al. 2023; Tudurachi et al. 2023).

α-tropomyosin (TPM1) ~5% of HCM cases: As the structural blockade that regulates crossbridge formation tropomyosin it accounts for many HCM mutations. These mutations generally cause an increase in the availability of actin binding sights ready to interact with myosin (Dorsch et al. 2021).

The troponin complex ~1-5% of HMC cases each: The troponin complex in the adult ventricle is made of Troponin C (TNNC1), Troponin T (TNNT2), Troponin I (TNNI3), and together these complexes sense calcium levels in the sarcomere and allow for the movement of tropomyosin during contraction. HCM mutations in these proteins generally increase the calcium sensitivity of the thin filament (Lu, Wu, and Morimoto 2013; Watkins et al. 1995).

α-actin (ACRC1) ~1-5% of HCM cases: Actin is the main structural component of the thin filament and HCM causing mutations in this portion are generally found in the myosin binding site associated with changes in how actin interacts with myosin (Vang et al. 2005).

Myosin regulatory (MYL2) and essential (MYL3) light chains ~1-5% of HCM cases: Both light chains are found at the head-rod junction of myosin and modulate myosin function and activation. The phosphorylation of the regulatory light chain promotes the activation of myosin

heads (Zaleta-Rivera et al. 2019). The essential light chain on the other hand can interact directly with actin and regulate crossbridge formation (Hernandez et al. 2007). Mutation in these proteins associated with HCM can lead to increased myosin activation and hypercontraction.

α-actinin (ACTN2) ~1% of HCM cases: α-actinin is a structural protein of the sarcomere that interacts with actin filaments to form the z-disk. Mutations in this gene make up a small but not insignificant number of HCM cases however the mechanism by which these mutations cause disease is still under investigation (Chiu et al. 2010).

Current treatments

They hypercontraction associated with HCM can be addressed in a few different ways. Beta-blockers can be used to slow the heart rate. Calcium channel blockers can be used to improve diastolic relaxation. In extreme cases of HCM where heart has hypertrophied enough that outflow from the ventricles is blocked by the septum surgical intervention to remove part of the heart muscle can help (Kindi and H. Yacoub 2018). Finally, the first myosin inhibitor drugs have recently been approved by the FDA meaning that force generation in the heart can be directly targeted to correct the hypercontractility associated with HCM (Bello and Pellegrini 2024; Braunwald et al. 2023).

Despite the importance of genetics in hypertrophic cardiomyopathy a patient's treatment is currently not informed based on their genotype (Maron and Maron 2013). Genotype screening is only used clinically to identify family members who may also suffer from HCM. One goal of the work presented here is to begin to bridge this gap between genotype information patient treatment by describing the molecular mechanisms that lead to disease.

Dilated Cardiomyopathy

Dilated cardiomyopathy (DCM) is characterized be a weakening and eccentric enlargement of the heart muscle, and is a key cause of heart failure and worldwide is the leading indication for cardiac transplant (Saeed et al. 2023). The dilation of the heart muscle characteristic of this disease means that the heart loses systolic force generation and cannot effectively contract to push blood throughout the body. Much like in HMC the morphological changes in the heart are not caused by cell proliferation or death but rather changes the morphology of cardiomyocytes themselves. In DCM cardiomyocytes add sarcomeres in series leading to elongated cells with an increased aspect ratio. DCM can be caused by a variety of etiologies and can be inherited, acquired, or idiopathic (Schultheiss et al. 2019). Studies in the 1990s found that of idiopathic DCM cases 20-50% can be attributed to genetic mutations (Burkett and Hershberger 2005). Unlike HCM mutation causing DCM are found not only in the sarcomere (**Figure 1-3**) but also in the sarcoplasmic reticulum, desmosome, nucleus, and gap junctions (Schultheiss et al. 2019).

This complex genetic landscape of DCM, where multiple genetic variants can contribute to each disease phenotype, presents a significant challenge for accurate diagnosis and targeted therapeutic interventions. Despite this some trends can be seen in the impact of mutations that cause DCM. DCM mutations often induce a decrease in myofilament sensitivity to calcium, leading to accelerated relaxation and necessitating a higher concentration of free cytosolic Ca^{2+} for adequate force generation (Lu et al. 2013). Notably, neither the extent of myocyte shortening nor the amplitude of the calcium transient alone provides a reliable predictor for distinguishing between hypertrophic and dilated ventricular remodeling—however the integral of force generated over time can predict disease progression and severity (Davis et al. 2016). The precise mechanisms through which mutations associated with DCM result in disease pathogenesis remain an active area of investigation (Schultheiss et al. 2019), to which this thesis intends to contribute. What is known about disease causing mutations in major cell compartments and organelles is summarized in the following section.

The sarcomere and sarcolemma

Mutations in contractile proteins are very common in DCM and account for approximately 30% of idiopathic DCM cases (Herman et al. 2012). These mutations include truncating mutations in titin (TTN), cardiac actin (ACTC1), myosin-binding protein C (MYBPC3), myosin heavy chains (MYH6, MYH7), myosin light chains (MYL2, MYL3), tropomyosin (TPM1), cardiac troponin C (TNNC1), troponin I (TNNI3), and troponin T (TNNT2) (Lu et al. 2013; Schultheiss et al. 2019).

Mutations found in proteins that make up the sarcoplasmic reticulum (SR) are also common in DCM including the ryanodine receptor (RYR2), which is responsible for calcium induced calcium release, and phospholamban (PLN) which regulates calcium reuptake into the SR through interactions with the calcium pump SERCA. Interestingly SERCA itself has not been seen mutated in cases of DCM (Schultheiss et al. 2019).

The membrane and the nucleus

Structural proteins such as desmin (*DES*), dystrophin (*DMD*), and laminin (*LAMA4*) have been linked DCM. These proteins are part of the complexes which connect a cell to its environment. Additionally nuclear envelope proteins such as lamin A/C (*LMNA*) and thymopoietin (*TMPO*) as well as the RBM20 (a regulator of nuclear organization) have been implicated in DCM (McNally, Golbus, and Puckelwartz 2013). These sets of proteins don't directly regulate force generation and their relationship to DCM is thus harder to explain. They do however regulate force transduction and nuclear organization. The connection here is mechanotransduction which is hypothesized to play a role in DCM disease progression (Barrick and Greenberg 2021).

Current treatments

The current standard of care for DCM primarily focuses on managing symptoms, slowing disease progression, and preventing complications (Altinier et al. 2019). This involves combining

pharmacological interventions with lifestyle modifications and, in advanced cases, device therapy or transplantation. Medications play a crucial role, including angiotensin-converting enzyme inhibitors or angiotensin receptor blockers to lower blood pressure and reduce cardiac workload; beta-blockers to slow heart rate and improve cardiac function; diuretics to alleviate fluid retention; and in some cases, medications like digoxin or antiarrhythmics to control heart rhythm. Additionally, lifestyle adjustments such as dietary sodium restriction, regular moderate exercise, and abstaining from excessive alcohol consumption are essential components disease management.

A newer area of interest involves myosin activating drugs, such as Danicamtiv (Voors et al. 2020). These drugs work by increasing the interaction between myosin and actin, the proteins responsible for cardiac muscle contraction. It should be noted however that these drugs have many different effects. They not only change myosin recruitment and activation but can also change the rate that myosin moves through the chemomechanical cycle (Kooiker et al. 2023). As these new drugs are developed there must be a thorough investigation of how exactly they interact with and change myosin structure and function. The goal is to improve cardiac contractility and therefore cardiac output. While promising, these drugs have limitations. Careful patient selection is needed, as they may not be suitable for all DCM patients—this is potentially where genetic screening can help. Finally, side effects and long-term efficacy are still being investigated. Further research is necessary to fully understand their role in DCM treatment and how to best integrate them into existing therapeutic strategies.

The Role of Loop 2 Electrostatics in Myosin Actin Interaction

Loops are flexible parts of proteins often found on the surface of proteins. Their flexible nature and solvent accessibility mean they are uniquely well-suited sub-structures for controlling protein dynamic action and regulating or modulating interactions between a protein and its various ligands. The stable amino acid structures of alpha-helices and beta-sheets are the rigid bones that make up structural supports of proteins. Flexible loops are the dynamic structures that let a protein interact with its environment. In this way loops are the fingers and hands that proteins use to interact with other proteins, ligands, and structures (Bartlett et al. 2002). The role that surface loops play in regulating myosin ATPase activity has been hypothesized for decades (Onishi, Mikhailenko, and Morales 2006), but the inability to resolve these loops via crystal structure has limited research in this area. Moreover, even if all these flexible loops could be resolved, they are inherently disordered and dynamic. A crystal or cryo-EM structure could never depict the movement that makes these loops functional.

Intrinsically disordered loops are challenging to study but very important in many biological systems. It is estimated that on average one third of protein sequences are made up of flexible loops, however fully half of protein sequences in enzyme active sites are flexible loops (Bartlett et al. 2002; Towel et al. 2011). Conformation changes in these flexible loops regulate enzyme function in many key biological systems (Malabanan, Amyes, and Richard 2010). While the movement of loop structures cannot be observed in in crystal structures, loop movements can be observed via NMR relaxation and happen across a wide range of time scales all the way form picoseconds to milliseconds (Gu, Li, and Brüschweiler 2015). Key to understanding the mobility of flexible loops is the concept of energy landscapes or energy state space where movement between semi-stable states requires activation energy (Wales 2003). Some loop structures have relatively simple on/open off/closed conformations that regulate ligand or substrate interaction (Zinovjev et al. 2024), but others can sample many different conformations with poorly understood

regulatory roles (Barozet, Chacón, and Cortés 2021). The stability or relative stability of the semi-stable states and the activation energy to move between them are yet another open question in the field of structural biology—especially when it comes to the surface loops of myosin.

Mutation studies changing the residues in myosin loop 2 have established the important role that the positive charges on loop 2 play in initiating the weakly bound state between myosin and actin (Murphy and Spudich 1999; Uyeda, Ruppel, and Spudich 1994; Yengo and Sweeney 2004). The positive charges on loop 2—five lysine residues in the case of beta-cardiac myosin—are hypothesized to form electrostatic interactions with the negatively charged residues on the N-terminus of actin facilitating the formation of the actomyosin weakly bound state (Klebl et al. 2025). While the ephemeral weakly bound state has been challenging to observe via crystal structure, the interactions of these charged residues can be clearly observed in crystal structures of the strongly bound actomyosin complex (Clobes and Guilford 2014; Doran, Rynkiewicz, Pavadai, et al. 2023). While biochemical and crystal structure studies have given insight into the role that loop 2 plays regulating actomyosin complex formation these techniques are unable to elucidate the dynamics of loop 2 movement during this complex biological process. Biochemical assays give an overview of millions of chemical interactions and crystal structures give a snapshot of structures frozen in non-physiological conditions. Molecular dynamics (MD) simulations are a powerful tool for understating how flexible loop structures move (Barozet et al. 2021). Given the dynamic nature of the myosin molecule the ability to understand how loop 2 changes dynamically during the actomyosin complex formation is critical. Additionally, understating how disease-causing mutations change this dynamics motion is an important step in developing drugs that target the root cause of myosin diseases.

Beta-Myosin Mutations E525K and V606M in Cardiomyopathy

The work presented in this thesis focus on two mutations associated with cardiomyopathy E525K and V606M. These two mutations have been used here to study the development of cardiomyopathy in general and the dynamics of the myosin loop 2 structure specifically. Both mutations were identified through genetic screening of patents with cardiomyopathy, but they have different disease phenotypes. The V606M mutation is associated with HCM, a hypercontractile phenotype, has been found in multiple patients, and has been directly linked to familial HCM (Blankenburg et al. 2014; Watkins et al. 1992). The E525K mutation on the other hand has only been identified as a *de novo* mutation in a single patient suffering from DCM (Lakdawala et al. 2012). Through that work E525K has been associated with DCM and a dilated cardiomyopathy phenotype but this mutation is less well established as a heritable and reproducible DCM mutation. The following sections delve into these two beta-myosin mutations, E525K and V606M, exploring their interplay with the contractile machinery and dissecting their potential contributions to the distinct phenotypes of HCM and DCM.

Two Mutations to Study Loop 2

While diverse etiologies contribute to cardiomyopathy pathogenesis, genetic factors are a robust tool to study disease. The location of E525K and V606M in myosin makes them particularly interesting for studying the loop 2 region of myosin. Neither of these mutations are in loop 2 itself which runs between the upper and lower 50 kDa domains of myosins. Rather, these mutations are “in the neighborhood of loop 2” and both a have clear allosteric pathways through which they may change the dynamic motion of loop 2 (**Figure 1-4**). V606M is found on the upper 50 kDa domain directly linked to the helix which leads to loop 2. E525K is found on the lower 50 kDa domain and while not directly linked to loop 2 has a direct allosteric pathway to loop 2 through altered salt bridges. The final reason these mutations were chosen for the loop 2 studies

presented here is that they have both been shown to alter the affinity of myosin for actin. Both E525K and V606M have been shown to increase binding affinity of myosin for actin (Duno-Miranda et al. 2024; Kinnear et al. 2024). These mutations are both near loop 2—a region of myosin important for electrostatic interaction with actin. This has led the hypothesis that these mutations may have a similar mechanism of action by which they increase the association between myosin and actin: they alter the dynamic motion of loop 2 and the presentation of the positive charges on loop 2.

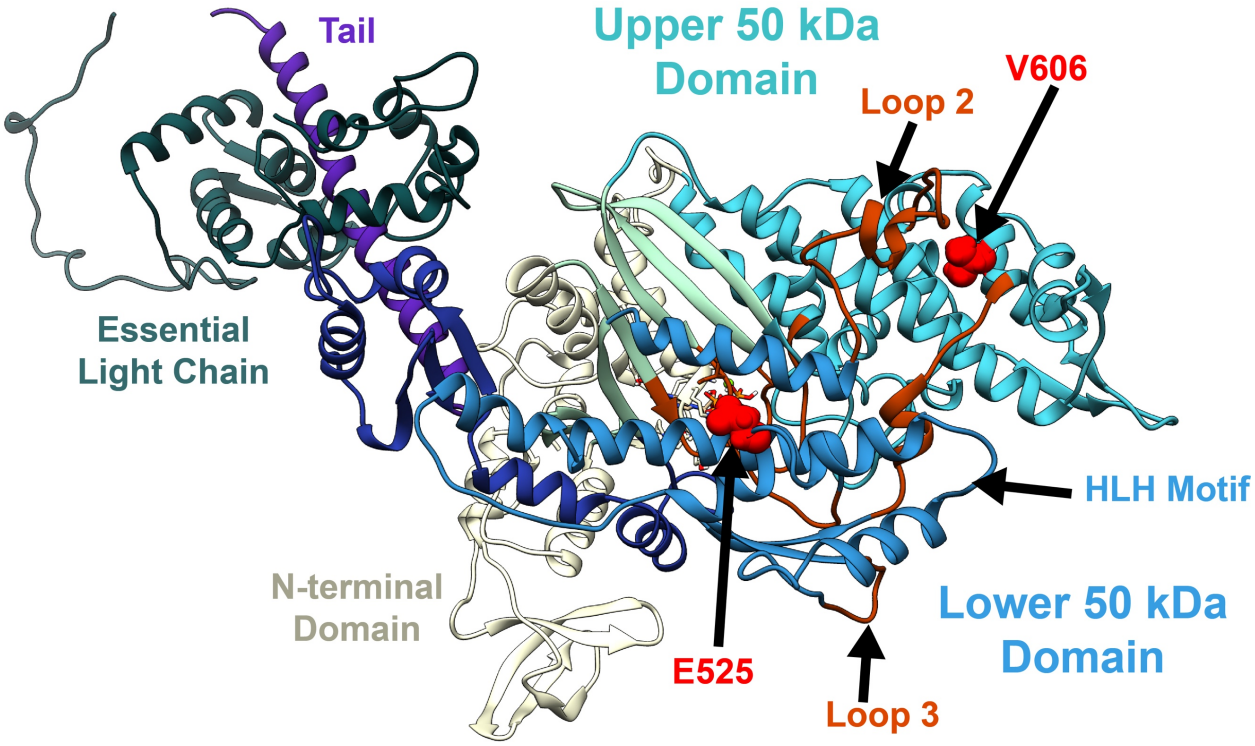

Figure 1-4 Location of the E525 and V606 residues in myosin.

Pre-powerstroke myosin S1 head ribbon diagram. The major domains of myosin are indicated. The subdomains of the actin binding surface are also noted: the helix loop helix (HLH) motif, loop 2, and loop 3. The locations of the E525 and V606 residues are highlighted in red.

E525K Drives both Hypocontraction Hypercontraction: A Disease Paradox

As has been discussed, a hypocontractile phenotype (a decrease in wringing out) is generally associated with DCM disease progression. However, the E525K mutation—while it was found in a patient suffering from DCM—has been associated with both hyper- and hypocontractile phenotypes (Rasicci et al. 2022). However, this mutation has exclusively been studied using

isolated myosin constructs produced via viral transduction in C2C12 cells (Bodt et al. 2024; Duno-Miranda et al. 2024; Rasicci et al. 2022), and has never been studied in contracting cardiomyocytes or under load. For this reason, this mutation was chosen for a deeper analysis using our stem cell derived cardiomyocyte model of disease (see Chapter 3).

The E525K mutation was originally identified and linked to DCM in a 2012 study where DCM patients were screened for genetic mutations in various DMC linked genes including MYH7 (Lakdawala et al. 2012). In this study 264 patients were screened, and one Hispanic patient was identified with the *de novo* mutation E525K. This mutation was classified as “Clinically Significant” based on three factors: (1) this mutation was not identified in any individuals from the control (no heart disease) data set. (2) This mutation was *de novo* meaning it was not found in either healthy parent. (3) The conservation of this residue in distantly related species. While this classification clearly points towards E525K being causal in the identified patient with DCM it should be noted that this mutation has only ever been identified in a single patient with DCM. Neither the age of this patient or nor the age of DCM diagnosis was reported and—given the complexity of DCM disease progression—this study does not directly link this mutation to DCM. It is probably true that this mutation alters myosin structure at the atomic level and alters contractility at the cell and tissue level but the exact link between the structural changes and physiological changes remains to be explored.

More recent work on the E525K mutation has used virally expressed and isolated myosin constructs to paint a picture of its role in DCM pathogenesis. These studies used myosin constructs with different tail lengths to investigate the relationship between myosin ATPase activity and the IHM state. By using a combination of biochemical approaches (ATPase activity as measured by mantATP turnover) and structural biology approaches (FRET and electron microscopy) they were able to demonstrate that the E525K mutation stabilizes the "OFF" state of myosin, where the motor heads remain inactive, significantly reducing the pool available for force generation. This translates to weakened contractility, impaired power output, and therefore could

contribute to DCM's characteristic hallmarks of dilated heart chambers and systolic dysfunction (Rasicci et al. 2022). Interestingly this work also found that in isolated E525K S1 constructs (without a tail and incapable of forming the IHM) the mutation actually led to an increase in ATPase activity (Bodt et al. 2024; Duno-Miranda et al. 2024; Rasicci et al. 2022). This type of increased activity could lead to a hypercontractile phenotype, but it is important to note that increased ATPase activity is not the same thing as increased contractility. The intramolecular mechanism by which E525K accelerates the ATPase activity of myosin is still under investigation but the above studies have identified accelerated phosphate release as a potential mechanism (Bodt et al. 2024). This result makes sense given the placement of the E525K mutation near the hypothesized “phosphate back door” (Cecchini, Alexeev, and Karplus 2010), however phosphate release is only rate limiting in myosin in the absence of actin (Sweeney and Houdusse 2010). The presence of actin and load slow ADP release meaning that this step becomes the rate limiting factor in contracting muscles (Geeves and Holmes 2005). To characterize this mutation, it must be studied under load. Mechanistically, the E525K mutation appears to alter electrostatic interactions within the lower 50 kDa domain. These changes seem to favor the inactive conformation “OFF” conformation and hinder efficient ATP hydrolysis. This "off-state stabilization" model could explain the contractile deficits observed in DCM hearts harboring the E525K mutation.

One critical limitation in the fields current understanding of E525K β-myosin biology is that no studies have measured contraction in an intact myofilament containing E525K mutation myosin molecules. As has been discussed isolated myosin can have very different kinetics and rate constantans than myosin under load (Campbell et al. 2018; Sweeney and Houdusse 2010). Isolated engineered myosin constructs are useful tools for understanding myosin biochemistry, but myosin is a molecular motor driving force generation and to understand this mutation its biochemical properties need to be observed in a sarcomere under load. This is especially important for this mutation as the stability of the interacting heads motif and the rate limiting step

of ATPase turnover are both known to be load dependent (Campbell et al. 2018; Vander Roest et al. 2021).

The V606M Mutation

The V606M mutation has a much clearer link to disease than the E525K mutation. The first report of this mutation in families with HCM came from a 1992 study looking specially at mutations in the MYH7 gene in cases of familial HCM (Watkins et al. 1992). This work noted that of the mutations studied V606M did not induce a charge change (valine and methionine are both hydrophobic) and families with the V606M mutations seemed to have less aggressive HCM with a later onset of disease and fewer sudden cardiac deaths. However, one child from the study with the V606M mutation died at 13 years of age, so this mutation is far from harmless!

More recent studies have looked more closely at this mutation by generating a mouse model of the V606M mutation (Blankenburg et al. 2014). This work was limited since it required the β-myosin mutation be engineered into α-myosin for expression in a mouse model. However, it was able to show that the V606M mutation created a mild HCM phenotype in mice. The penetrance for this mutation therefore appears to be relatively low, and its presence alone cannot definitively diagnose the condition. This is not unusual for HCM mutations, especially when studied in mice (Feest et al. 2014; Maron and Maron 2013; Wang et al. 2012).

Since the publication of this mouse study the use of patient derived stem cells to study cardiomyopathies has been used to gain further insight into V606M and its relationship to HCM (Kinnear et al. 2024). This work again focused on patient (and patient stem cells) from individuals suffering from familial HCM. The use of human stem cells removed the need to rely on an α-myosin model as all human patients carry this mutation in β-myosin. This work also used CRISPR to reverse the mutation and showed a reversal in disease phenotype, further codifying the V606M mutation as causal in HCM. Interestingly the authors were also able to use a myosin inhibitor to reverse the disease phenotype.

None of this work has explored the mechanism by which the V606M mutation leads to increased hypertrophy, except for an increased affinity for actin described by actomyosin pulldown assays (Kinnear et al. 2024). While the result that disease phenotype can be reversed with a myosin inhibitor drug is exciting, further work is needed to understand how this mutation alters the myosin chemomechanical cycle and how drugs targeting myosin my interact with this mutation.

Summary

The details of what has already been studied with regard to these two mutations highlights the remarkable complexity of how seemingly subtle alterations in myosin structure can lead to dramatic changes in contractile phenotypes. Understanding these intricate pathways not only holds immense promise for deciphering the pathogenesis of HCM and DCM but also paves the way for developing targeted therapeutic strategies aimed at modulating myosin function and alleviating disease progression. Chapter 2 of this thesis will dissect the roles of E525K and V606M in the context loop 2 and the electrostatic interactions between myosin and actin. Chapter 3 of this thesis will focus on the E525K mutation and cardiomyopathy development, offering valuable insights into the intricate dance between molecular perturbations and the clinical manifestations of debilitating heart conditions.

Chapter 2 — Conformational State of Myosin's Disordered Loop 2 Structure Mediates Actomyosin Association During Crossbridge Formation

Kalen Z. Robeson[1,2,4], Matthew Carter Childers[1,2], Kieran J. Fruebis[3,4], Rachelle Soriano[4,5], Jennifer Davis[1,2,4], Michael Regnier[1,2,4]*

1. Department of Bioengineering, University of Washington, Seattle, WA, USA
2. Center for Translational Muscle Research, University of Washington, Seattle, WA, USA
3. Department of Biology, University of Washington, Seattle, WA USA
4. Institute For Stem Cell and Regenerative Medicine, University of Washington, Seattle, WA, USA
5. California State University, Los Angeles, CA, USA

*Corresponding Author

Email: mregnier@uw.edu

Phone: 206-221-0504

Running title: Myosin's Loop 2 Mediates Actomyosin Association

Total number of manuscript pages: 33 (3 pages of supplemental figures included)

Total number of figures: 5 with 4 additional supplemental figures

Description of supplementary material: All supplement figures are included in this manuscript

Big Idea: To date, no structures resolve the complete loop 2 sequences, but the functional importance of this disordered region is well established. The goal here is to model its structure and assess its role in the functional context of crossbridge formation.

Abstract

The binding of myosin to actin to form crossbridges is a critical step for force generation by sarcomeres. A recent cryo-electron microscopy structure has resolved the weakly-bound actomyosin complex (AM.ADP.Pi); however, the structural and dynamic factors that influence actin-myosin association are unclear. The disordered loop 2 of myosin is thought to mediate actomyosin interactions in complex, chemomechanical state-dependent fashion; however, the loop is usually unresolved in structural studies due to its intrinsic disorder. Here, we utilize a combination of molecular dynamics simulations and electrostatic calculations to investigate the dynamics of these actin binding regions of myosin. Our results show that loop 2 experiences disordered dynamics and that specific conformations sampled by loop 2 modulate the strength of the associative electrostatic force between actin and myosin. Variation in the actin-myosin associative force was associated with the presentation and orientation of positively charged residues in loop 2. We provide an in-depth analysis of the conformational state space occupied by loop 2 during nine 500 ns molecular dynamics simulations of pre-powerstroke human β-myosin S1, with three replicates each of wildtype and two different mutant (E525K and V606M) myosin structures. This dataset allowed for exploration of how loop 2 conformational sampling is altered by these two mutations which have been clinically and experimentally associated with cardiomyopathy and altered actin binding affinity. The E525K and V606M mutations altered the conformational ensemble sampled by loop 2 and were associated with associative actin binding strength. These results highlight the importance of the positive charges on loop 2 for actomyosin interactions and demonstrate how disease-causing mutations outside of loop 2 can still affect it.

Introduction

Contractions in muscle are a product of myosins binding to actin to form crossbridges that cycle to produce force and shorten. In cardiac muscle, identifying the residues in myosin that interact with actin before and during the formation of the weakly-bound actomyosin complex is a vital step towards understanding the regulation of force development and how this may be altered by disease-causing mutations, as well as for the development of novel treatments for cardiomyopathies. In the weakly-bound state (AM.ADP.Pi), the actin binding surface of myosin is made up of the helix loop helix (HLH) motif of the lower 50 kDa domain, loop 3, which is also on in the lower 50 kDa domain, and loop 2, which spans the cleft between the upper and lower 50 kDa domains (**Figure 2-1A**)(Childers, Geeves, and Regnier 2024; Thomas and Roopnarine 2002). Loop 4 and the cardiomyopathy loop also contribute to actin interactions in force-bearing states of the crossbridge cycle. The positively charged lysine residues on loop 2 are known to interact with negatively charged residues on the N-terminus and Asp-containing N-terminal hairpin loop of actin during weak and strong (AM.ADP*) binding (Clobes and Guilford 2014:2; Klebl et al. 2025; Murphy and Spudich 1999; Nowakowski, Regnier, and Daggett 2017; Uyeda et al. 1994). However, to date, no structures resolve the complete loop 2 structure for any myosin isoform or in any chemomechanical state. In this study we explore the dynamics of loop 2 in the pre-powerstroke (M.ADP.Pi) state and report on how disordered dynamics modulate the presentation of positive charges by myosin.

To investigate the dynamics of the actin interacting myosin domains we developed an *in-silico* assay for actomyosin crossbridge formation by coupling molecular dynamics (MD) simulations with electrostatic calculations using *DelPhiForce*(Li, Chakravorty, and Alexov 2017). Two cardiomyopathy associated mutations (E525K and V606M) that are near, but not in, loop 2 and increase myosin's affinity for actin(Bodt et al. 2024; Kinnear et al. 2024; Rasicci et al. 2022) were used to perturb myosin's structure. Comparison of WT and mutant behavior highlighted the

importance of loop 2 and led us to an in-depth structure-function analysis that explores the relationship between sequence and the conformational state space occupied by loop 2.

The two mutations surround loop 2 (residues 621-646): E525K is in the lower 50 kDa domain and V606M in the upper 50 kDa domain (**Figure 2-1A**). The E525K mutation involves a charge inversion, disrupting key salt bridges that connect the E525 residue to the helix where loop 2 is anchored in the lower 50 kDa domain. This mutation could therefore lead to allosteric changes in the conformational ensemble sampled by loop 2. The V606M mutation extends the hydrophobic side chain of V606 and increases the likelihood of hydrophobic interactions inside the upper 50 kDa domain. This mutation is found on a helix in the upper 50 kDa domain which leads to loop 2 and, again, could lead to allosteric changes in the conformation of loop 2 (**Figure 2-1A**). These two mutants perturb the structure of myosin in the region where loop 2 interfaces with the upper and lower 40 kDa domains. We hypothesize that both mutations change the dynamic presentation of the charges in loop 2.

Previous work has established the importance of loop 2 via both mutation screening(Murphy and Spudich 1999; Uyeda et al. 1994) and MD simulations of myosin(Ma et al. 2023; Nowakowski et al. 2017). Indeed, myosin mutations that neutralize a positively charged residues in loop 2 are associated with dilated cardiomyopathy and a decrease in myosin's affinity for actin(Parker and Peckham 2020). Despite the importance of loop 2 for crossbridge formation, this study represents the first in-depth exploration of both loop 2's dynamic movement and the impact of that movement on electrostatic interactions between myosin and actin. We modeled the pre-powerstroke (M.ADP.Pi) conformation of human MYH7 performing three replicate simulations of each myosin variant (WT, E525K, V606M), to resolve an ensemble of loop 2 conformations. The *DelPhiForce* tool generated by Li *et al.*(Li, Chakravorty, et al. 2017) was then used to calculate the electrostatic force from actin on myosin with singe atom resolution. In depth analysis of these results suggested that loop 2 conformation is responsible for the changed actin affinity observed with these myosin mutations. This work provides a mechanistic groundwork for

understanding the role of loop 2 and how mutations that influence its structure and mobility change myosin's affinity for actin.

Results

Electrostatic Modeling Identifies Residues That Initiate Actin Binding and Highlights the Importances of Loop 2 in Crossbridge Formation and Cardiomyopathy

First, we performed conventional MD simulations of WT, E525K, and V606M human cardiac β-myosin in the pre-powerstroke (M.ADP.Pi) state. The *DelPhiForce* tool developed by Li *et al.* was used to calculate the electrostatic forces that occurred between a model actin filament (an unregulated pentamer) and different MD-derived conformations of myosin(Li, Chakravorty, et al. 2017). Structures from MD simulations of pre-powerstroke human β-myosin S1 were sampled at 1 ns resolution (500 structures per simulation) and aligned 30 Å away from the central myosin binding sight on the actin pentamer (**Supplemental Figure 2-3A**). *DelPhiForce* was then used to calculate the electrostatic attraction felt by myosin from actin for each atom in the myosin model for each sampled snapshot.

The calculated binding force for each timestep in replicate simulations for both WT and mutant myosins was variable (**Figure 2-1B and Supplemental Figure 2-1B**), but the average binding force calculated across all E525K and V606M timesteps and simulations replicates was elevated compared to WT (**Figure 2-1B** dashed lines). Additionally, high binding energy (>25 nN) conformations were sampled more frequently in E525K and V606M simulations compared with WT simulations (**Figure 2-1B**). To investigate the electrostatic contribution of each residue to binding force calculations, residues that resulted in > ± 0.01 Kt/Å binding energy during any *DelPhiForce* calculation were selected for further analysis (**Supplemental Figure 2-1A**). The analysis allowed us to define residues that have electrostatic interactions with actin during early myosin binding to actin with high resolution. We identified charged residues in known actin binding elements including the HLH motif, loop 2, and loop 3. Quantification of the binding force from each

of these residues shows that the positively charged residues in the HLH motif and loop 2 experienced the strongest attractive force (**Figure 2-1C**). To predict the effects of E525K and V606M on myosin affinity for actin, we calculated the precent change in electrostatic force between the WT and mutant simulations. For most residues, the attractive or repulsive force on myosin from actin was relatively unchanged between WT and mutant simulations. However, the positively charged Lys residues in loop 2 had the greatest changes in binding force compared to WT (**Figure 2-1D** and **Supplemental Figure 2-1**). Also, as expected, the charge inversion of the E525K mutation led to a shift from a repulsive force to an attractive force at this location (**Figure 2-1D**).

Together these results indicate that isolated, static structures are not adequate to explain the changed actin affinity seen with these mutations. Instead, conformational ensembles are required to capture the range of electrostatic forces between actin and myosin during the early stages of crossbridge formation. The temporal and spatial resolution provided by MD simulations more accurately samples the relationship between structural heterogeneity and actomyosin interaction of loop 2. The changes in actin affinity appear to be driven by conformations of loop 2 that are only seen in E525K and V606M simulations and never sampled by WT simulations. This result prompted a deeper investigation of how these mutations alter loop 2 movement and how this relates to myosin activation and crossbridge formation.

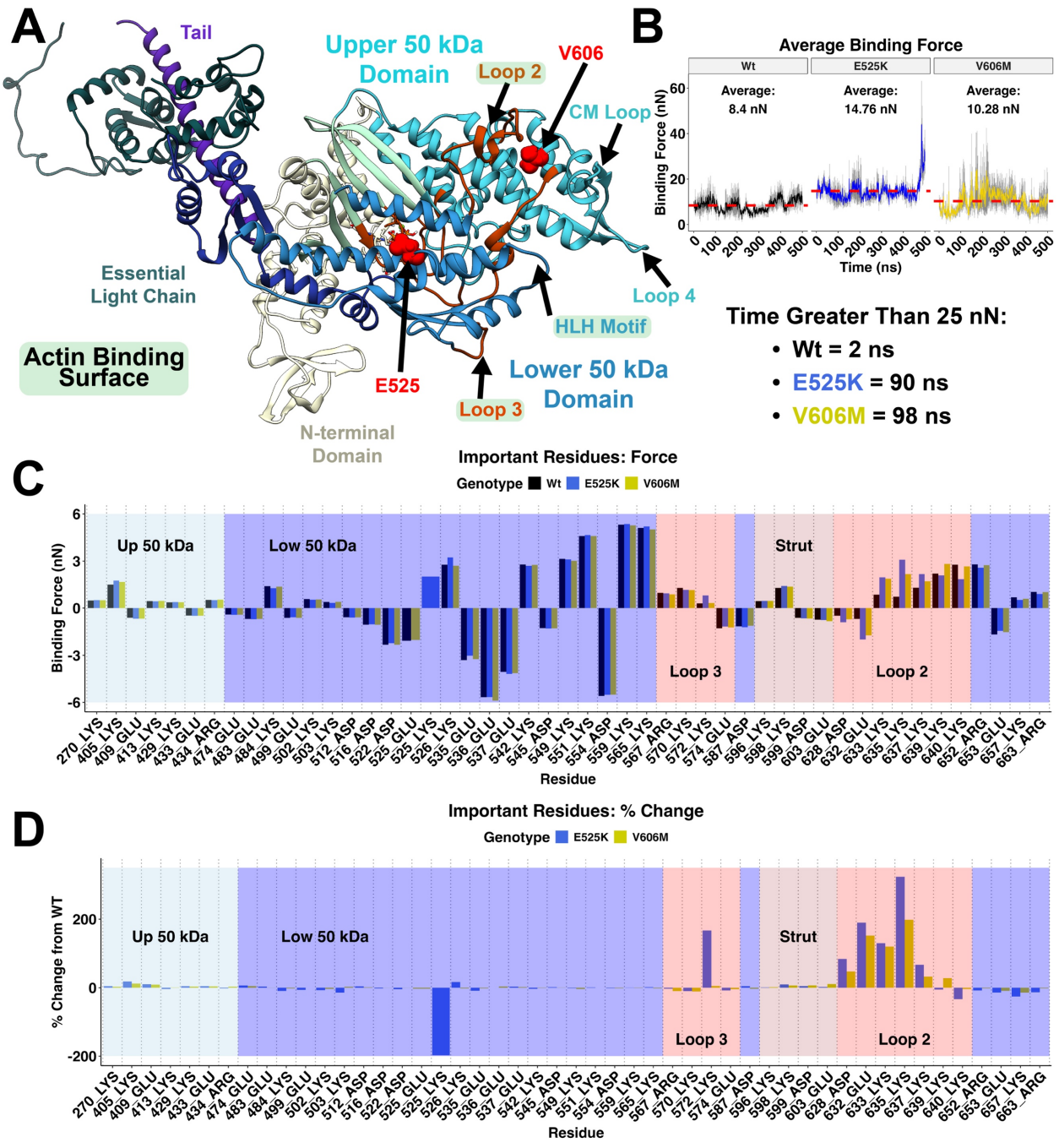

Figure 2-1: Loop 2 Drives Observed Changes in E525K and V606M Myosins' Affinity for Actin.

(A) Pre-powerstroke human β-myosin S1. The major structural domains as well as the location of the E525K and V606M mutations are labeled. Structures of the actin binding surface are highlighted in teal. (B) Average binding force calculated with *DelPhiForce* across simulation time in three replicate simulations of each genotype (Mean + SEM; dashed lines represent mean across all simulations of a given genotype. High binding energy (pro-actin binding) conformations are sampled in E525K and V606M simulations (bottom). (C) Quantification of binding force felt at the single amino acid level in residues that experienced > ±0.0 kT/Å during any (WT or Mutant) *DelPhiForce* simulation. (D) Percent change from WT binding force for each residue in C. The positively charged lysine residues in loop 2 can be seen driving increased actin

affinity in E525K and V606M. The charge change due to the E525K mutation is also identified in E525K simulations.

The Dynamics of Loop 2 are Changed by The E525K and V606M Mutations

We next investigated the hypothesis that myosin mutations near the interface of loop 2 with the upper and lower 50 kDa domains can disrupt its movement and the presentation of loop 2's positive charges to actin. Contact pair analysis of E525K and V606M MD simulations showed that the contacts formed by loop 2 during simulations were changed by both mutations. The E525K mutation in the lower 50 kDa domain resulted in a charge change (negative to positive) and disrupted salt bridges on adjacent helices (**Figure 2-2A-B**). One of these helices leads directly to loop 2, and the contacts formed by loop 2 during MD simulations of E525K myosin were significantly altered compared to WT simulations (**Figure 2-2C**). In MD simulations of V606M myosin the increased hydrophobic side chain length induced a hydrophobic interaction between the 606 reside and residue 434 on an adjacent helix in the upper 50 kDa domain (**Figure 2-2D-E**). This interaction twisted the helix where residue 606 is located and led to allosteric shifts in loop 2 as seen by altered loop 2 contacts in V606M simulations (**Figure 2-2F**). This analysis showed that there are intramolecular pathways where each of these mutations changes the allostery of and contacts formed by loop 2.

These two mutations represent a framework to study the role of not only the positive charges in loop 2 but the dynamic movement of these charges and the conformational states populated by the motion and coiling of loop 2. We hypothesize that the conformational ensemble sampled by loop 2 plays a critical role in regulating actomyosin complex formation and that E525K and V606M both alter loop sampling. In turn these changes to Loop 2 conformation may result in changed electrostatic interaction between myosin and actin observed in both mutations.

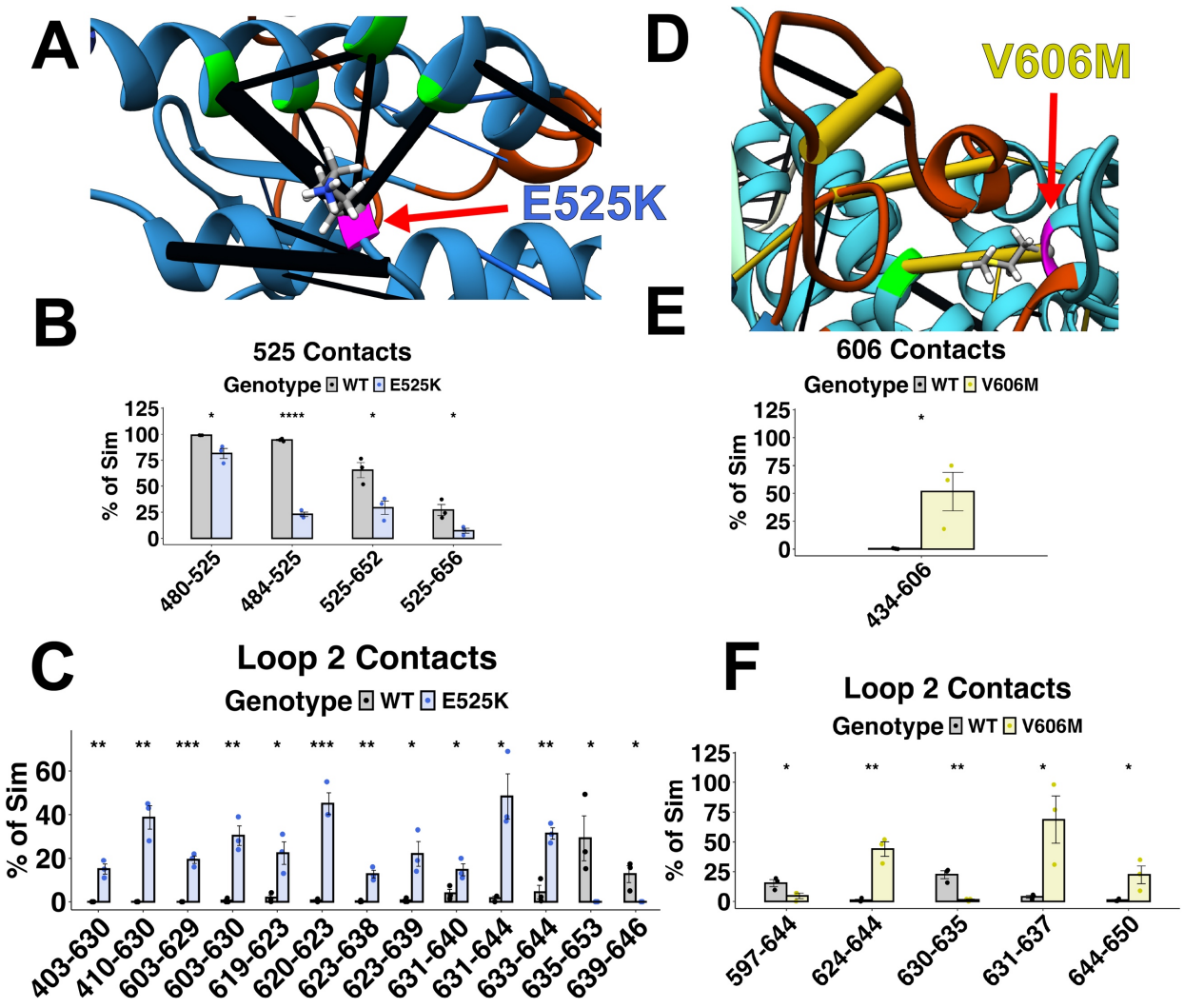

Figure 2-2: The allostery of myosin's loop 2 is disrupted by the E525K and V606M mutations.

(A) Zoomed in contact pair image of residue 525 in myosin showing how the E525K charge change disrupts key salt bridges on adjacent helices. Blue bars indicate increased contact time and black bars indicate decreased contact time compared to WT. (B) Quantification of contact pairs involving residue 525 during the WT (black) and E525K (blue) simulations. (C) Quantification of altered contact pairs involving loop 2 during E525K simulations compared to WT simulations. (D) Zoomed in in contact pair image of residue 606 showing how the V606M mutation forms a hydrophobic interaction with residue 434. Yellow bars indicate increased contact time and black bars indicate decreased contact time compared to WT. (E) Quantification of contact pairs involving residue 606 during the WT (black) and V606M (yellow) simulations. (F) Quantification of changed loop 2 contact pairs during V606M simulations compared to WT simulations. Contact pairs that were present for significantly ($p < 0.05$, two-tailed Student's t-test) more or less time than WT simulations are depicted. The pseudo-bond radii are proportional to the difference in contact time: thicker pseudo-bonds correspond to greater contact populations.

The E525K and V606M Mutations Shift Loop 2 Towards the Actin Binding Cleft

Loop 2 sampled many different conformational states during the 500 ns simulations. To identify and compare characteristic conformations (representative states) observed for WT and mutant myosin we performed principal component analysis (PCA), focusing on the Cartesian coordinates of the C_α atoms for each amino acid within loop 2. This dimensionality reduction allowed us to group similar structures along the different principal components. Principal component 1 (PC1) explained 45% of the observed variance and separated most mutant simulations from WT simulations, except for one V606M simulation. PC2 and PC3 did not show separation of WT and mutant simulations but described distinct types of loop 2 movement (**Figure 2-3A**). The contribution of each residue's Cartesian coordinate to each principal component helps to explain the dynamic way in which these two mutations changed the conformational state space occupied by loop 2. PC1 was dominated by a negative shift in the x-coordinate of loop 2 C_α positions. This represents a movement of loop 2 parallel to the HLH motif and actin binding surface (**Figure 2-3B**). Since this principal component separates most mutant from WT simulations it appears that both mutations led to loop 2 spending more time near the tip of the 50 kDa domain and the actin binding cleft. PC2 is dominated by a positive shift in the y-coordinate of the loop 2 C_α position associated with movement that was orthogonal to the HLH motif and actin binding surface (**Figure 2-3C**). Notably V606M simulations separated from the WT and E525 structures along this axis. Finally, PC3 is made up of a negative shift in some loop 2 C_α coordinates and a positive shift in other loop 2 C_α coordinates describes a twisting of the flexible loop 2 structure (**Figure 2-3D**).

These results demonstrate a method for quantifying the movement of loop 2 through time during MD simulations and show how two different myosin mutations, on either side of loop 2, can have similar allosteric impacts on its movement. They also suggest how these allosteric changes in loop 2 impact the presentation of loop 2's positive charges and may be important for actomyosin

complex formation. As such, this result promoted a much deeper analysis of how loop 2 coils and twists during simulations of pre-powerstroke myosin.

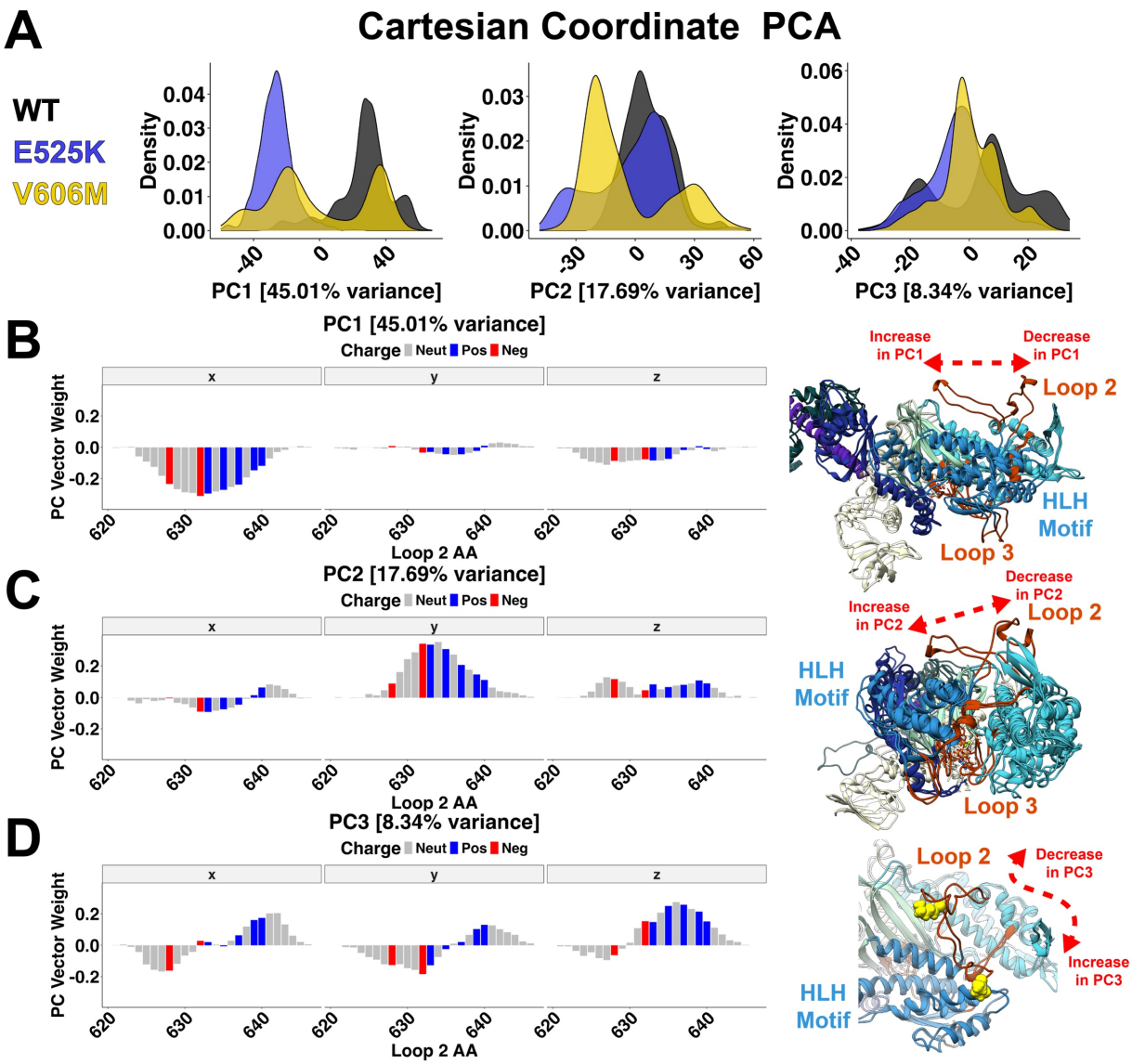

Figure 2-3: Movement of loop 2 is shifted towards the actin binding cleft by the E525K and V606M mutations.

(A) Principal component analysis of loop 2 C_α position during 3 replicate simulations of each genotype showing mutant vs. WT separation primarily along PC1 with some contributions from PC2 and PC3. (B-D) Principal component weight analysis (left) with representative (min and max PC weight) structures from one WT simulation (right). PC1 (B) describes waving of loop 2 in the x direction (left) representing movement along the myosin head (right). PC2 (C) describes waving of loop 2 in the y direction (left) representing movement up and down between the 50 kDa domains (right). PC3 (D) describes twisting of loop 2 in x, y, and z (left) describing twisting of loop 2 (right).

Expanded Conformations of Loop 2 Favor Actin Binding

Thus far, simulations demonstrated that loop 2 was responsible for changed electrostatic interactions with the E525K and V606M mutations and, in turn, these mutations changed the position of loop 2 in similar ways. We next investigated how the specific conformation of loop 2 may change the presentation of positive charges in the loop. We correlated the distance between the center of mass of positive charges in loop 2 and negative charges the N-terminus of actin (spheres in **Figure 2-4A**) with the binding force calculated for the whole myosin S1 head (**Figure 2-4B**). This correlation showed that the position of loop 2 alone explains 62% of the calculated binding energy for the whole myosin S1 head. Additionally, single timesteps from E525K simulation 2 and V606M simulation 3 can be seen that occupy conformations with very low distances and very high forces.

Loop 2 is long and flexible enough that it can form both interactions with itself and interactions with other myosin domains. To compare more compact vs more extended conformations of loop 2, we performed dihedral angle principal component analysis (PCA) on the backbone (ϕ/ψ) dihedral angles along loop 2. In comparison to the C_α PCA discussed earlier, this analysis used an internal reference frame within loop 2's structure, enabling a deeper analysis of internal versus overall motion in the ensembles sampled by loop 2. Results of this dihedral angle analysis showed that each simulation formed a dense cluster in PC space. Notably, E525K simulation two and V606M simulation three formed a less dense cluster near each other and away from all other simulations (**Figure 2-4C**). This indicates that these mutations may alter the conformational state space occupied by loop 2, populating conformations that are never or seldom seen in the WT structures.

The importance of these different conformational states can be seen by mapping the distance and force values calculated earlier onto the dihedral angle PCA plot (**Figure 2-4D & E**). Most simulations are tightly clustered with themselves and occupy high distance, low force conformations for most of the simulation time. However, the less dense cluster formed by E525K

simulation two and V606M simulation three contains simulation timesteps with unusually small distances between loop 2 and actin's N-terminus (**Figure 2-4D**) and unusually high electrostatic force (**Figure 2-4E**).

K-means clustering was used to define four conformational states that were occupied by loop 2 during these nine simulations (**Figure 2-4F and Supplemental Figure 2-4A**). The optimal k-value for clustering was based on the elbow point in the inertia plot of within-cluster sum of squares (**Supplemental Figure 2-4B**). By plotting the distance (**Figure 2-4G**) and force (**Figure 2-4H**) calculated earlier for each timestep within a cluster, we can see that cluster three stands out with significantly lower distance and significantly higher force compared to all other clusters. The mechanism behind this difference is elucidated by representative structures from each of the other clusters (**Figure 2-4I**). Structures from cluster one and cluster two formed helical twists where loop 2 interacted with itself. This twisting sequestered the positive charges in loop 2 away from the actin binding cleft and the negative charges present in the N-terminus of actin. Notably, timesteps from WT simulations made up the majority of these two "unfavorable actin-binding" states. The representative structure from the less dense cluster three was expanded, not twisted and shifted towards the actin binding surface and the HLH motif. This expanded state moved the positive charges in loop 2 much closer to the negative charges in actin's N-terminal domain and represents a "favorable actin binding" state. Finally cluster four was also expanded but here loop 2 was not shifted directly toward the myosin binding surface and we observed only a modest increase in binding force for this cluster (**Figure 2-4H**). Importantly both expanded, "favorable actin-binding" states identified here were populated almost exclusively by mutant (E525K or V606M) simulations.

These results collectively demonstrate that conformational states of loop 2 (defined by dihedral angles) when combined with electrostatic modeling can predict myosin's affinity for actin. These findings also underscore loop 2's significant role in regulating actomyosin cross-bridge formation and clearly illustrate how mutations near loop 2 can allosterically influence its

conformation, consequently affecting myosin's binding affinity for actin. The ability of loop 2 to sample conformations that have variable long-range electrostatic interactions with actin may play an important regulatory role in myosin activation, and here are demonstrated to be causal in the increased actin affinity observed in two cardiomyopathy mutations.

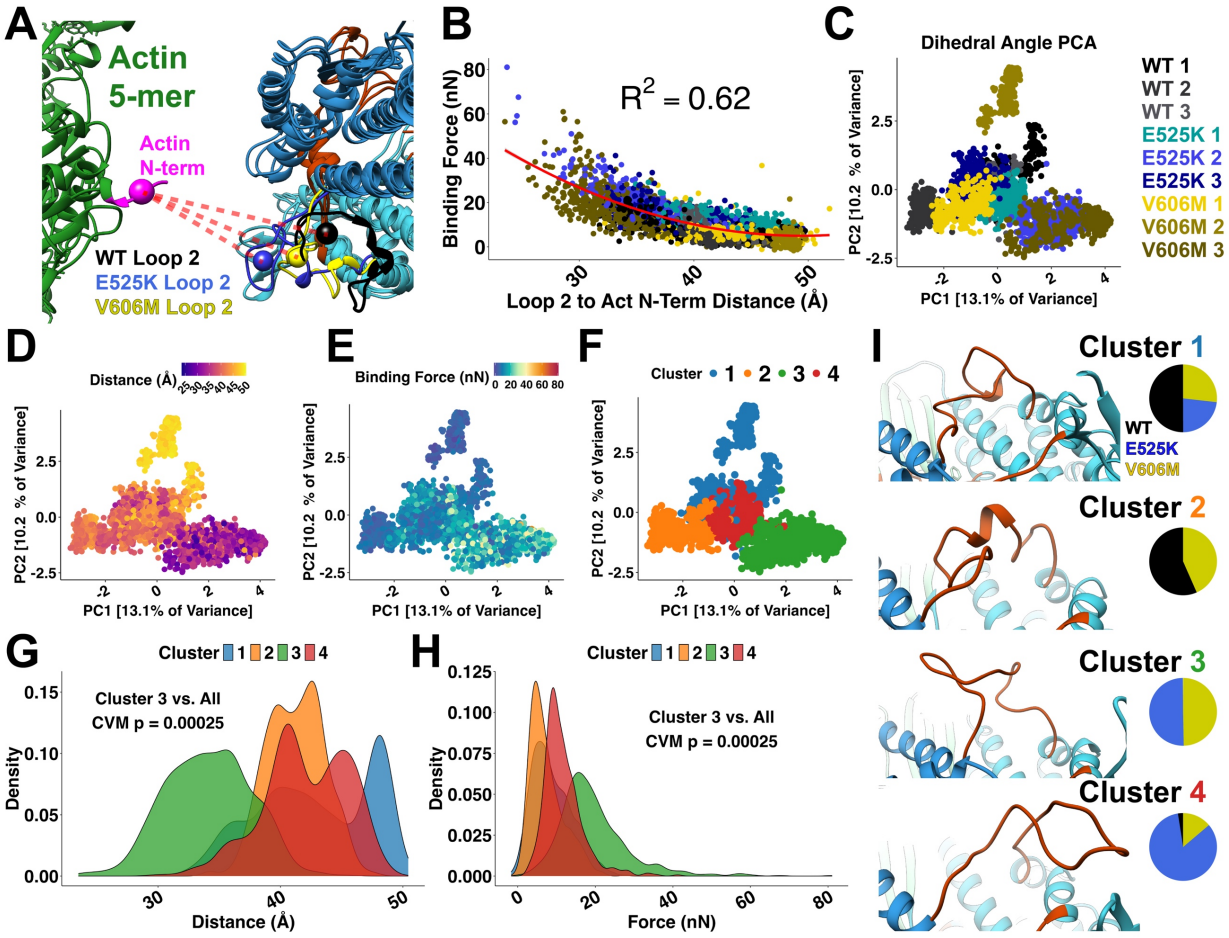

Figure 2-4: Dihedral angle analysis identifies loop 2 condensed and expanded states which regulate electrostatic binding energy.

(A) Alignment of myosin 30 Å from its binding site on actin used for *DelPhiForce* electrostatic calculations. The center of mass is indicated for the negative charges on the actin N-terminus (pink sphere) and the positive charges in loop 2 (black-WT, blue-E525K, and yellow-V606M spheres). (B) The relationship between distance (spheres in A) and calculated force is fit with a second order exponential. (C) Principal component analysis of loop 2 dihedral angles during 3 replicate simulations of each genotype. E525K Sim 2 and V606M Sim 3 can be seen forming a dispersed cluster distal from all other simulations. (D) Distance and (E) force mapped onto the dihedral angle PCA clusters. The dispersed cluster of E525K Sim 2 and V606M Sim 3 contains structures with unusually low distances and unusually high forces. (F) K-means clustering on the dihedral angle PCA identified 4 clusters. (G) Density of distance values (spheres in A) measured within each cluster. Cluster 3 shows a significant shift towards lower distances between loop 2 and the actin n-terminus. (H) Density of force values calculated within each cluster. Cluster 3 shows a significant shift towards higher binding energy states—representing a shift to a pro-actin binding

conformational state of loop 2. A Cramer Von Mises Test (CVM) was used to test for differences in the distribution of distance and force. (I) Representative structures and genotypic make up for each cluster. Representative structures were selected as those that most closely matched the mean force value calculated within each cluster.

Discussion

Loop 2 Electrostatically Mediates Actomyosin Interaction. Protein loops are often regulators of function and enzymatic activity in biological systems,(Gu et al. 2015; Malabanan et al. 2010) and structural disorder of a loop often imparts functional benefits(Berlow, Dyson, and Wright 2015). Spudich and coworkers established that changes in the sequence, length, and charge of loop 2 affects actin-myosin kinetics(Goodson, Warrick, and Spudich 1999) as well as ATPase activity(Murphy and Spudich 1999; Uyeda et al. 1994). While these vary substantially across myosin classes, loop 2 consistently demonstrates impact on actin-myosin association for many myosins. Yu *et al.* used AI-generated models and MD simulations of myosin to explore the relationship between loop 2 length and actomyosin interaction(Yu, Park, Ryu, et al. 2024). They report that longer loop 2 isoforms formed a more complex salt bridge network (involving actin's N-terminus and a hairpin turn in actin subdomain 1) than did short loop 2 isoforms (few to no interactions with actin's N-terminus) in strongly-bound states(Yu, Park, An, et al. 2024). Yengo and Sweeney studied variants of the processive myosin V(Yengo and Sweeney 2004). They observed that changing the charge on loop 2 modified the kinetics of actin-myosin binding with fewer effects on other steps of the cycle. They also postulated that the length and charge of loop 2 is essential for the processive properties of myosin V. Elfrink *et al.* studied the single-headed, processive type IX myosin that contains a >100 residue insertion in loop 2(Elfrink et al. 2014). They found that deletion of the loop 2 insertion or increased ionic strength diminishes processive behavior. Prior studies from this group also show that loop 2 assists with the directionality required for processive motion in a single headed myosin(Liao, Elfrink, and Bähler 2010). Onishi *et al.* tested the molecular mechanisms by which mutations in loop 2 affect actin-activated ATPase and speculate that charged residues in loop 2 contribute to complex formation and that hydrophobic residues contribute to the coupled process of myosin cleft closure and phosphate release(Onishi et al. 2006). Thus, across multiple myosin isoforms, loop 2 is shown to have a net positive charge,

a role in mediating actin-myosin association, and a substantial impact on cross-bridge cycling kinetics.

To date, few studies have explored the relationship between loop 2 structure and actin-myosin association(Clobes and Guilford 2014:2; Murphy and Spudich 1999). This is due to the intrinsic structural disorder in the loop. Dynamic regions of proteins do not resolve well in X-ray and cryoEM structures. While loop 2 is generally unresolved in X-ray structures of myosin alone, fragments of loop 2 are frequently observed in some cryoEM structures of the actomyosin complex. Doran *et al.* solved cryoEM structures of force-bearing-like conformations of human cardiac actomyosin(Doran, Rynkiewicz, Rasicci, et al. 2023) and their structures show residues F644-K639 interacting with the D24-D25 hairpin turn of actin. Risi *et al.* detail how changes in the length of loop 2 across myosin isoforms affects its resolution in cryoEM structures, with shorter loops being better resolved. However, N-terminal residues of actin may also not resolve in cryoEM, leaving the possibility of a 'fuzzy cloud' of disordered interactions(Risi et al. 2021). In a recent study, Klebl *et al*. collected cryoEM structures of the weakly-bound, primed actomyosin complex using a myosin-V construct with mutations near the phosphate 'back door' and deletions in loop 2 that slow the phosphate release step(Klebl et al. 2025). Their structure shows the C-terminal end of loop 2 sandwiched between the negatively charged hairpin turn and N-terminus of actin. Together these studies provide strong evidence that loop 2 interacts electrostatically with actin in both weakly-bound and strongly bound states. However, no studies have resolved the full structure of loop 2 and none indicate the structural mechanisms through which loop 2 mediates actomyosin association. The formation of a weakly-bound crossbridge leads to stronger binding that is needed for force generation and shortening in the sarcomere as interaction between myosin and actin facilitates the lever arm swinging. The simulations performed here contain the full structure of loop 2 and our models show that loop 2 structure interconverts among multiple conformations on nanosecond timescales (**Figure 2-3**). *DelphiForce* measures indicate that loop 2 contributes meaningfully to the electrostatic association force between actin and myosin (**Figure**

2-1) and that neutralization of loop 2 charged residues diminishes this force (**Supplemental Figure 2-3**). Finally, our conformational analysis of loop 2 showed that loop 2 can sample compact conformations with unfavorable anti-binding properties and more extended conformations that favor actin binding (**Figure 2-4**). These data suggest that the conformational ensemble that loop 2 samples can regulate a key step leading to contractions by modulating initial crossbridge formation. Our results provide a model wherein the coiling of loop 2 serves as a regulatory axis for the number of crossbridges formed and force generation within the heart (**Figure 2-5**).

Links Between Conformational Shifts in Loop 2 and Cardiomyopathy. Over 1000 mutations in human striated muscle myosis are associated with disease(Parker and Peckham 2020). This includes several mutations within loop 2 of β-cardiac myosin (e.g. K637E(Møller et al. 2009) and K639E(van Waning et al. 2018) are associated with dilated cardiomyopathy; G636S(Homburger et al. 2016) and S642L(Daehmlow et al. 2002) are associated with hypertrophic cardiomyopathy). The E525K and V606M mutations studied here are not found in the loop 2 sequence and are instead located on either “side” of this loop (**Figure 2-1A**). However, our results show that these mutations can result in structural changes that affect the conformational ensemble sampled by loop 2 (**Figure 2-2**). Our current findings represent an atomistic mechanism behind the increased actin affinity observed in both cardiomyopathy mutations. Other cardiomyopathy mutations or myosin binding drugs may alter the conformational sampling of loop 2. For example, we reported similar allosteric effects on loop 2 for the small molecule 2’-doexy-ATP when it is in the nucleotide binding pocket of myosin, resulting in enhanced binding to actin(Childers et al. 2021; Ma et al. 2023; Nowakowski et al. 2017; Teitgen et al. 2024). Thus, loop 2 coiling may represent an important modality for understanding myosin function and we have developed methods this in the context of cardiomyopathy linked mutations that could easily be expanded to include other mutations and to study small molecules for drug development.

Computational Predictions from Disordered Data. Simulation to simulation variability and disordered dynamics are dual features and limitations of atomic scale simulations. The intrinsic disorder of loop 2 prevents its full resolution in X-ray crystal structures and leads to high variability within and between computational simulations. While our simulations allowed for an overview of loop 2 movement and generated insights into how mutations may influence loop 2 dynamics, they do not exhaustively sample the conformational space of loop 2 (i.e. *the sampling problem*(Childers and Daggett 2018)*)*. As illustrated here, even conformations of this loop that are transiently sampled can have dramatic impacts on myosin function. Less compact, more extended conformations of loop 2 are more structurally variable but may increase the probability of an association event between actin and myosin via the 'fly casting mechanism'(Shoemaker, Portman, and Wolynes 2000) of intrinsically disordered protein regions. Despite the *sampling problem* our work shows a strong correlation between the orientation of loop 2 and the associative force between actin and myosin prior to weak binding. Our simulations suggest molecular mechanisms by which certain disease-associated mutations affect cross-bridge cycling. Future efforts should use longer myosin simulations or enhanced sampling strategies to better assess loop 2 conformational space. Loop 2 is also known to have a structural role in cross-bridge cycling kinetics. Simulations like those performed here should improve our understanding of the functional roles of loop 2.

While our simulations are imperfect and incomplete, they are useful to serve for generating hypotheses for future exploration. First, loop 2 may act as an electrostatic 'tractor beam' to guide myosin motors toward their binding sites on the thin filament. Second, the disorder of loop 2 may allow it to moonlight in several roles with different behaviors in unbound, strongly-bound, and weakly-bound conformations(Berlow et al. 2015; Uversky 2016). Finally, prior simulations and structures indicate that loop 2 can form interactions between myosin heads in the interacting heads motif state(Childers et al. 2024) and it remains to be seen whether these interactions meaningfully contribute to IHM stability, and consequently thick-filament regulation. As the next

generation of myosin targeting drugs are developed, their intended or unintended allosteric effects on myosin structures such as loop 2 should be considered. At the molecular level myosin targeted compounds alter myosin's function allosterically. The present study has clearly shown that allosteric effects can propagate through myosin and alter the coiling of loop 2 to changing the affinity of myosin for actin. Drugs that directly interact with myosin have the potential to target heart disease at a mechanistic level of individual proteins, which is very exciting. As the importance of loop 2 conformational dynamics is recognized, identifying the mutations and molecules that change loop 2 kinetics through local and long-range effects is critical and the work presented here defines a paradigm for this analysis.

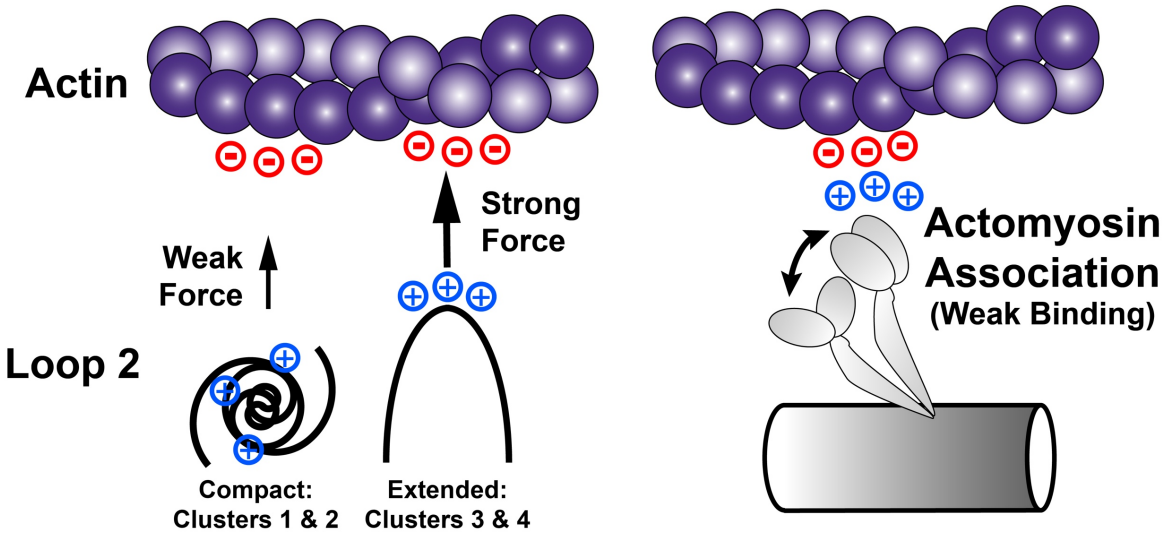

Figure 2-5: A model for the regulatory role of loop 2 in myosin activation.

The loop 2 structure of myosin adopts compact semi-stable conformations where the positive charged residues in loop 2 are sequestered away from their negatively charged binding partners on the N-terminal domain of actin. Loop 2 can adopt extended less-stable conformations where these same positive changes are available to interact with actin. Here two cardiomyopathy mutations that increase myosin molecules' affinity for actin were shown to disrupt loop 2 coiling demonstrating a mechanism for this regulatory role of loop 2 in disease progression.

Acknowledgements

This research was supported by the University of Washington Center for Translational Muscle Research (CTMR) via the National Institute of Arthritis and Musculoskeletal and Skin Diseases of the National Institutes of Health award nos. P30AR074990 and R01HL128368 to M.R. and award nos. NHLBI R01 HL141187, HL142624, and HL162229 to JD. MCC was supported by grants T32HL007828 and K99HL173646 from the National Heart, Lung, and Blood Institute. The content is solely the responsibility of the authors and does not necessarily represent the official view of the NHLBI or the NIH.

Conflicts of Interest

The authors have no financial conflicts of interest that may be construed to these data.

Author Contributions

Conceptualization – MCC MR

Methodology – MCC

Project Administration – MR JD

Resources – MR JD

Supervision – MCC MR JD

Visualization – KZR KJF RS

Original Draft Preparation – KZR

Review and Editing – KZR KJF MCC MR JD

Data Curation – KZR MCC

Formal Analysis – KZR MCC KJF RS

Funding Acquisition – MR JD MCC

Investigation – KZR MCC

Methods

Model Preparation

Homology models of pre-powerstroke (M.ADP.P_i) human cardiac myosin (gene: MYH7) were prepared with *Modeller*(Eswar et al. 2006) using the a bovine cardiac myosin structure as a template. The template structure was the 2.45 Å X-ray crystal structure of bovine cardiac β-myosin in complex with the essential light chain, ADP, vanadate, and Mg^{2+} solved by Planelles-Herrero *et al*. (PDB: 5N69) (Planelles-Herrero et al. 2017). Crystallographic waters and other molecules were removed. Trimethylated lysine residues were converted to lysine. The X-ray study by Planelles-Herrero *et al*. included a complementary structure of pre-powerstroke myosin in the absence of OM, but residues in the tail and ELC were not resolved (PDB: 5N6A), so we used the OM-bound structure to generate our model but removed OM prior to model generation. The bovine ELC found in 5N69 was similarly used as a template for the human ELC. HIS protonation states at pH 7.0 were predicted using the *H*++ webserver (Anandakrishnan, Aguilar, and Onufriev 2012). Structures of the E525K and V606M myosin were generated by computationally introducing mutations into the modeled structure. This yields three separate all-atom molecular systems: WT, E525K, and V606M myosin all containing ADP.Mg^{2+}.Pi in the active site and all in complex with ELC.

Molecular Dynamics Simulation

The resulting systems were prepared for molecular dynamics simulation using the Amber 20(Case et al. 2023) simulation package and the ff14SB force field(Maier et al. 2015). Water molecules were treated with the TIP3P force field(Jorgensen et al. 1983). Metal ions were modeled using the Li and Merz parameter set(Li and Merz 2014; Li, Song, and Merz 2015a, 2015b). ADP and Pi (modeled as H_2PO_4)(Kiani and Fischer 2014) molecules were treated with the GAFF2 force field(He et al. 2020). Partial charges for ADP and P_i were derived from a

restrained electrostatic potential (*resp*) fit to quantum mechanics calculations performed with ORCA(Neese et al. 2020). The SHAKE algorithm was used to constrain the motion of hydrogen-containing bonds(Miyamoto and Kollman 1992). Long-range electrostatic interactions were calculated using the particle mesh Ewald (PME) method. Hydrogen atoms were modeled onto the initial structure using the *leap* module of *AMBER,* and each protein was solvated with explicit water molecules in a truncated octahedral box and neutralizing counterions were added. Each system was minimized in three stages. First, hydrogen atoms were minimized for 1000 steps in the presence of 100 kcal/mol restraints on all heavy atoms. Second, all solvent atoms were minimized for 1,000 steps in the presence of 25 kcal/mol restraints on all protein atoms. Third, all atoms were minimized for 8,000 steps in the presence of 25 kcal/mol restraints on all backbone heavy atoms (N, O, C, and C_α atoms). After minimization, systems were heated to 310 K using the NVT (constant number of particles, volume, and temperature) ensemble and in the presence of 25 kcal/mol restraints on backbone heavy atoms. Next, the systems were equilibrated over five successive stages using the NPT (constant number of particles, pressure, and temperature) ensemble. During the first four stages, the systems were equilibrated for 5 ns in the presence of 25 to 1 kcal/mol restraints on backbone heavy atoms. During the final equilibration stage, the systems were equilibrated for 5 ns in the absence of restraints. A 10 Å nonbonded cutoff was used for all preparation and production simulations. Separate equilibrations were run for replicate simulation for each genotype. The equilibrated systems were then simulated using conventional molecular dynamics protocols in the NVT ensemble in triplicate for 500 ns each (3 systems, three replicate simulations per system, 500 ns sampling per replicate simulation = 4.5 μs total sampling) and coordinates were saved every 10 ps.

DelPhiForce Calculations

To assess the impact of loop 2 residue variations on electrostatic interactions, we employed *DelPhiForce*(Li, Jia, et al. 2017; Li, Chakravorty, et al. 2017) to compute the

electrostatic binding forces between representative timeframes extracted from MD simulations and a pre-equilibrated actin pentamer derived from the 8EFH PDB structure(Doran, Rynkiewicz, Rasicci, et al. 2023). *DelPhiForce* calculates electrostatic forces by numerically solving the Poisson-Boltzmann (PB) equation, which accounts for the distribution of ions and the dielectric properties of the solvent and protein. This approach allowed us to determine the electrostatic contributions to the interaction energy between the loop 2 variants and the actin pentamer, providing insights into how residue substitutions modulate binding affinity.

Alignment of myosin with actin in a pre-weakly bound sate was achieved using a reference structure of the human cardiac actin-tropomyosin-myosin complex in complex with ADP-Mg2+ (PDB: 8EFH). All alignments were generated using the MatchMaker function in Chimera (UCSF). An equilibrated actin pentamer was aligned to actin such that the central actin monomer was interacting with myosin. Frames from each simulation (with a resolution of 1 frame/ns) were then aligned to actin using the 8EFH reference. Importantly the reference structure represents a strongly bound actomyosin complex. To generate a weakly bound conformation myosin structures from MD simulation were only aligned to the HLH motif of the reference structure (residues 515-550 and 530-553 respective). Myosin was then shifted 30 Å away from action to simulate pre-binding conditions. To achieve this a plane of actin and myosin interaction was defined by the list of clashing atoms between the two molecules. Myosin was then shifted 30 Å normal to this plane away from actin. This alignment can be seen in **Supplemental Figure 2-3**. Protein structures were prepared for electrostatic modeling using *DelPhiPka* (Wang, Zhang, and Alexov 2016) and *DelphiForce* was used to calculate electrostatic binding force. Default parameters were used for all *Delphi* programs.

Molecular Dynamics Analyses

Dihedral angles were calculated for every residue in loop 2 in every timestep of every simulation using the *cpptraj* command *multidihedral* for residues 615-651. Based on resulting Ramachandran coverage loop 2 was defined as residues 621-646 (**Supplemental Figure 2-2**).

The center of mass of the positively charged Lys residues in loop 2 was calculated using the *cpptraj* command *vector* to identify the center of mass for the C_α of residues 633, 635, 637, and 639 (**Figure 2-4A**). The location of the center of mass of the negatively charged N-terminal residues in the actin molecule used was calculated using the *define centroid* command in *Chimera* based on the C_α of residues 2-5. Finally, *cpptraj* and the *contacts* command was used to calculate the contact pairs for each residue in myosin simulations. Two residues were considered in contact with one another if at least one pair of heavy atoms were within 5 Å of one another.

Principal Component Analysis of Loop 2 C_α Position and Loop 2 Dihedral Angles

Principal component analysis was used to define loop 2 position and coiling as previously described(Childers, Towse, and Daggett 2016, 2018; Palma and Pierdominici-Sottile 2023). Briefly, to account for movement of the myosin molecules during simulation, all myosin molecules used for analysis (1 frame/ns from each simulation) were aligned to their 50 kDa domains (residues 215-231, 266-453, 604-621, 645-665, 472-590). The C_α position of each residue as well as the dihedral angels of each residue in loop 2 was then extracted from the simulations (residues 621-646). These data were then used for PCA analysis. For the dihedral angle PCA the first 100 ns (100 frames) of each simulation were omitted to allow the simulations to acclimate as they were highly variable. Additionally, the four glycine residues in loop 2 were omitted (residues 626, 634, 636, 641) since glycine dihedral angels are extremely variable. Additionally, the dihedral angle PCA was performed on the sin() and cos() components of the phi/psi dihedral angles to avoid circular statistics as previously described(Altis et al. 2007). All frames/timesteps and all loop 2 residues were used for the Cartesian coordinate C_α PCA analysis.

Supplemental Figures

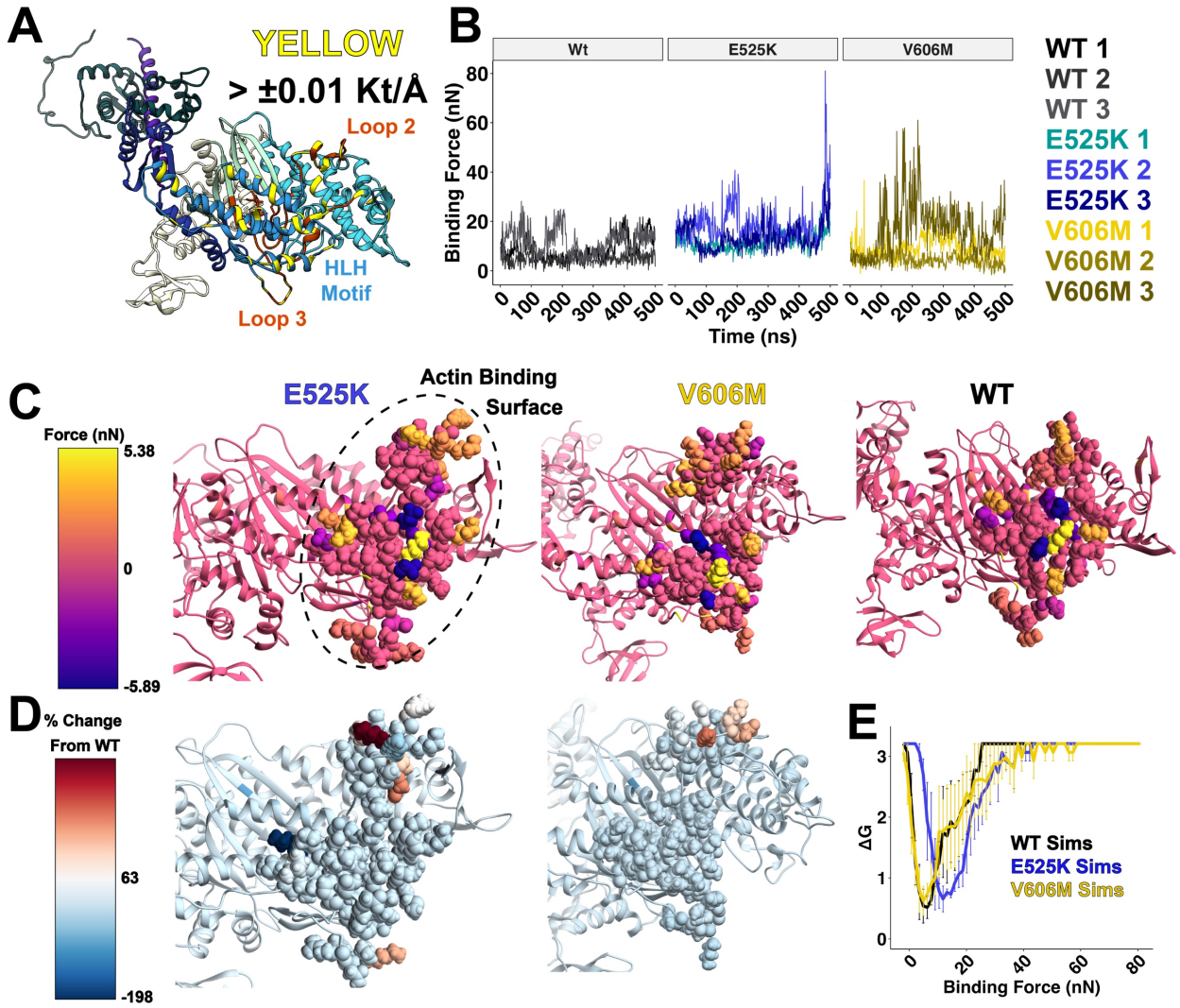

Supplemental Figure 2-1: Binding force felt by each residue in the actin binding surface.

(A) Pre-powerstroke human β-myosin S1 head where residues that experienced > ±0.0 kT/Å during any (WT or Mutant) *DelPhiForce* simulation are highlighted in yellow. Key charged residues in the actin binding surface can be seen including the HLH motif, loop 2, loop 3, and the strut. (B) Binding force calculated with DelphiForce across simulation time in each of three replicate simulations of each genotype. (C) Myosin S1 actin binding surface colored by average binding energy felt at that residue during three replicate simulations. Loop 2, loop 3, and the HLH motif are depicted with a space filling model to highlight the changes in these areas. (D) Myosin S1 actin binding surface depicted as in C but colored by percent change in average binding force felt by that residue when compared to WT simulations. (E) Boltzmann free energy distribution showing the distribution of WT, E525K, and V606M simulations that sample different binding energies for the whole myosin S1 head.

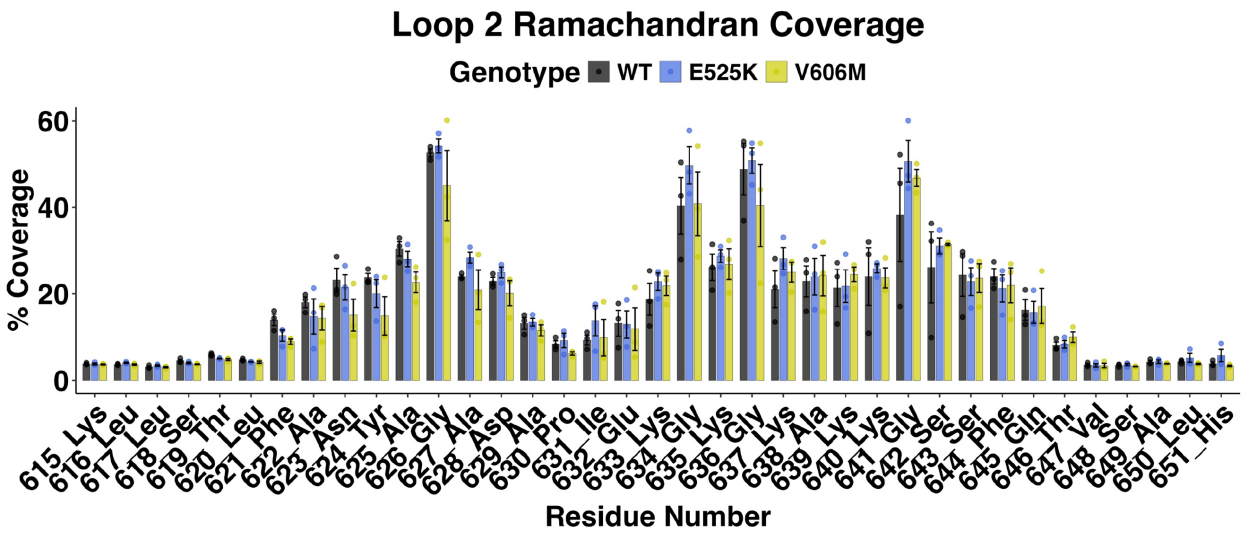

Supplemental Figure 2-2: Identification of loop 2 residues in simulation

Dihedral angles were recorded for resides in the vicinity of loop 2 for each simulation. Loop 2 was defined for all myosin molecules in all simulations as residues 621 to 646 due to the increase in Ramachandran plot coverage in this region.

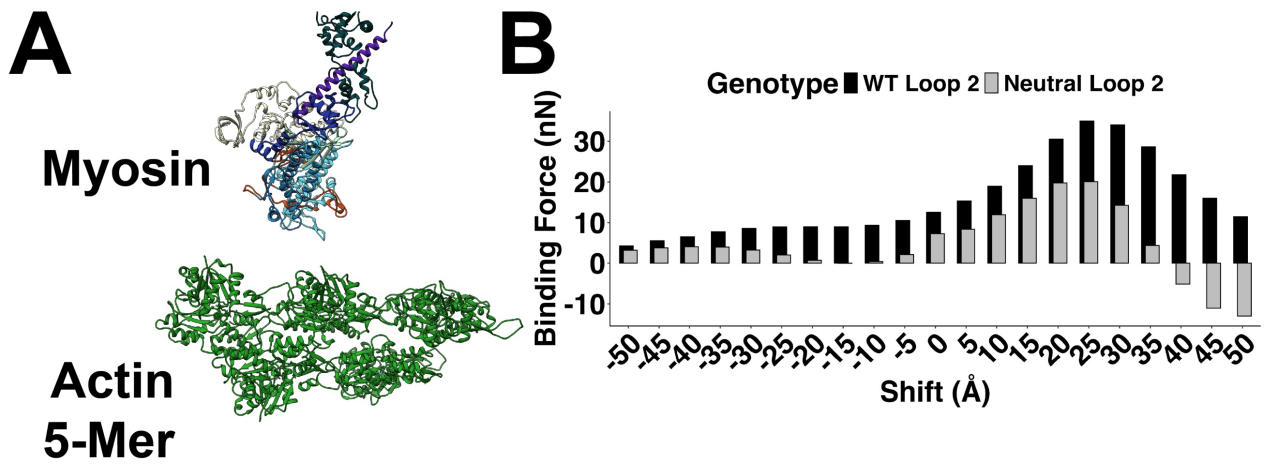

Supplemental Figure 2-3: Setup of *DelPhiForce* simulations and validation of *DelPhiForce*

The alignment of myosin and actin was achieved as discussed in the methods section. (A) A depiction of the alignment of a WT myosin S1 head 30 Å from its binding site on an actin 5-mer. (B) To confirm that the *DelPhiForce* tool would model electrostatic interactions between myosin and actin a test simulation was run where a WT myosin S1 head was shifted along the axis of actin and the binding force was calculated after each 5 Å shift (black in B). Additionally, to confirm this tool could identify the electrostatic force generated by the charged lysine residues of loop 2 these residues were computationally changed to glutamine residues (630, 632, 634, 636, and 637). A reduction in the binding force between myosin and actin can be seen when the lysine residues of loop 2 are neutralized (gray in B).

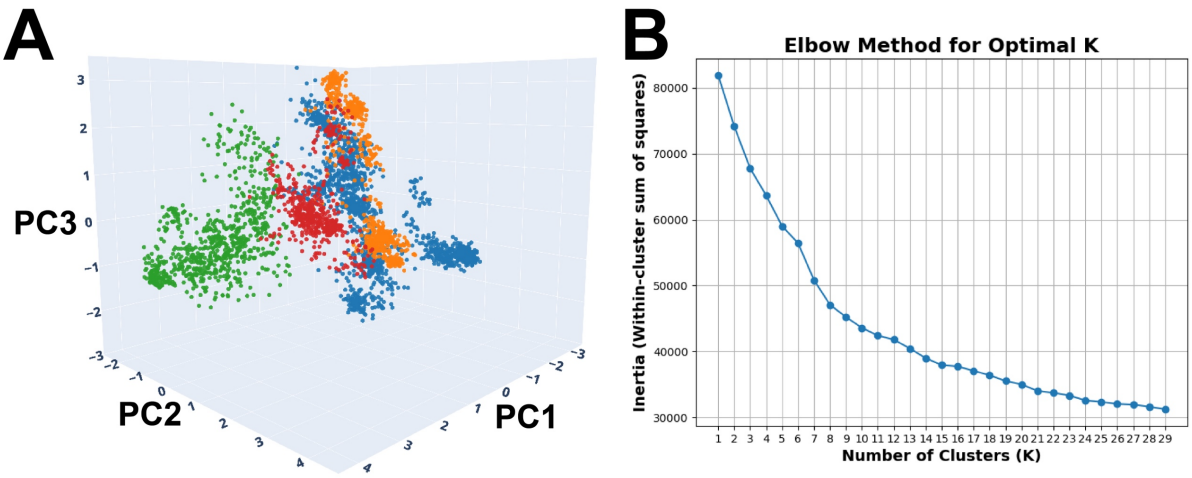

Supplemental Figure 2-4: K-means clustering of loop 2 dihedral angle PCA and loop 2 secondary structure

(A) 3D depiction of the four clusters identified showing distinct grouping of clusters. (B) Inertia plot (within-cluster sum of squares) used to determine optimal number of clusters for k-means analysis.

Chapter 3 — Effect of The E525K Myosin Mutation on The Myofilament: Understanding Hypocontraction and Hypercontraction

Kalen Z. Robeson[1,2,3], Tim McMillen[1,2,3], Kristi Kooiker[1,2,3], Kerry Kao[1,2,3], Kieran Fruebis[1,2], Rachelle Soriano[3,4], Andrew P. Wescott[3,5] Jennifer Davis[1,2,3], Michael Regnier[1,2,3]*

1. Department of Bioengineering, University of Washington, Seattle, WA, USA
2. Center for Translational Muscle Research, University of Washington, Seattle, WA, USA
3. Institute For Stem Cell and Regenerative Medicine, University of Washington, Seattle, WA, USA
4. California State University, Los Angeles, CA, USA
5. Division of Cardiology, University of Washington, Seattle, WA, USA

*Corresponding Author

Email: mregnier@uw.edu

Phone: 206-221-0504

Abstract

The *de novo* myosin mutation E525K was identified in 2012 in a single patient diagnosed with dilated cardiomyopathy (DCM). Recent work on isolated engineered myosin constructs has led to the hypothesis that this mutation has two main effects: (1) stabilization the interacting heads motif (IHM) and (2) increasing myosin ATPase activity of isolated S1 heads. This ultimately leads to hypocontractility due to impaired myosin recruitment and, perhaps, faster crossbridge cycling. Here, we present the first force and contractility measurements from human induced pluripotent stem cell (hiPSC)-derived cardiomyocytes (CMs) carrying the heterozygous E525K mutation.

These cells were generated on the WTC11 background with a green fluorescent protein (GFP) tag on α-actinin. Our data revealed a 65% reduction in sarcomere contraction in single E525K/WT cells and a 39% decrease in maximal twitch force in engineered heart tissues (EHTs). Paradoxically, isolated myofibrils showed a 45% increase in peak force under high calcium stimulation (pCa 4.0). To validate these findings, we introduced the E525K mutation into a different hiPSC genetic background (the UC2 background), generating wild-type, heterozygous, and homozygous lines. This confirmed reduced force generation at the tissue level in a stepwise manner (WT/WT > E525K/WT > E525K/E525K). However, myofibrils from these new lines also showed decreased force, mirroring the EHT results. Interestingly, we observed no change in contractile kinetics, suggesting no alteration in myosin cycling rate under loaded conditions, which contrasts with previous findings in isolated myosin. This difference may be due to changes in myosin function under loaded conditions. Our results highlight the critical need for comprehensive biochemical and biophysical investigations of myosin mutations and emphasizes the importance of understanding the interplay between the myosin chemomechanical cycle and myosin recruitment in disease pathology and therapeutic development.

Introduction

The heterozygous E525K mutation in MYH7 was identified in 2012 through a genetic screen of patients with dilated cardiomyopathy (DCM). It was found in one patient diagnosed with DCM but the mechanism though which this mutation might cause a contractile deficit and a DCM phenotype remained unclear (Lakdawala et al. 2012). More recently studies have used isolated myosin constructs to study the biochemical properties of myosin carrying the E525K mutation. These studies have given the first insight into how this mutation may be changing recruitment of myosin (Rasicci et al. 2022), as well as the activation and cycling of myosin heads (Bodt et al. 2024; Duno-Miranda et al. 2024).

So far it has been shown that the E525K mutation increases the actin dependent ATPase activity of myosin S1 heads (which cannot form the auto-inhibited OFF state of myosin) but decreases the ATPase activity of myosin HMM constructs (which can self-inhibit) (Duno-Miranda et al. 2024; Rasicci et al. 2022). An increase in the auto-inhibition of myosins with the E525K mutation could therefore be responsible for the hypocontractile phenotype associated with DCM disease progression. The increased actin dependent ATPase activity of S1 heads has been attributed to an increase in actin affinity and an increase in the phosphate release rate for E525K myosin (Bodt et al. 2024). These biochemical studies have been extremely insightful but E525K myosin has still never been studied in the myofilament and in the context of load.

Under conditions of high load, such as during strenuous muscle contraction the release of ADP from the myosin head is significantly slowed (Doran, Rynkiewicz, Rasicci, et al. 2023; Sweeney and Houdusse 2010). This means that load (and the presence of actin) changes the rate limiting step in the myosin cycle from phosphate release to ADP release. Additionally, the recruitment of myosin heads out of the auto-inhibited OFF state is also facilitated by increased force (Campbell et al. 2018). Since product release and myosin recruitment are the mechanisms

by which the E525K mutation has been theorized to change myosin activity, it is important to confirm these findings in intact myofilaments and in the context of loaded contraction.

Here we build on the previous biochemistry work done with the E525K by measuring the contractile force and kinetics of E525K myosin in human induced pluripotent stem cell (hiPSC) derived cardiomyocytes (hiPSC-CMs). We found that the E525K mutation does alter force generation in cells and tissues, but we saw no evidence that the kinetics or enzymatic activity of E525K myosin was altered. This emphasizes the importance of studying myosin mutations at multiple scales. A great deal can be learned from experiments using isolated myosin to understand how the biochemistry of myosin is changed. However, myosin chemomechanics are highly load dependent and regulated by the larger cellular process of EC coupling—it is therefore critical to study myosin mutations at the cell and tissue level to understand how they contribute to disease progression.

Results

Engineered heart tissues with the E525K mutation show hypocontractility with unchanged kinetics

Induced Pluripotent Stem Cells (iPSC) carrying the heterozygous E525K mutation as well as wildtype (WT) controls were kindly provided by the Allen Institute for Cell Science. Cells lines were differentiated into mature cardiomyocytes that expressed β-cardiac myosin following a standard differentiation protocol (**Supplemental Figure 3-1A-B**). All experiments were carried out at day 45 of differentiation unless otherwise indicated.

Engineered heart tissues (EHTs) were used to investigate force generation in cardiac tissues with the E525K/WT heterozygous mutation and compared with EHTs with no mutation (WT/WT). EHTs with the E525K mutation showed decreased force generation in isometric twitches paced at 1 Hz (**Figure 3-1A**). With twitches showing both a decreased peak force and a decreased tension time integral (**Figure 3-1B-C**). Interestingly the rate of force generation and

rate of relaxation in these tissues was unchanged by the mutation as seen in the time to peak and time to baseline measurements (**Figure 3-1 D-E**). While the morphology of these tissues did vary the cross-section area (CSA) of these tissues was comparable between genotypes (**Figure 3-1 F**).

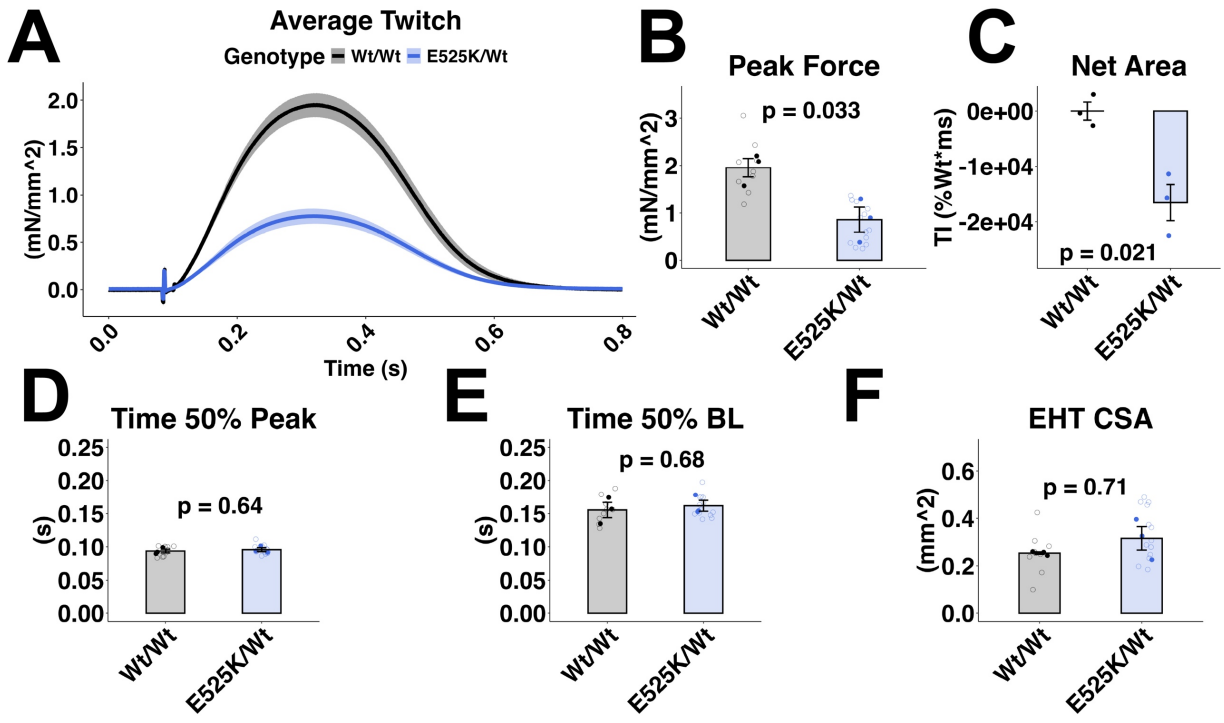

Figure 3-1: Isometric twitch force is reduced in E525K engineered heart tissues (EHT).

(A) Average trace of isometric twitch contraction (Mean +/- SEM). (B) Peak isometric twitch force is reduced with the E525K mutation. (C) The tension time integral was reduced with the E525K mutation. (D-E) Contraction and relaxation rates were unchanged with the E525K mutation. (F) EHT cross section area (CSA) was unchanged. Open circles represent technical replicates (individual EHTs), filled circles represent biological replicates (separate differentiations). All data is represented as the mean +/- SEM. All statistics represent a student's T-test; N = 3 differentiations and n = 9-13 EHTs per genotype.

<u>Single cardiomyocytes with the E525K mutation show a hypocontractile phenotype</u>

While perhaps more physiologically relevant EHTs introduce heterogeneity by including multiple cell types. To bypass this limitation and directly measure how contraction is changed in cells with the E525K mutation the contraction of single cells was observed using live cell imaging. An endogenous eGFP tag on α-actinin allowed for live imaging/tracking of sarcomere movement

in WT/WT and E525K/WT cell lines. To generate elongated and aligned myofibrils stem cell derived cardiomyocytes were matured to day 45 of differentiation and grown on elongated patterns for one week prior to imaging. Both WT/WT and E525K/WT cells were able to form elongated myofibrils and contract when paced at 1 Hz (**Figure 3-2 A**). However, E525K/WT cells contracted less as measured by pixel displacement over time (**Figure 3-2 B-C**). Area under the curve analysis of these displacement twitches revealed a decrease in the tension time integral consistent with a dilated cardiomyopathy phenotype (**Figure 3-2 D**). This decrease in cell contraction was driven by a decrease in sarcomere shortening as measured by percent change in the distance between Z-disks during contraction (**Figure 3-2 E**). Interestingly, as in tissues, there was no change in the rate of contraction or rate of relaxation in cells carrying this E525K mutation (**Figure 3-2 F-G**).

Together these results show that at both the single cell and the tissue level there is a decrease in contraction when cardiomyocytes carry the heterozygous E525K mutation. Additionally, there was also no change in the rate of contraction or relaxation at either scale of analysis. This points towards a change in the number of actively cycling myosin heads driving the change in force generation rather than a change in the rate at which myosin moves through the crossbridge cycle.

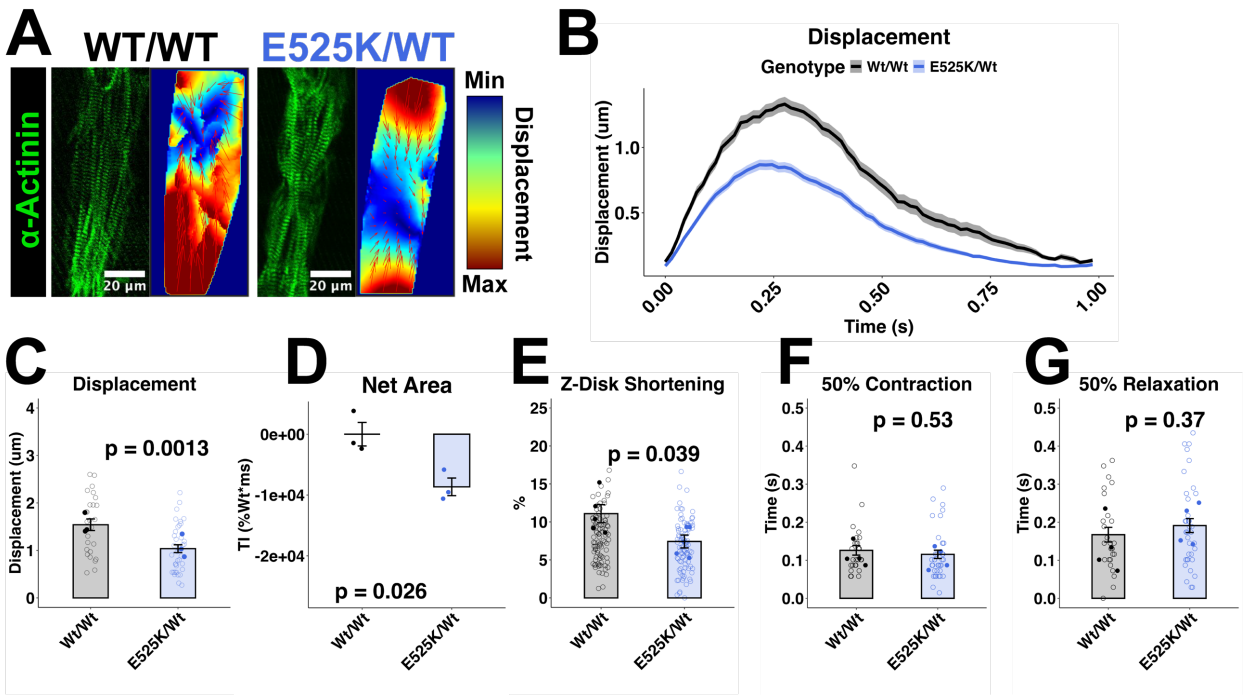

Figure 3-2: Live cell contraction analysis shows decreased contraction in E525K cardiomyocytes.

(A) Patterned day 45 cardiomyocytes with endogenous α-actinin eGFP tag. Representative displacement tracking images are shown. (B) Average traces showing displacement over time for live imaged cardiomyocytes (Mean +/- SEM). (C) Average cell displacement decreased with the E525K mutation. (D) The tension time integral calculated based on the displacement traces was decreased with the E525K mutation. (E) Sarcomere shortening measured at the Z-disks was also decreased with the E525K mutation. (F-G) Time to 50% of peak and time from peak to 50% of baseline were unchanged with the E525K mutation. Open circles represent technical replicates (individual cells), filled circles represent biological replicates (separate differentiations). Students T-test, N = 3-5 differentiations n = 91-94 cells per genotype.

Myofibril mechanics show increased max force generation in fibrils with E525K myosin

To get a better picture of how the chemomechanics of activation, relaxation, and force generation are changed myofibrils were isolated and activated at various calcium concentrations. Both WT/WT and E525K/WT myofibrils were robustly formed enough to be isolated after 45 days of culture and patterning, moreover myofibrils from both genotypes were able to activate and generate force in response to elevated calcium (**Figure 3-3 A**). Surprisingly, unlike in cells and tissues, myofibrils isolated from cells with the heterozygous E525K mutation generated more force than WT/WT myofibrils when stimulated with a calcium concentration higher than physiologically relevant (pCa 4.0). When stimulated at calcium levels more consistent with

intracellular systolic calcium (pCa 5.6 and 5.8) E525K/WT myofibrils no longer showed a statistically significant increase in force (**Figure 3-3 B**). This finding demonstrates that E525K myofibrils are still competent to contract and, at least under some conditions, can generate more force than WT myofibrils. Once again, the kinetics of all phases of activation and relaxation were unchanged by the mutation—this was true at all calcium levels tested (**Figure 3-3 C-E**). Scaled and zoomed in versions of these average traces can be seen in **Supplemental Figure 3-2**. Finally, to investigate if the calcium sensitivity of the thin filament was altered in E525K/WT myofibrils the percent of maximum force generated under submaximal calcium stimulation was investigated. The fragile nature of myofibrils isolated from hiPSC-CMs made it impossible to run these fibrils through a full force pCa curve, but two physiologically relevant, submaximal stimulations were investigated (pCa 5.6 and pCa 5.8). There was a significant difference in percent of max force generated between WT/WT and E525K/WT myofibrils at pCa 5.6 (**Figure 3-3 F**) but not at pCa 5.8 (**Figure 3-3 G**). This indicates that there may be a change in the calcium sensitivity of myosin in E525K/WT myofibrils. Notably, as with results at the tissue and cell level, this assay indicates that the differences in force generation are driven by differences in myosin recruitment, and not by changes in the rate at which E525K mutant myosin moves through the crossbridge cycle.

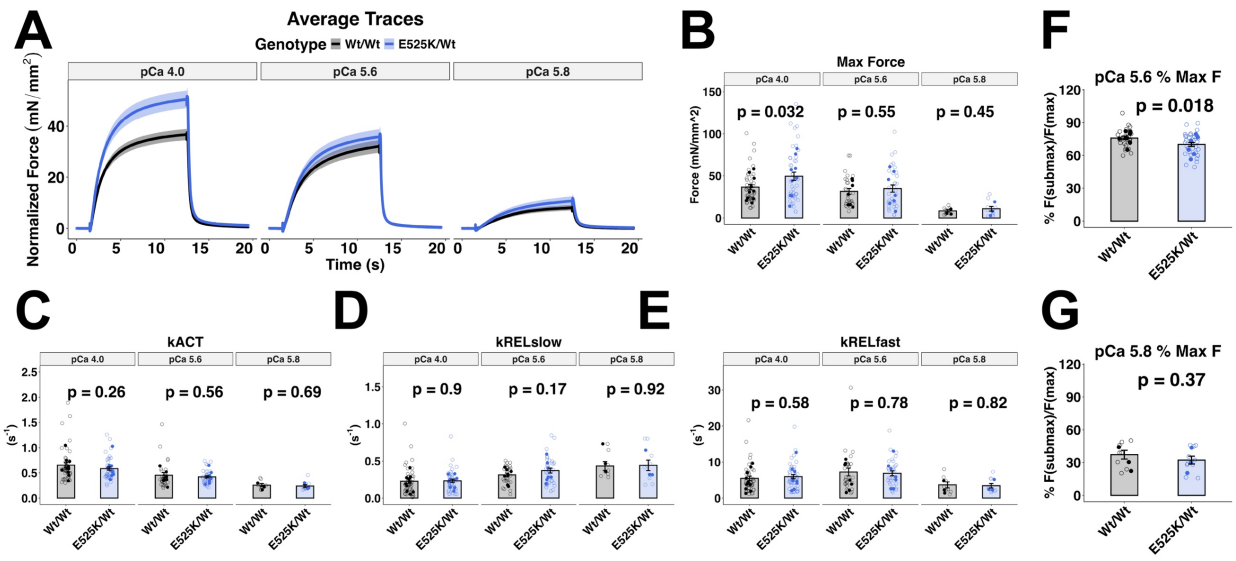

Figure 3-3: Myofibril mechanics show increased force generation with the E525K mutation under high calcium conditions.

(A) Average traces of normalized force over time (Mean +/- SEM) at maximal (pCa 4.0) and submaximal (pCa 5.6 or pCa 5.8) stimulation. (B) Max force increased with the E525K mutation stimulated at pCa 4.0 but was not significantly elevated when stimulated at lower calcium concentrations (pCa 5.6 or 5.8). (C-E) The kinetics of contraction and relaxation were unchanged under all conditions tested. (F) The percent of maximum force generated at submaximal calcium stimulation (pCa 5.6) was reduced. (G) This difference was not significant at pCa 5.8. Open circles represent technical replicates (individual myofibrils), filled circles represent biological replicates (separate differentiations). T-test, N = 3-10 differentiations n = 8-43 myofibrils. Due the inherent variability of this assay significance was calculated based on technical replicates.

Sarcomere formation and organization is decreased in E525K/WT cells and tissues

To investigate sarcomere formation in the absence of external morphometric cues day 45 un-patterned cardiomyocytes were fixed in blebbistatin and imaged using the α-actinin eGFP reporter (**Figure 3-4 A**). Images of single cardiomyocytes were then blindly ranked based on sarcomere formation and organization from 1-disorganzed to 5-organized. Cardiomyocytes carrying the E525K/WT mutation formed fewer less well-organized sarcomeres (**Figure 3-4 B**). WT/WT and E525K/WT patterned day 45 cardiomyocytes both formed sarcomeres and elongated myofibrils (**Figure 3-4 C**). However, dispersion angle analysis on z-disks from these images showed that myofibrils and z-disks from E525K/WT cardiomyocytes were less well aligned with the axis of contraction/patterning (**Figure 3-4 D**).

Together these results show that the formation and organization of sarcomeres is inhibited in hiPSC-CMs carrying the E525K mutation. This result could partially explain the decrease in force generation observed in cells and tissues (**Figures 3-1 and 3-2**). Notably, the isolation and purification of myofibrils—required for the myofibril assay—may discard malformed myofibrils, and analysis at the single myofibril level also eliminates any impact from myofibrils that are not aligned with each other or the axis of contraction inside a patterned cardiomyocyte.

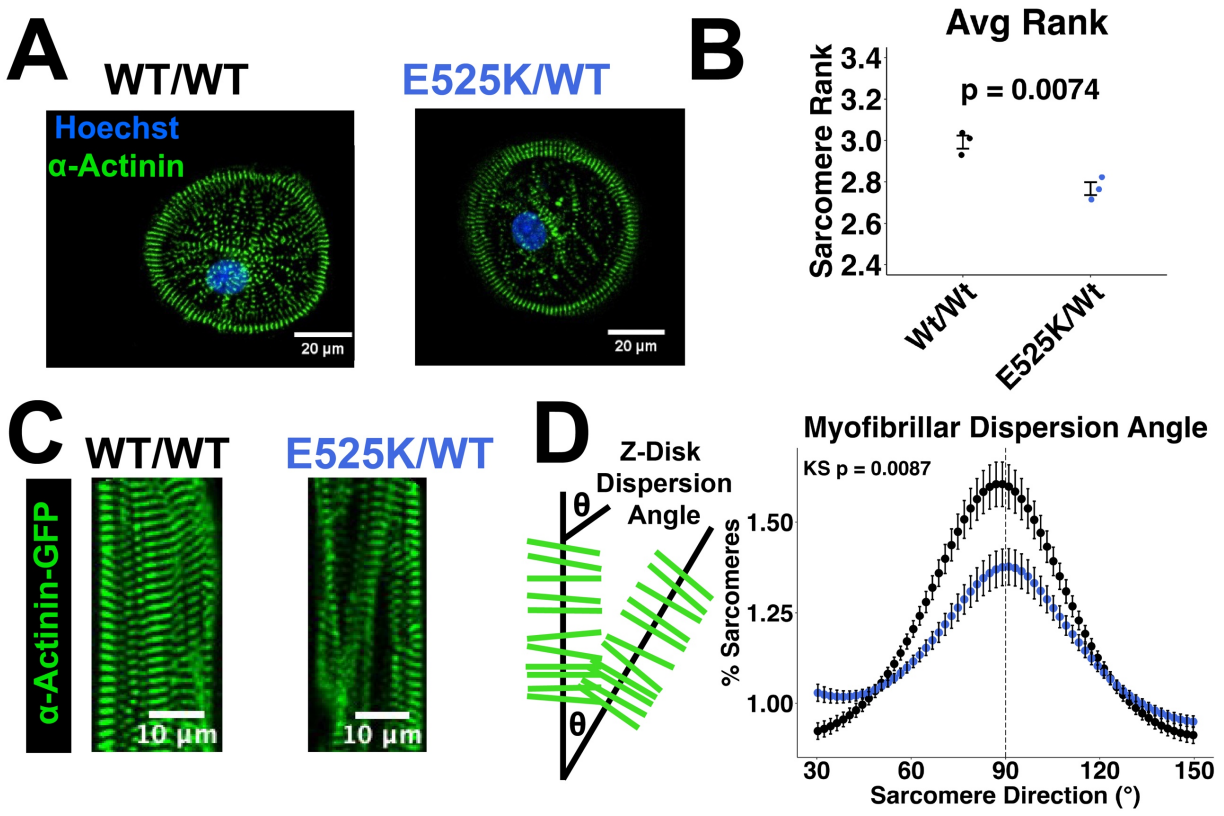

Figure 3-4: Sarcomere formation and organization is decreased in E525K/WT patterned and un-patterned cells.

(A) Representative day 45 un-patterned single cardiomyocytes. (B) Blind ranking of sarcomeres in single cells demonstrates a decrease in sarcomere formation and organization (scale from 1-poorly formed sarcomeres to 5-well formed sarcomeres). T-test, N = 3 differentiations n = 828-989 ranked cells per genotype. (C) Representative day 45 patterned single cardiomyocytes. (D) Dispersion angle analysis on whole patterned E525K cells shows that E525K myofibrils & Z-disks are less in register with one another than WT controls—Kolmogorov-Smirnov Test, N = 5 differentiations.

Calcium transients are unchanged in E525K/WT patterned cells

The results presented so far represent a kind of paradox. We see decreased force in cells and tissues carrying the E525K mutation, but we see increased force in myofibrils isolated from the same cells. One difference between these assays is that at the cell and tissue level calcium is regulated by excitation contraction coupling within each cardiomyocyte or syncytium of cardiomyocytes. In isolated myofibrils on the other hand, the amount of calcium available to activate the thin filament is controlled exogenously by the solution bath. It is also important to note that the pCa 4.0 condition is a higher than physiologically relevant level of calcium. Even under systolic conditions calcium in the sarcomere is closer to pCa 5.8 (Bers 2002). To more closely observe the intracellular concentrations of calcium in hiPSC-CMs we used Calbryte™ 590 AM (a fluorescent calcium reporter compatible with the endogenous GFP tag in this cell line). Calcium transients were assayed in patterned day 45 cardiomyocytes (**Figure 3-5 A**). The amplitude of calcium transients was not significantly changed in E525K/WT cells (**Figure 3-4 B**). Additionally, both the baseline fluorescence (**Figure 3-5 C**), and the kinetics of the calcium transient were unchanged (**Figure 3-5 D-E**) in E525K/WT cells.

These results indicate that the calcium handling in these cells is not changed by the E525K mutation—this is consistent with the location of this mutation in the thick filament rather than the thin filament. If the direct calcium transient isn't altered, it also suggests that the mechanism by which elevated calcium leads to increased force in E525K/WT myofibrils is not due to the gross properties of the calcium transient itself. Instead, the focus should shift to how myosin responds to thin filament activation or the sensitivity of the thin filament to calcium.

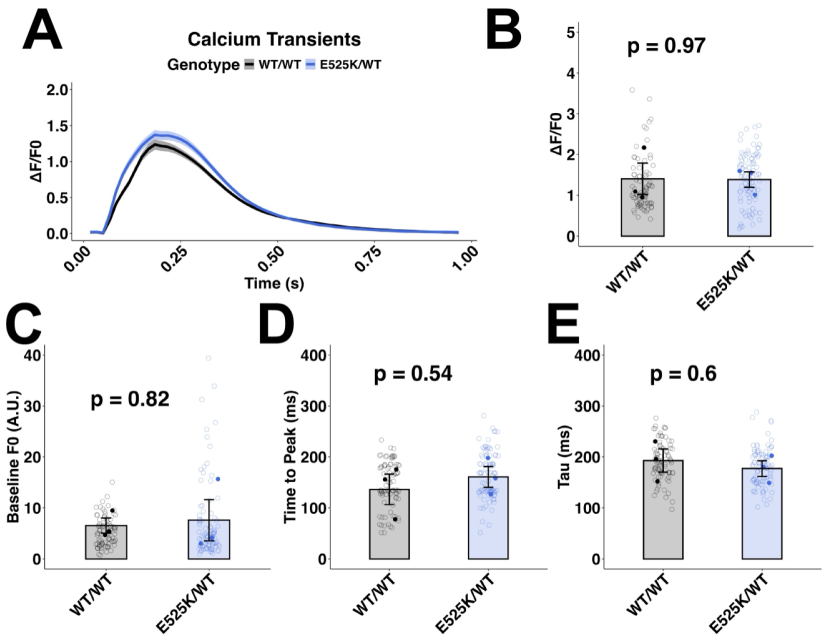

Figure 3-5: Calcium transients are unchanged in E525K patterned cardiomyocytes.

(A) Average calcium transient from day 45 patterned cardiomyocytes paced at 1 Hz (Mean +/- SEM). (B) Transient amplitude was not changed in E525K/WT cardiomyocytes. (C) Baseline fluorescence was not changed in E525K/WT cardiomyocytes. (D) Time to peak was not changed in E525K/WT cardiomyocytes. (E) The decay constant (Tau) was also not changed. T-test, N = 3 differentiation, n = 82-92 cells.

E525K myosin has an increased affinity for actin

Previous work has shown that E525K myosin S1 constructs have an increased actin dependent ATPase activity (Duno-Miranda et al. 2024; Rasicci et al. 2022), moreover modeling from our previous work has shown that the E525K mutation may increase myosin's affinity for actin through a disruption of loop 2 folding (**See Chapter 2**). To biochemically test the affinity of E525K myosin for actin an ATP-induced dissociation of pyrene-actin+S1 assay was used to determine the relative percent of myosin S1 bound to actin at various concentrations of S1 (**Figure 3-6 A**). These data form a hyperbolic titration curve which can be fit by the classical quadratic equation to define the dissociation constant of S1 for actin: K_{actin} (**Figure 3-6 B**). These data show that E525K myosin has an increased affinity for actin which could explain the increased force generated by E525K/WT myofibrils stimulated with elevated calcium.

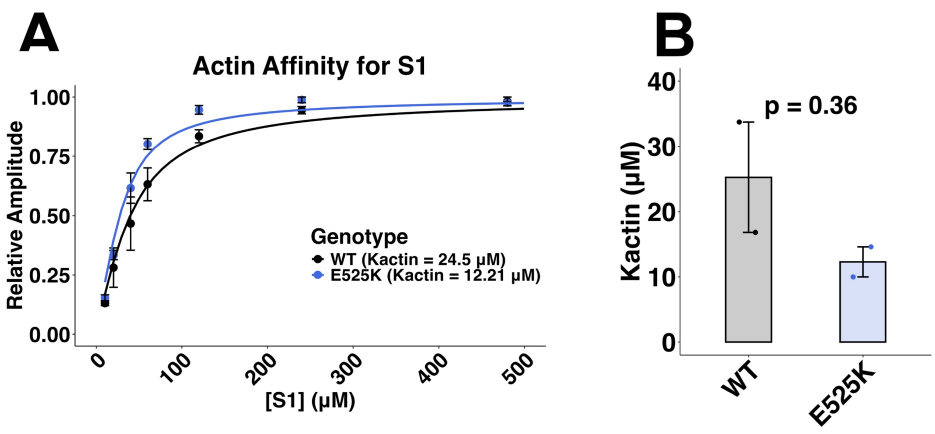

Figure 3-6: E525K myosin has an increased affinity for actin

Stopped flow biochemistry was used to measure the affinity of WT and E525K myosin S1 constructs for pyrene labeled actin. (A) The relative decrease in pyrene-actin florescent amplitude at various concentrations of myosin S1 was fit with the standard quadratic equation. (B) Myosin K_{actin} value for each replicate of the pyrene actin assay. T-test N = 2 replicates.

Phenotypic Comparison of The E525K Mutation with UC2 Background Cells

All mechanics work presented so far has used cell lines engineered on the WTC11 background. To investigate the penetrance of the E525K mutation we also engineered this mutation into a second background. These cells underwent the same Cas9 engineering to introduce the E525K mutation however in addition to a heterozygous clone (E525K/WT) a homozygous clone (E525K/E525K) was also isolated. As for the WTC11 background cells myosin isoform was assayed after differentiation (**Supplemental Figure 3-1C**). There was not a full transition from α- to β-myosin in these cells following the same protocol, however most of the myosin in all UC2 cell lines was β-myosin by the day 45 endpoint for all EHT and myofibril assays.

Engineered heart tissues with the E525K mutation on the UC2 background show hypocontractility with unchanged kinetics

As previously described EHTs were used to investigate force generation in cardiac tissues with the E525K mutation. Here cells on the UC2 background with no mutation (WT/WT) were

compared with heterozygous (E525K/WT) and homozygous (E525K/E525K) mutants. EHTs with the E525K mutation showed a stepwise decreased force generation with heterozygous cells generating less force than WT/WT cells and homozygous cells generating still less force (**Figure 3-7 A**). These isometric twitches showed both a decreased peak force and a decreased tension time integral (**Figure 3-7 B-C**). The rate of force generation and rate of relaxation in these tissues was unchanged by the mutation as seen in the time to peak and time to baseline measurements (**Figure 3-7 D-E**). The morphology of these tissues did vary, but the cross-section area (CSA) of these tissues was comparable between genotypes (**Figure 3-7 F**). The results of this experiment show that UC2 background cells recapitulate findings on the WTC11 background at the EHT level.

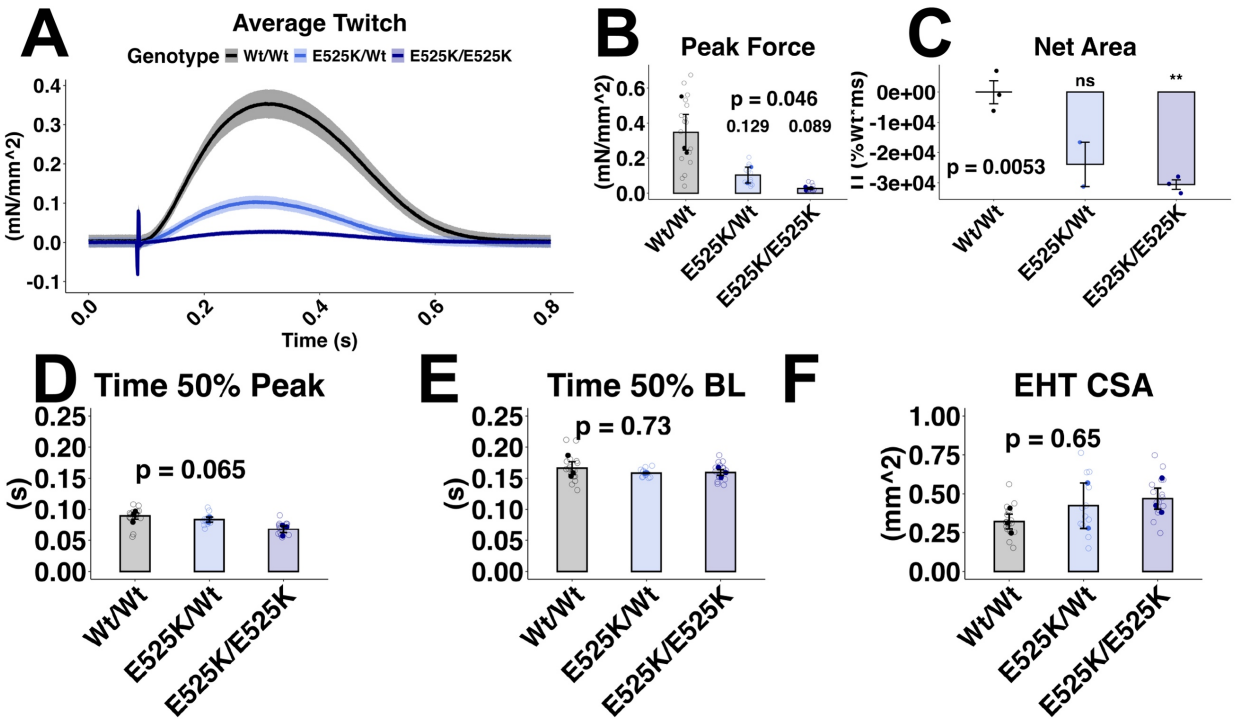

Figure 3-7: Isometric twitch force is reduced in E525K engineered heart tissues (EHT) on the UC2 background.

(A) Average trace of isometric twitch contraction (Mean +/- SEM). (B) Peak isometric twitch force is reduced with the heterozygous E525K mutation and further reduced by the homozygous mutation. (C) The tension time integral was reduced with the E525K mutation and further reduced by the homozygous mutation. (D-E) Contraction and relaxation rates were unchanged with the E525K mutation. (F) EHT cross section area (CSA) was unchanged. Open circles represent technical replicates (individual EHTs), filled circles represent biological replicates (separate differentiations). All data is represented as the mean +/- SEM. All statistics represent an ANOVA with a post hoc T-test; N = 2-3 differentiations n = 12-17 EHTs per genotype.

Myofibrils with the E525K mutation on the UC2 background show hypocontractility with unchanged kinetics

Surprisingly, unlike in myofibrils isolated from WTC11 background cells, UC2 background myofibrils with the E525K mutation (heterozygous or homozygous) generated less force than WT/WT myofibrils (**Figure 3-8 A**). This was true at all levels of calcium stimulation (**Figure 3-8 B**). This finding—while inconsistent with the results from the WTC11 background cells—is consistent with hypocontraction and a dilated cardiomyopathy phenotype. The kinetics of all phases of activation and relaxation were unchanged by the mutation; this was also true at all calcium levels tested (**Figure 3-8 C-E**). Scaled and zoomed in versions of these average traces can be seen in **Supplemental Figure 3-3**. Finally, there was a significant difference in percent of max force generated between WT/WT and E525K/E525K myofibrils at pCa 5.6 (**Figure 3-8 F**), but this was not significant in E525K/WT cells or at pCa 5.8 (**Figure 3-8 G**). Notably, as with results from the WTC11 background hiPSC-CMs, these results indicate that the differences in force generation are driven by differences in myosin recruitment and activation—not by changes in the rate at which E525K mutant myosin moves through the crossbridge cycle.

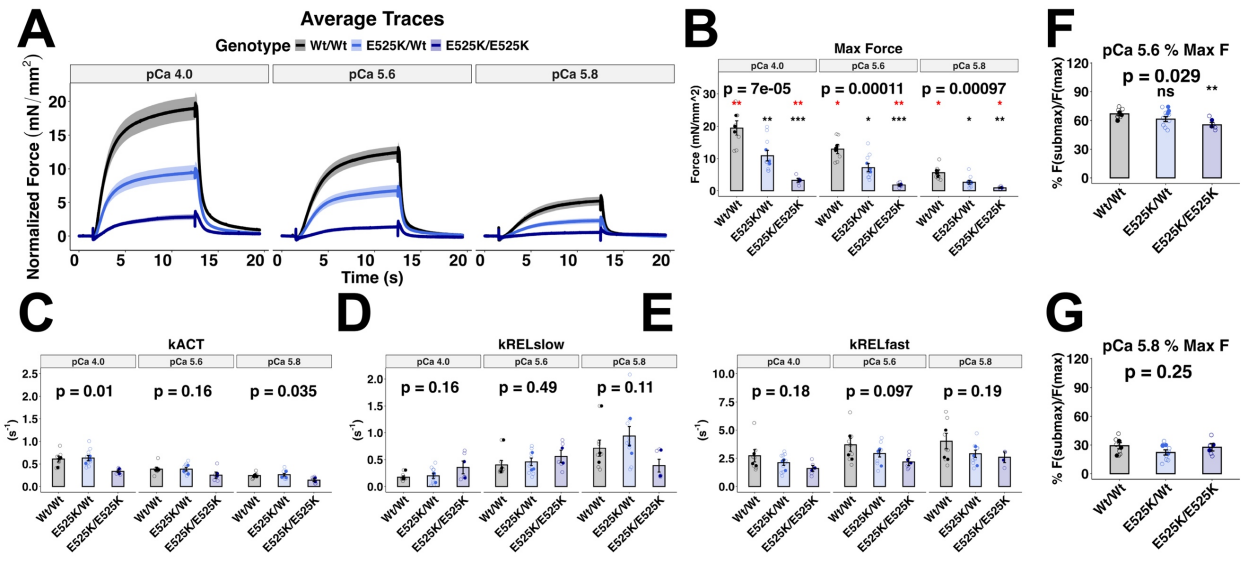

Figure 3-8: Myofibril mechanics from UC2 background cells show decreased force generation with the E525K mutation under all calcium conditions.

(A) Average traces of normalized force over time (Mean +/- SEM) at maximal (pCa 4.0) and submaximal (pCa 5.6 or pCa 5.8) stimulation. (B) Max force decreased with the E525K mutation in a stepwise fashion with heterozygous cells weaker than WT cells and homozygous cells weakest of all at all calcium stimulations. (C-E) The kinetics of contraction and relaxation were unchanged under all conditions tested. (F) The percent of maximum force generated at submaximal calcium stimulation (pCa 5.6) was reduced only in homozygous cells compared to WT cells. (G) This difference was not significant at pCa 5.8. Open circles represent technical replicates (individual myofibrils), filled circles represent biological replicates (separate differentiations). ANOVA with post hoc T-test, N = 2-3 differentiations n = 5-10 myofibrils. Due the inherent variability of this assay significance was calculated based on technical replicates.

Discussion

The results presented here represent the first analysis of how E525K myosin impacts cardiomyocyte and myofibril contraction. Cells and tissues with the heterozygous or homozygous form of the E525K mutation generated significant less tension over time, consistent with a DCM phenotype (Davis et al. 2016). Surprisingly however single myofibrils from mutant cells stimulated with high calcium did not follow this trend—instead generating more force or less force than WT cells depending on the background cell line of the engineered cells. This result highlights the importance of understanding how a given mutation interacts with the greater context of the cell line's or patient's genetic background. This phenomenon of variable "penetrance" of a mutation is a major limitation of current efforts to include a patient's relevant genetic background when designing therapeutic intervention (McGurk et al. 2023). This work is consistent with previous studies showing that the impact of the E525K mutation is primarily through changing the number of myosin heads which interact with actin. Unlike previous work, we saw no evidence that the cycling rate of individual myosin heads was changed in all kinetic measurements assay here—from the single myofibril level to the single cell level, and even at the whole tissue level.

These findings demonstrate the complexity of trying to understand how a myosin mutation changes myosin function at all scales of contraction. Myosin function is clearly changed by this mutation and is consistently decreased at the cell and tissue level no matter the background of the cells. However, the fact that we saw increased force and decreased force depending on background means there is something more complicated going on here. The decreased myofibrillar alignment leads to misaligned inefficient force generation. Conversely, the enhanced actin affinity imparted by the E525K mutation may help with the cooperative activation of myosin heads. This increased affinity could facilitate the augmented force production seen under some myofibril conditions. Together these results present a picture of how some phenotypes are consistently changed by the E525K mutation and some phenotypes are not (**Figure 3-9**).

Previous work using isolated E525K myosin has shown that this mutation stabilizes the IHM state while also increasing the intrinsic ATPase activity of the myosin head. The decrease in tension generation over time associated with DCM was attributed the stabilization of the IHM state and a decrease in the recruitment of myosin (Duno-Miranda et al. 2024; Rasicci et al. 2022). Notably, both myosin recruitment (Campbell et al. 2018; Vander Roest et al. 2021) and myosin ATPase activity (Sweeney and Houdusse 2010) are load-dependent processes. The observation that ADP release limits the crossbridge cycle under load, combined with load-induced myosin recruitment, could explain the apparent differences between our results and previously published work.

This underscores the need for investigating myosin mutations at various scales to fully understand how these mutations change contraction. Since force generation at the organelle level was variable based on cell background, the observed reduction in cellular and tissue force generation is likely attributable to multiple factors. We observed myofibrillar disorder here, but the established E525K-related impairment of myosin recruitment observed by others (Bodt et al. 2024; Rasicci et al. 2022) is also likely playing a role.

As new drugs are developed to specifically target cardiac myosin it is critical to understand how specific mutations will respond to drug treatment. Novel myosin modulating drugs have been identified using myosin ATPase assays as a screening approach (Bello and Pellegrini 2024; Hartman et al. 2024; Planelles-Herrero et al. 2017; Voors et al. 2020). The results presented here emphasize that the interaction between these drugs and myosin may be different under load and that these drugs may have different or unpredictable interactions with specific myosin mutations. Future work on the E525K mutation should investigate how this mutation interacts with myosin activator drugs since (under some conditions) it appears that the E525K mutation can lead to both hypocontraction and hypercontraction.

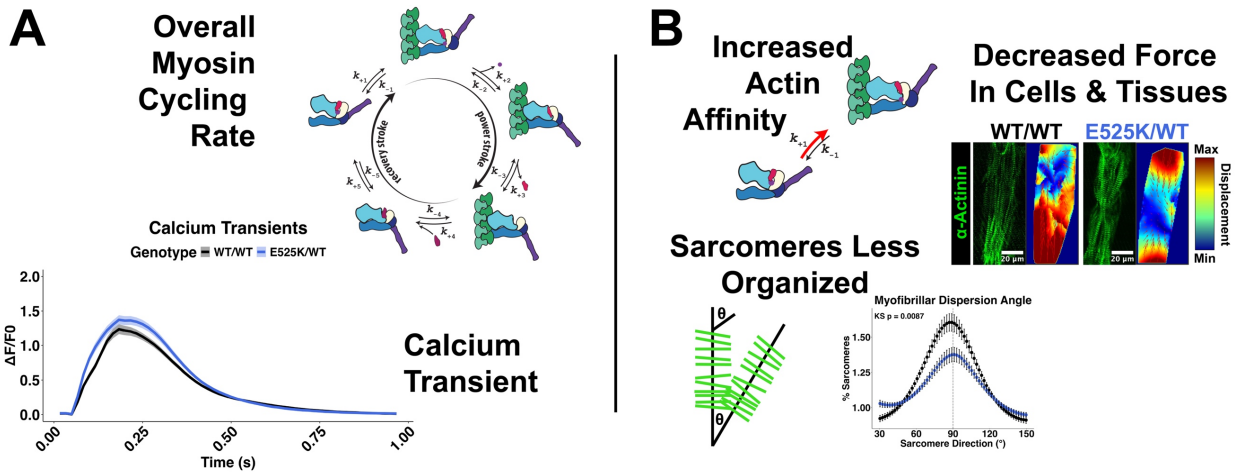

Figure 3-9: How the E525K mutation changes or does not change contraction in cardiomyocytes

(A) Parameters not changed in E525K hiPSC-CMs: The overall rate that myosin moves through the crossbridge cycle was not changed in any assay we measured here and the calcium transients of intact cardiomyocytes with the E525K mutation was not changed. (B) Parameters changed in E525K hiPSC-CMs: Force generation is depressed in cardiomyocytes and tissues with the E525K mutation, and this may be due in part to decreased myofibrillar alignment. The increased affinity for actin demonstrated by E525K myosin—leading to an increase in crossbridge formation—may help to explain the increased force generation observed in single myofibrils under some conditions.

Methods

Cell line generation and cardiomyocyte differentiation

All WTC11 background hiPSC were generously provided by the Allen Institute for Cell Science. All UC2 background hiPSC were generated by the Elison Stem Cell Core at the University of Washington. The genetic engineering approach was the same. Briefly, CRISPR Cas9 was used to edit hiPSC cells and incorporate the E525K mutation into the *MYH7* gene. Cells that went through Cas9 editing but did not receive the E525K mutation were used as wildtype controls for all experiment. Line validation including pluripotency testing and karyotyping.

Undifferentiated cells (6×10^4) were seeded in Matrigel-coated 12-well dishes in mTeSR supplemented with 10 μM Y-27632 ROCK inhibitor (day -2). After 24 hours media was change dot mTeSR supplanted with 1 μM Chiron 99021. The following day (day 0), media was replaced with RBA media (RPMI supplemented with 0.5 mg/ml bovine serum albumin and 0.214 mg/ml ascorbic acid) and 5 uM Chiron 99021. On day 2, media was changed to RBA with 2 uM WNT C-59. Day 4 media was changed to RBA with no small molecule. On day 6 media was changed RPMI with B-27 supplement. Cells were cultured in RPMI with B-27 with media changes every 2–3 days. To purify cardiomyocytes cells were replated at day 14 and cultured in DEME with no glucose supplemented with 4 mM sodium lactate. Cells were maintained in lactate media for 6 days with media changes every 2 days before being returned to RPMI with B-27. Media was changed every 2-3 days until cells until cells reached the endpoint or protocol described.

Patterning, and maturation

Elongated, mature myofibrils are needed to perform myofibril kinetics experiments. To achieve this from iPSC-CMs the cells were cultured on lined patterns of stamped Matrigel, created using a high-fidelity photoresist double lift-off patterning method. Lined patterns for stamping (1 cm x 1 cm area and 15 um line width) were generated by pouring polydimethylsiloxane (PDMS,

Silgard 184, Electron Microscopy Sciences) over a silicon wafer master, cured overnight and then gently peeled off. Ethanol sterilized PDMS stamps were then coated in Matrigel overnight. This Matrigel was then stamped onto an 18 mm cover glass, which was peeled off and then subsequently placed facedown onto a 10 kPa polyacrylamide gel base (0.025 g/mL bis-acrylamide and 0.5 g/mL acrylamide polymerized with 10% APS and TEMED) adhered to plasma treated, glass-bottom 6-well culture dish wells using bind-silane. After hydrating these patterns with phosphate buffered saline (PBS) overnight at 4°C, 300-500,000 iPSC-CMs per well (day 38) were replated onto the patterns in replating media (RPMI, 1X B27 supplement, and 10 mM Y-27632 ROCK inhibitor) and allowed to adhere in a concentrated, 0.4 ml bubble only on top of the patterned area for 2 hours in a 37°C incubator. After 2 hours, each well was topped up with replating media for overnight incubation. 24 hours after replating, media was replaced with 50:50 RPMI:DMEM minus glucose media with 1X B27 supplement to begin increasing the concentration of Ca^{2+} from 0.4 mM to 1.1 mM. After 2 days, Ca^{2+} concentration was further increased from 1.1 mM to 1.45 mM by replacing media with 25:75 RPMI:DMEM minus glucose media with 1X B27 supplement. Cells were maintained in this media for 4 days with one media change after 48 hours (for a total of 7 days on the patterned surface).

EHT Casting, culture, and force measurements

Tissue constructs were generated following established protocols (Bielawski et al. 2016; Schaaf et al. 2014). Briefly, rectangular 2% w/v agarose/DPBS casting molds (12 mm length, 4 mm width, ~4 mm depth) were prepared in 24-well plates using 3D-printed spacers. PDMS posts were positioned centrally, upside down, with a 0.5 mm gap between the post tip and mold bottom. Each tissue consisted of 97 µL of a fibrinogen-media solution (87 µL RPMI with B-27 and insulin, 10 µL of 50 mg/mL bovine fibrinogen, Sigma-Aldrich) containing 5×10^5 iPSC-CMs (day 24) and 5×10^4 HS27a human bone marrow stromal cells (ATCC). Immediately before casting, 3 µL of 100 U/mL thrombin (Sigma-Aldrich) was added. The mixtures were incubated at 37 °C for 90 min

to allow fibrin gel polymerization around the posts. Gels were then lubricated with media and transferred to fresh EHT media (RPMI with B-27, insulin, and 5 mg/mL aminocaproic acid, Sigma-Aldrich) in a 24-well plate. Media was replaced three times weekly (2 mL/well). Tissues were cultured for 3 weeks and harvested for force measurements at day 45 of differentiation.

For isometric force measurements tissues were removed from posts and mounted on an IonOptix Intact Muscle Chamber System. Tissues were bathed in DMEM/F12 supplemented with $CaCl_2$ to a final Ca^{2+} concentration of 1.8 mM. Tissues were field stimulate with 5-10 V and paced at 1 Hz. Paced tissues were allowed to acclimate to the pacing protocol for 5-10 minutes before twitches were recorded for 30 s. Average traces, max twitch force, and contraction/relaxation parameters where calculated using the IonOptix software.

Live cell sarcomere imaging

Patterned day 45 cardiomyocytes were placed in a custom-built live cell imaging chamber on a Nikon A1R Confocal (37°C and 5% CO_2). Cells were bathed in Normal Tyrode's buffer (1.8 mM Ca^{2+}), stimulated with 5-10 V, and paced at 1 Hz. Live cell recordings of the α-actinin eGFP signal were recorded for 8-10 seconds at a frame rate of 69 FPS. Sarcomere shorting was measured in one relaxed and one contracted frame by hand using ImageJ line scans of two myofibrils form each cell. The angular dispersion of myofibrils and Z-disks was calculated from one relaxed frame of for each cell using the local gradient orientation plugin in ImageJ. Displacement and kinetics of contraction were calculated using the LifeAct software with default settings (Ribeiro et al. 2017).

Myofibril isolation, and force measurements

For myofibril isolation, day 45 cells on patterned surfaces were directly treated with pCa 9.0 relaxation solution (supplemented with 50 mM Tris, 100 mM KCl, 2 mM $MgCl_2$, 1 mM EGTA, 1x protease inhibitor cocktail Sigma, and 1% Triton X-100 Acros Organics) for 10 min on ice. Cells

were then washed twice with pCa 9.0 and 1:100 PIC without Triton X-100, gently lifted off the plate with a cell scraper, and then collected off the plate with a pipet. After isolation, iPSC-CM myofibrils were mounted between two glass microprobes, one microprobe was attached to a motor arm and the other served as an optically based force probe, and into a custom-built apparatus with rapid Ca^{2+} solution switching (15°C) to measure myofibrillar contraction and relaxation kinetics at the millisecond timescale. Myofibrils were maximally activated in a pCa 4.0 solution and then subsequently activated in sub-maximal pCa 5.6 and pCa 5.8 solutions.

Imunocytocemestry and immunohistochemistry

Cells and tissues were relaxed in blebbistatin (25 mM) or KCl (140 mM) respectively, then fixed in 4% PFA for 15 minutes. Tissues were embedded in optimal cutting temperature compound (OCT) and sectioned at 5 um. Cells and tissues were washed with PBS stained with Hoechst 33342 (1:2000) for 10 minutes and mounted in Mowiol 4-88 (Sigma Aldrich). Images were taken on a Nikon AX-R Confocal Microscope and analyzed using ImageJ.

Live cell calcium transient imaging

Calcium transients were visualized as previously described (Psaras et al. 2021). The previously described protocol was adjusted as follows. Patterned day 45 cardiomyocytes were loaded with Calbryte™ 590 AM (AAT Bioquest) to avoid spectral overlap with α-actinin eGFP tag. Cells were consistently loaded for 10 minutes and washed out for 10 minutes. Cells were then placed in a custom live cell imaging chamber (37°C and 5% CO_2) on a Nikon AX-R Confocal Microscope and bathed in Normal Tyrode's buffer (1.8 mM Ca^{2+}). Cells were stimulated with 10-20 V and paced at 1 Hz. Cells were paced for 30s pacing prior to imaging to allow calcium regulation to reach to steady state. Images were acquired for 9-10 seconds using NSPARC resonant scanning at a frame rate of 50 FPS. NSPARC detector with near 0 noise floor allowed use of lower laser power with high Signal to Noise. ImageJ was used to select a cytosolic region

of patterned cells for analysis avoiding the nucleus and endoplasmic/sarcoplasmic reticulum. All cells were analyzed simultaneously using the same settings with the CalTrack automated software in MatLab (Psaras et al. 2021).

Stopped flow actin affinity assay

Stopped-flow kinetics were performed at 20°C using a Hi-Tech 'KinetAsyst' stopped-flow (SF-61DX2, TgK Scientific, UK). Measurements were performed at 120 mM KCl, 5 mM $MgCl_2$, 20 mM MOPS, 1 mM DTT, pH 7.0. Pyrene fluorescence was measured by excitation at 365 nm and emission through a GG 400 nm cutoff filter. Actin affinity (K_{actin}) was assessed via ATP-induced dissociation of pyrene-actin and S1 complex. Briefly, 0.25 μM actomyosin (sS1 + pyrene-actin) was rapidly mixed with 20 μM ATP. An average trace of at least eight individual traces was generated for each condition and fit with a double exponential. The relative amplitude of fluorescence increase (pyrene-actin dissociation from S1) was plotted vs. S1 concentration and fitted with the classical quadratic equation to define the dissociation constant of S1 for actin (K_{actin}) as described previously (Kao and Geeves 2024).

Myosin Separation Gels

Cell pellets were flash frozen in liquid nitrogen and stored at -80°C until ready to use. Cell pellets were resuspended in ~3x volumes myofibril lysis buffer (5% SDS, 50 mM Tris (pH 8.5), 0.75% sodium deoxycholate, and 1x protease inhibitor cocktail). Sarcomeres and proteins were denatured by boiling samples for 10 minutes. Concentration was measured by blotting for total protein and adjusting loading as needed. Myosin separation gels were made by combining a stacking gel (2.95% Acrylamide with 10% glycerol at pH 8.8) and resolving gel (6% Acrylamide with 10% glycerol at pH 8.8). Separation gels were run for 2 hours and 15 min at 32 mA in a cold room (4°C). Gels were stained for total protein using One-Step Lumitein™ Protein Gel Stain, 1X

following manufacturer instructions. Gels were imaged on a BioRad ChemiDoc using SYPRO Ruby protein stain setting.

Supplemental Figures

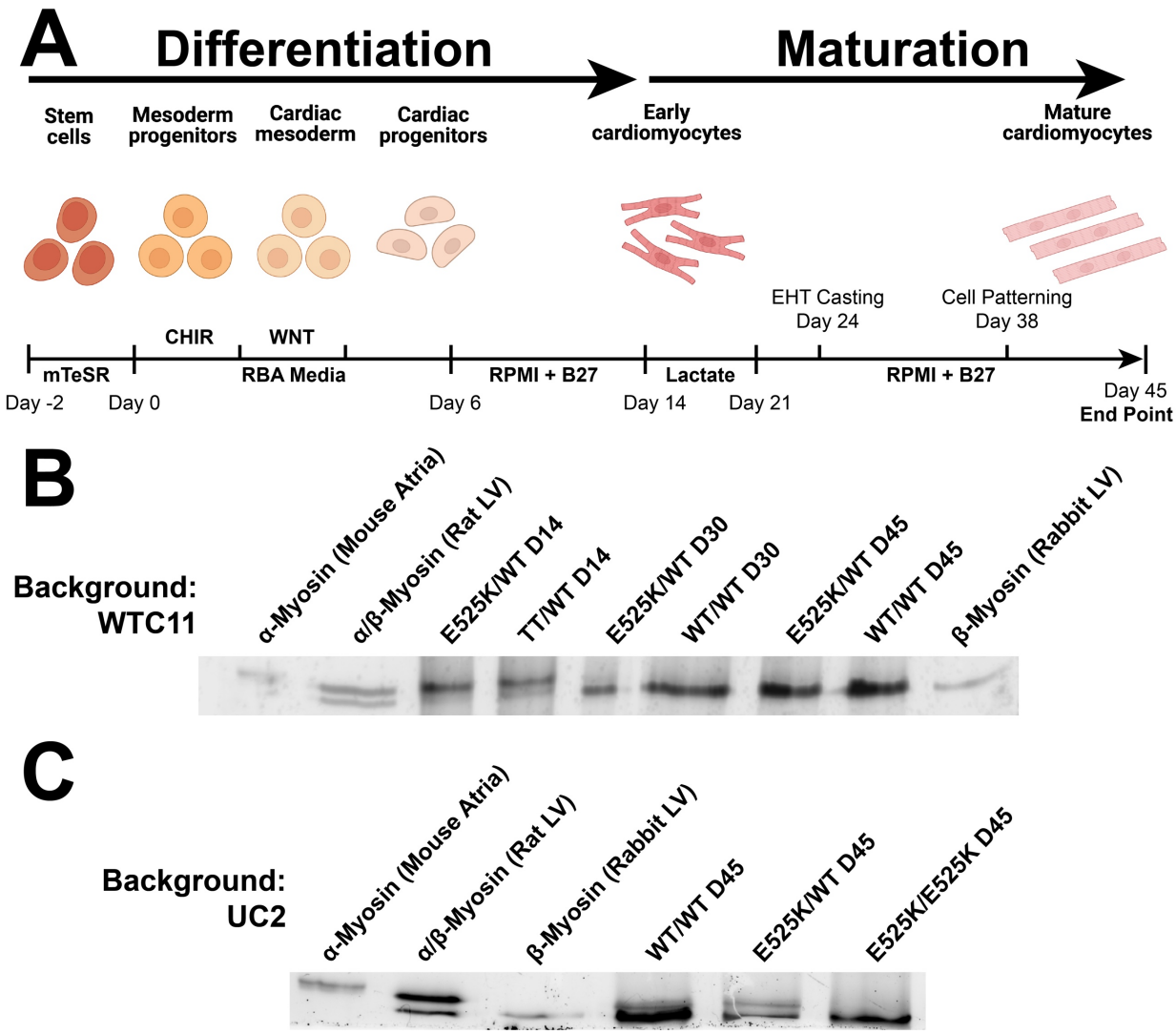

Supplemental Figure 3-1: Differentiation and maturation of iPSC derived cardiomyocytes

(A) Protocol for the differentiation and maturation of stem cell derived cardiomyocytes from iPSCs. All cell lines underwent the same differentiation and maturation protocol. Differentiated cardiomyocytes were purified by lactate selection from day 14 to day 21. Engineered heart tissues (EHTs) were cast on day 24 and cultured for 21 days on posts. Patterned cells were generated by seeding cells onto patterns on day 38 and cultured for 7 days on patterns. All end point assays were carried out on day 45 of differentiation. (B) The expression of β-myosin was confirmed in the WTC11 cell lines via myosin blotting. Day 14 (pre-lactate selection) cardiomyocytes of both genotypes expressed a mixture of α- and β-myosin. After purification (day 30 and day 45) all genotypes expressed only β-myosin. Animal heart tissue was used as positive controls for α-myosin (mouse atria), α- and β-myosin (rat left ventricle), and β-myosin (rabbit left ventricle). (C) The same experiment was run for the UC2 cell lines and WT/WT and E525K/WT cell lines did not show complete conversion to β-myosin.

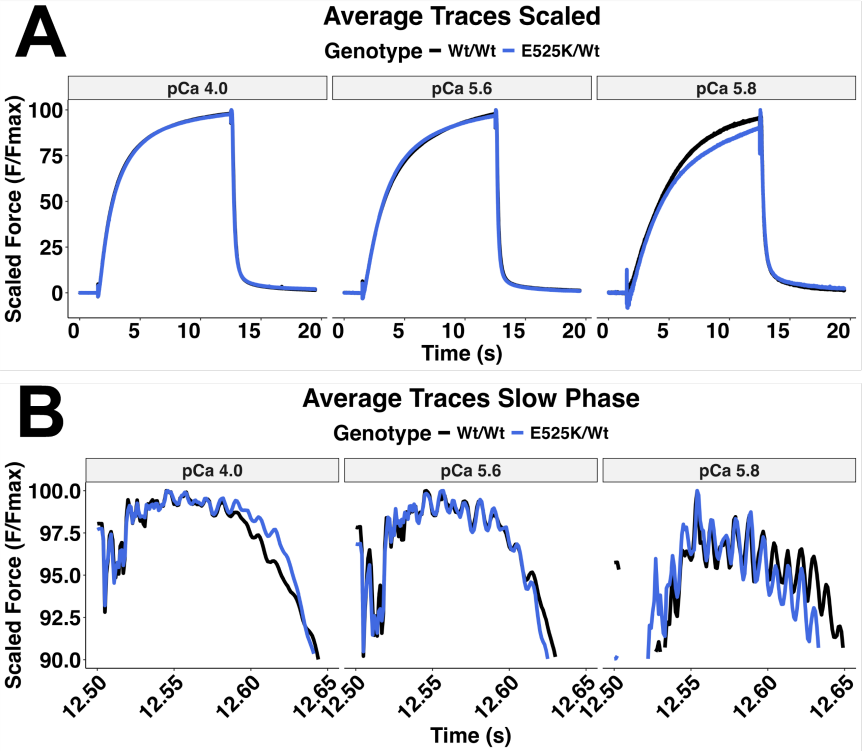

Supplemental Figure 3-2: Scaled traces for WTC11 E525K myofibrils.

Whole myofibril traces scaled to max force to compare the shape of the traces for WT/WT and E525K/WT myofibrils (A) and partial traces zoomed in to show the slow phase of relaxation (B).

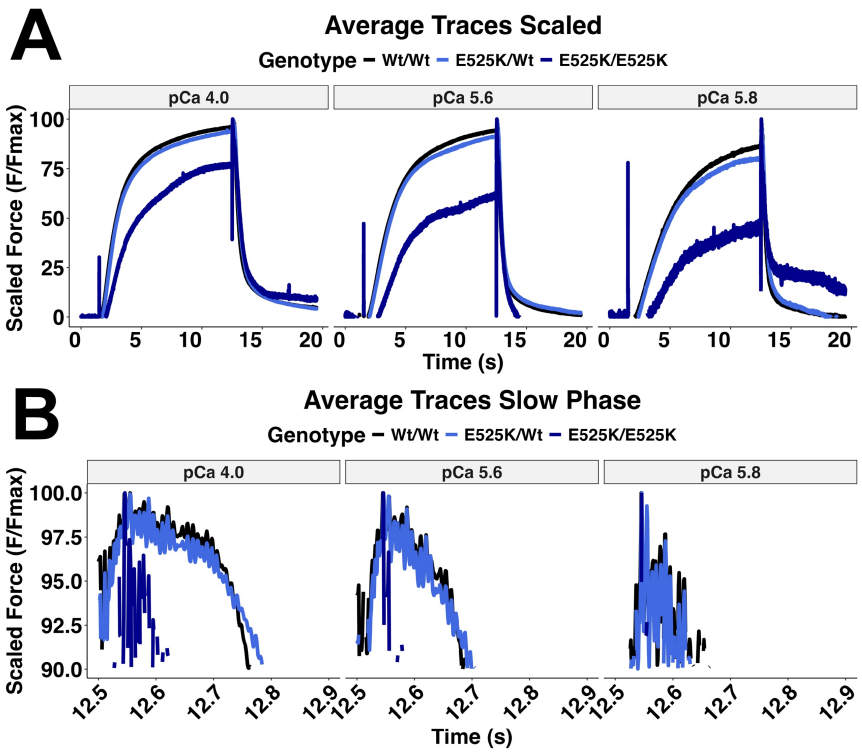

Supplemental Figure 3-3: Scaled traces for UC2 E525K myofibrils.

Whole myofibril traces scaled to max force to compare the shape of the traces for WT/WT and E525K/WT myofibrils (A) and partial traces zoomed in to show the slow phase of relaxation (B). Increased noise can be seen due to the extremely weak nature of these myofibrils as well as the (relatively) low N of 2-3 biological replicates.

Future Work on the E525K Mutation

This investigation into the E525K mutation has yielded interesting results, but it has also highlighted several key areas for future work. These open questions will form the basis of my initial post-doctoral research, extending the current findings to develop a more comprehensive understanding of the mutation's effects. Ultimately, comparing results between the two different genetic backgrounds (WTC11 and UC2) presents inherent challenges. It is difficult to completely isolate the effect of a single mutation when there are thousands of other small genetic differences between the cell line backgrounds that could be playing a role. Furthermore, the WTC11 background cell line used in this study has a pre-existing eGFP tag on the α-actinin protein, a sarcomeric protein. This modification could alter the contractile properties of the cell, making direct comparisons with the UC2 background less straightforward. For these reasons, future work will primarily focus on comparing results within a given genetic background to understand the impact of the E525K mutation more accurately. However, the comparison between different genetic backgrounds remains valuable for investigating the penetrance of the mutation—that is, the extent to which the mutation expresses its phenotype across different genetic contexts.

<u>The importance of mechanical load in destabilizing the autoinhibited state of E525K myosin is a critical area for further study.</u>

Work from others has shown that this mutation stabilizes the IHM state which is the structural basis of the autoinhibited sate of myosin (Duno-Miranda et al. 2023, 2024; Rasicci et al. 2022). Future experiments will focus on applying different levels of mechanical load/tension to isolated myofibrils with the E525K mutation to determine the precise conditions under which the inhibited sate of myosin is destabilized (see **chapter 4**). This will provide crucial insights into

the mechanosensitive nature of the mutation and its potential role in the progression of heart disease.

Transcriptomic and proteomic analysis of the E525K mutation.

A deeper understanding of the molecular consequences of the E525K mutation will be achieved through advanced proteomics and transcriptomics. By analyzing the protein and gene expression profiles of engineered heart tissues (EHTs) carrying the E525K mutation, we can identify specific pathways that are altered. This approach will allow us to move beyond observing functional changes to pinpointing the underlying molecular mechanisms. This is of particular interest given the conflicting results in some assays depending on the background of the cell line investigated. This analysis could find dysregulation of specific signaling pathways or a change in the expression of structural proteins, providing a more complete picture of how the mutation contributes to the disease phenotype.

Characterize another clonal cell line for each genotype and each background.

To enhance the rigor and reliability of these findings, we could characterize another clone of each genotype for both genetic backgrounds used in this study. These cell lines have already been engineered, but would need to be expanded, differentiated, and characterized. A wild-type control and an E525K/WT mutant for the WTC11 background, and a wild-type, a heterozygous (E525K/WT), and a homozygous (E525K/E525K) line for the UC2 background. This replication would be a demanding but highly rigorous approach, as it would help to rule out any potential clonal artifacts or off-target effects from the gene-editing process. While costly in terms of time and resources, this step would ensure the reproducibility and validity of our conclusions.

Full characterization of the UC2 background cells

A significant portion of the future work will focus on fully characterizing the cell lines from the UC2 genetic background. This includes several key steps. We will strive to improve the efficiency of both differentiation and maturation, aiming for a complete switch from the fetal α-myosin to the adult β-myosin in all cell lines by day 45 of differentiation. This is important because the mature isoform of myosin is critical for adult cardiac function. We also need to complete a full histologic characterization of the UC2 EHTs to confirm their cellular composition, such as the percentage of the tissue composed of cardiomyocytes versus other cell types. This will ensure that we are comparing tissues of similar quality and composition, which is a prerequisite for drawing valid conclusions about the effects of the E525K mutation.

Summary

Future research will expand upon the foundational work presented in this chapter by exploring the mechanosensitive nature of the E525K mutation, detailing its molecular consequences through proteomics and transcriptomics, and strengthening the study's rigor by characterizing additional cell clones. Furthermore, we will complete the full characterization of the UC2 genetic background cell lines, ensuring the quality and validity of our model system. While acknowledging the inherent challenges in comparing different genetic backgrounds, this future work is designed to address the remaining questions about these cell lines. Providing a more comprehensive and robust understanding of how the E525K mutation contributes to cardiac dysfunction.

Chapter 4 — Future Work: The ON/OFF State of Myosin in Human Myofibrils

One limitation of my work PhD work (as seen in Chapter 3) is that quantifying the ON/OFF population of myosin in intact myofibrils from humans is extremely challenging. The Kad Lab at the University of Kent has developed an assay to measure the ATPase rate of individual myosin molecules in a myofibril with sub-sarcomere resolution allowing for quantification of ON/OFF populations (Pilagov et al. 2022). For my post-doctoral work, I plan to work with the Kad Lab to establish the use of stem cell derived muscle for this assay so that any mutation of interest engineered into stem cells and can be studied in intact myofibrils. The following is an excerpt from my application for the Marie Skłodowska-Curie Actions (MSCA) post-doctoral fellowship to pursue this work—this project was titled STEM MUSCLE:

STEM MUSCLE – Unlocking Myosin's Secrets: How Our Muscles' Motor Moves from Idle to Drive

1. Excellence

1.1 Quality and pertinence of the project's research and innovation objectives (and the extent to which they are ambitious, and go beyond the state of the art)

Worldwide, disorders of the heart and skeletal musculature represent a leading cause of disability and morbidity (Cieza et al. 2020). Developing novel myosin-targeted drugs offers a promising avenue to address these diseases at their fundamental level: muscle contraction. However, effective targeting requires a complete understanding of how altered myosin function contributes to disease. In all muscles myosin in the thick filament interacts with actin in the thin filament to generate force in an ATP powered process. A key element of myosin regulation is the dynamic transition between its OFF state (where it is sequestered away from actin) and its ON state (where it is free to interact with actin) (Mohran et al. 2024). In all striated muscle (both cardiac and skeletal) myosin exists in a homeostasis between these ON (ready) and OFF

(reserve) states. The OFF-state acts as a reserve pool available to increase the contractile strength of muscle (**Figure 4-1**). Disruption of the homeostasis between these two states is strongly linked to cardiac (Barrick and Greenberg 2021; Toepfer et al. 2020) and skeletal (Carrington et al. 2023) myopathies. Due to the difficulty in obtaining diseased human tissue, disease-causing myosin mutations are often studied using animal models; but these models do not fully recapitulate the disease phenotypes observed in humans. To bridge this gap muscle tissue (cardiac and skeletal) can be generated from human induced pluripotent stem cells (hiPSCs). This offers unprecedented flexibility for studying disease in a human context; augmented by the ability to use gene editing to introduce single amino acid variants enabling the study of any disease-causing mutation of interest.

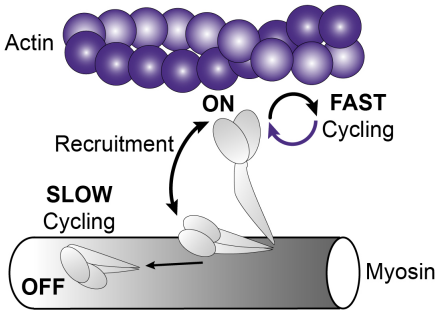

Figure 4-1: The ON/OFF states of myosin and myosin recruitment.

My PhD work at the University of Washington used state of the art methodology to measure contraction and muscle mechanics in hiPSC derived muscle tissue harboring disease causing mutations. I used these mechanics measurements to investigate the molecular mechanisms of disease-causing mutations. However, an inability to accurately quantify the ON/OFF population of myosins in hiPSC derived muscle has been a major limitation in this field. This has recently been resolved by the technology developed in the Kad Lab at the University of Kent that allows for the ON/OFF population to be assayed in intact myofibrils (the organelle responsible for muscle contraction) and has been used to study muscle tissue from animals and humans (Pilagov et al. 2022, 2025). This approach uses single molecule super-localization microscopy, enabling the ON/OFF population to be assayed with unparalleled spatial precision, down to that of individual molecules within individual sarcomeres (the smallest subunit of myofibrils). I will

use this assay to ask questions about both the function and the incorporation of mutant myosins in myofibrils with single molecule resolution.

Objectives: the **OVERALL AIM** of the STEM MUSCLE proposal it to develop an assay to quantify ON/OFF myosin populations in intact human sarcomeres generated from induced pluripotent stem cells. This project will achieve this objective through the following **three objectives**:

Objective 1: Measure the spatially explicit ratio of ON to OFF myosin with single molecule super-localization molecular imaging in human stem cell derived skeletal muscle myofibrils. Sarcomeres within myofibrils are extremely well organized with fixed positions of myosins and associated proteins; this means that super-localization microscopy can reliably report the ON/OFF state for each myosin and how this is modulated by mutation and the local environment. I will start with hiPSC skeletal muscle (hiPSC-SkM) since current protocols for the generation of skeletal muscle from stem cells robustly generate long, well-organized myofibrils. I will leverage single-fluorescent molecule super-localization microscopy with Cy3-ATP to directly quantify the ON and OFF myosin populations in intact human myofibrils. Unlike bulk biochemistry assays, this novel approach, developed by the Kad Lab, uniquely determines the sub-sarcomeric localization of myosin recruitment in response to mutations, thereby elucidating its impact on contractile properties. Importantly, the Regnier lab already possesses a catalogue of different myosin mutant cell lines—many of which are thought to affect ON/OFF state homeostasis—I have access to these and will investigate a subset in this study (**Table 5-1**). This available resource will allow us to immediately begin characterizing the effect of these mutations.

Objective 2: Upgrade existing technologies for quantification of ON/OFF myosin states under conditions where mechanical tension is applied. The super-localization microscopy assay outlined in objective one does not currently allow for measurements in myofibrils under tension. This is a limitation because tension on myofibrils is hypothesized to promoting the recruitment of myosin heads out of the OFF state (Campbell et al. 2018). In this objective two micromanipulators will be mounted on the left and on the right side of the super-localization microscope so that individual myofibrils can be picked up and positioned in frame for imaging. This technological improvement will allow for both the length and tension to be controlled during quantification of ON/OFF myosin populations.

Objective 3: Optimize the maturation and morphology of stem cells derived cardiac myofibrils for use with super-localization imaging. While I have regularly generated myofibrils from cardiac muscle in the past, the maturity and morphology of myofibrils generated from hiPSC cardiac muscle (hiPSC-CM) is less robust than that for hiPSC-SkM. For this reason, tissue engineering approaches (e.g. long-term culture and patterning, or 3D culture) may be needed to generate cardiac myofibrils with the organization and maturity required for the super-localization microscopy approach. The ability to measure ON/OFF state populations in intact human cardiac myofibrils would be extremely valuable in classifying cardiomyopathy-associated mutations and developing personalized medicine for patients this class of diseases.

1.2 Soundness of the proposed methodology

1.2.1 Interdisciplinary Approach and Research Design

The Problem: To effectively address contractile abnormalities linked to disrupted myosin ON/OFF homeostasis, a robust assay capable of measuring myosin ATPase activity within intact human sarcomeres is crucial for achieving the European Commission's goal of personalized medicine. The STEM MUSCLE project tackles this by combining the expertise I

have developed during my PhD in the Regnier Lab at the University of Washington and the expertise of Kad Lab at the University of Kent.

My Expertise: During my PhD I regularly generated muscle tissue and myofibrils from hiPSCs for mechanics and biochemical assays. This means I am uniquely placed to carry out in-depth studies of mutations impacting myosin ON/OFF homeostasis. I also have extensive experience measuring the biomechanical properties of muscle at all scales, from whole organs to single myofibrils. Additionally, my PhD Lab has developed a catalogue of myosin mutation lines, suitable for studying myosin's ON/OFF population which will be available for this project (**Table 5-1**).

Table 5-1: Myosin Mutants

MYH3 Lines	**Predicted Effect of Mutation**
S292C	Destabilize OFF
T178I	Unchanged OFF
R672C	Unchanged OFF
MYH7 Lines	**Predicted Effect of Mutation**
G256E	Destabilize OFF
E525K	Stabilize OFF
H251N	Destabilize OFF

Kad Lab Expertise: The Kad Lab has developed an assay to measure the ATPase rate of individual myosin molecules in a myofibril with sub-sarcomere resolution (Pilagov et al. 2022). This assay uses fluorescent Cy3-ATP in conjunction with super-localization microscopy to monitors myosin ATPase activity in intact sarcomeres. In collaboration with the Regnier lab, they have recently used this assay to demonstrate that 50% of cardiac myosins are in the energy conserving OFF state (Pilagov et al. 2025).

Together, the STEM MUSCLE project will enable me, for the first time, to study the **ON/OFF populations of myosin** variants associated with myopathy **in human myofibrils with any disease-causing mutation**.

1.2.2 Research Methodology for Objectives

<u>Objective 1 Experimental Design:</u> Measure the spatially explicit ratio of ON to OFF myosin with super-localization molecular imaging in human stem cell derived skeletal muscle myofibrils.

Production of Skeletal Muscle Myofibrils: During my PhD work I developed a protocol for the robust differentiation of skeletal muscle myotubes from hiPSCs as well as the isolation of intact myofibrils from these cells. The natural progression of myosin isoform expression in developing skeletal muscle is MHY3 → MYH8 → MYH7, with significant isoform overlap during transitions. To modulate the expression of myosin isoforms I treat cells with siRNA targeting MYH3, MYH7, or MYH8 at the myoblast stage. After 24 hours of transfection the media is replaced, and the cells are differentiated into myotubes via serum starvation. **Figure 4-2A** demonstrates that hiPSC-SkM are predominantly MYH3 at day 3 (D3) of secondary differentiation, then MYH8 increases expression on D4-5. siRNA for MYH8 was effective in suppressing MYH8 to provide a predominant MYH3 isoform out to D5-7. **Figure 4-2B** shows quantitative measure of isoforms MYH3, 7 and 8, relative to β-actin for D3 (left) and D5 (center) with knock-down of MYH7 and MYH8. siRNA for MYH3 causes greater expression of MYH 8 and 7 (right). **Figure 4-2C** shows the elongated and mature morphology of muscle cells generated with this protocol. This demonstrates my ability to produce pure and mixed populations of myosin isoforms in hiPSC-SkM. This demonstrates I will be able to generate myofibrils made up from pure populations of MYH3, MYH8, or MYH7 for ON/OFF population analysis. This will allow for the first ever measurements of ON/OFF homeostasis in these isoforms in their native myofibril context.

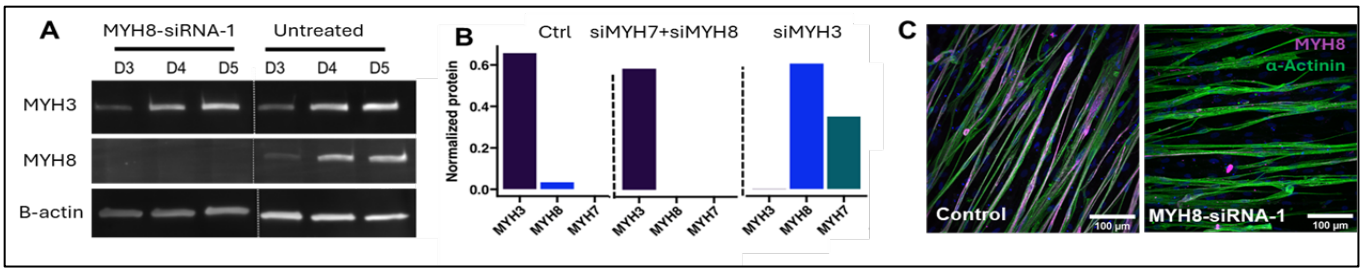

Figure 4-2: MYH3 enriched hiPSC-SkM cells.

(A, B) siRNA knockdown of MYH7 & 8 produces myocytes with predominantly MYH3 myosin, while siRNA knockdown of MYH3 results (B) in a mixed MYH8/7 population. (C) Myotube fusion in culture produces skeletal muscle cells with elongated morphologically mature myofibrils.

The ON and OFF state of myosin: I will measure the ON and OFF myosin populations using single fluorescent molecule (Cy3-ATP) super-localization microscopy, to determine the ratio of ON to OFF myosin in intact myofibrils. These myosin states are defined biochemically, where a fast-cycling rate (ATPase rate) of (~0.02-0.05 s^{-1}) defines the ON state and a slow-cycling rate (~0.002-0.005 s^{-1}) defines the OFF state (2). Using the assay developed by the Kad Lab (University of Kent, UK) I will determine the sub-sarcomeric location of ON and OFF myosins in the P (proximal), C (central), and D (distal) zones of the sarcomere (**Figure 4-3A**). I will further investigate how myosin recruitment from OFF to ON states is changed by mutations associated with muscle disease.

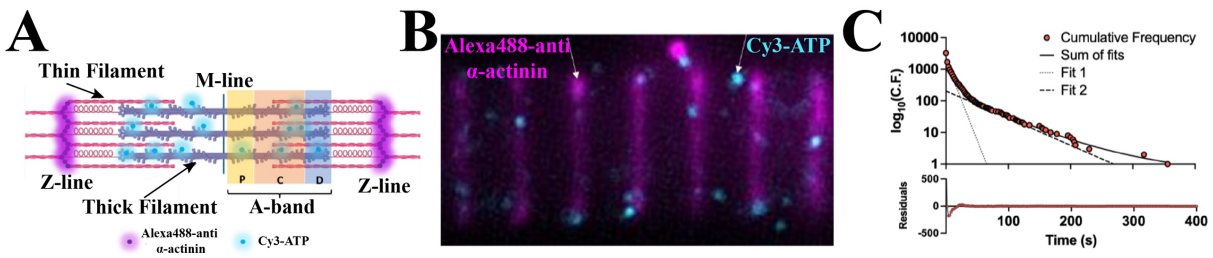

Figure 4-3: The super-localization assay.

(A) A schematic representation of a single sarcomere. P-, C-, and D-zones of the thick filament are labelled accordingly. 233 Alexa 488 – labelled α-actinin is denoted with magenta circles, while Cy3-ATP binding to the thick filament is 234 represented as cyan circles. (B) An enlarged section of a representative porcine cardiac left ventricular myofibril as observed during the super-localization microscopy assay. (C) Cumulative residence time histogram showing the distribution of ATP attachment events. The Cy3-ATP turnover rates per zone are then used to calculate the relative population ON (Fit 1) and OFF (Fit 2) myosin heads based on a triple exponential fit.

Super-localization imaging: This novel approach is based on super-localization single molecule microscopy to directly visualize the landing and subsequent release of ATP molecules within myofibrils by using Cy3-ATP, which is highly fluorescent and does not affect myosin activity. To measure discrete events the [Cy3-ATP] is kept at ~5 nM, with addition of 5 mM unlabeled (dark) ATP to ensure relaxed (non-rigor) myofibrils. Each time a fluorophore lands on a myosin it can be easily visualized (**Figure 4-3A-B**) and the center of its point spread function super-localized with ~30 nm accuracy (Pilagov et al. 2022; Smith et al. 2021). Cy3-ATP molecules remain bound until released as Cy3-ADP, providing an ATPase cycling rate. From a population of such measurements, lifetimes within each zone of the sarcomere are plotted (**Figure 4-3C**), which is subsequently fit to a multi-exponential decay to reveal two populations ON (amplitude of Fit 1) and OFF (amplitude of Fit 2). From their amplitudes the relative populations can be derived and assigned to the subzones of the myofibril's sarcomere (P-, C-, and D-zones; **Figure 4-3A**). Importantly, hiPSC-SkMs have the mature sarcomere structure (**Figure 4-4A**) required for high-resolution measures of myosin populations within the three thick filament zones (**Figure 4-3A-B**).

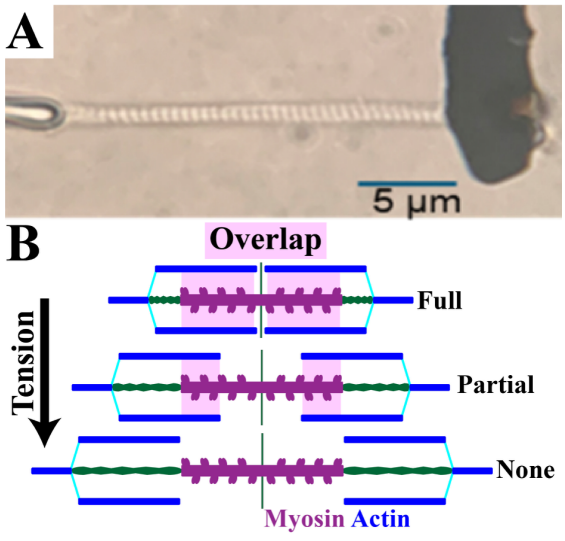

Figure 4-4: Example hiPSC-SkM myofibril and sarcomere overlap.

(A) Single myofibril from hiPSC-SkM suspended between two micromanipulators. (B) Schematic of sarcomere overlap

<u>Objective 2 Experimental Design:</u> Upgrade existing technologies for quantification of ON/OFF myosin states under conditions where mechanical tension is applied.

Technology Development for Super-Localization Microscopy: Currently the super-localization assay is performed using a microfluidic chamber with fluorescently tagged myofibrils adhered to the surface. Buffer containing the Cy3-ATP is flowed into the chamber and then imaged. This setup does not allow for individual myofibrils to be placed under tension. I propose to extend the use of this single molecule assay to include tension using my experience of working with micromanipulators to suspend individual myofibrils between glass microneedles (**Figure 4-4A**). I have used this approach in the past to study the response of single myofibrils to changes in solution conditions while maintaining known loads. The Kad lab have acquired the micromanipulators required and together with my experience I intend to augment the Kad Lab's existing setup and then take the first single molecule resolution measurements of myosin ON/OFF homeostasis in myofibrils under tension. By extending the sarcomere to different lengths I will be ablet to investigate the impact of different regions of the thick and thin filaments overlapping. At full overlap (low tension) I can ensure that the C and D zones are overlapped, medium extensions will lead to only the D zone overlapping, and large extensions (high tension) will lead to a complete loss of overlap between the actin and myosin filaments (**Figure 4-4B**). This is extremely exciting because I will be able to isolate the contributions of each of these zones to the generation of force and determine in relaxing conditions which sections control the ON/OFF equilibrium. This approach will revolutionize our understanding of how muscle works, providing insights into the early phases of activation that are not accessible by any other techniques. This crucial advancement will enable the investigation of the mechano-sensing properties of myosin and how mechanical load directly impacts its ON/OFF state transitions.

<u>Objective 3 Experimental Design:</u> Optimize the maturation and morphology of stem cells derived cardiac myofibrils for use with super-localization imaging.

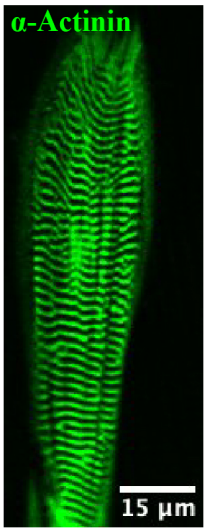

Figure 4-5: Patterned hiPSC-CM.

Production of Cardiac Muscle Myofibrils: The generation of hiPSC-CM is an established protocol, however the myotubes generated by this protocol are less elongated and less mature than those generated from the skeletal muscle differentiation. I have established in multiple cell lines carrying MYH7 mutations that expression of the MYH7 myosin isoform is not altered hiPSC-CM cells. To generate myofibrils with the high degree of organization required for the super-localization imaging outlined in objective #1 I anticipate the need to augment the established differentiation protocol to induce further maturation of the myofibrils in hiPSC-CMs. Based on my previous experience hiPSC-CM can be matured in three main ways: First, long term culture: aging hiPSC-CM reproducibly matures their myofibril morphology (Karbassi et al. 2020). Second, patterning: hiPSC-CM are remarkably susceptible to external morphometric cues and develop mature structure when forced into an elongated shape (Karbassi et al. 2020); my preliminary results show the high degree of organization achieved by patterning hiPSC-CMs (**Figure 4-5**). Third, 3D culture and long-term stimulation: encapsulating hiPSC-CM in 3D engineered tissues and “exercising” them via long term electrical pacing can lead to advanced maturation (Ronaldson-Bouchard et al. 2018). The generation of morphometrically mature cardiac myofibrils is ambitious, but the capacity to assess the ON/OFF state within intact human cardiac myofibrils would be exceptionally beneficial in the classification and treatment of cardiomyopathy mutations. Finally, the techniques and technologies developed in objectives #1 and #2 will be applied to measure lengthen and tension dependence for the first time in intact human cardiac myofibrils.

1.2.3 Gender Dimension and Diversity Aspects

Biological sex as well as racial background are important dimension of many myopathies (Vinciguerra et al. 2023). While disorders linked directly to myosin mutation are not dependent on biological sex or racial background these factors play an important role in disease progression as well as disease diagnosis (Butters, Lakdawala, and Ingles 2021). For all work proposed here stem cell lines with a diversity of biological sex/background will be selected to ensure samples represent the patient population suffering from the muscle diseases. Findings related to gender/race/background differences in myopathy disease progression would be an excellent basis for future scientific publication.

1.2.4 Open Science Practices

In alignment with the European Commission open science policy all scientific papers resulting from this work will be published in open access academic journals, pre-prints will be made available on bioRxiv and all accepted manuscripts will be published with supporting data on the Kent academic repository (https://kar.kent.ac.uk/). Additionally, a GitHub repository has been established for the Kad Lab and all modelling and analysis code used in my work will be made open source and available to other researchers and the public (https://github.com/Kad-Lab/).

2. Impact

2.2.1 The magnitude and importance of the project's contribution to the expected scientific, societal and economic impacts

Mutations in myosin are major contributors to genetic muscle disease. Worldwide it is estimated that 1.7 billion people suffer from some form of heart or skeletal muscle disease (Cieza et al. 2020). Mechanistic understanding of the relationship between mutations and disease lags the association of the two and is an obstacle to determining the pathogenicity of

new mutations. I will bridge this gap by utilizing biochemical and analytical approaches to visualize how mutations alter myosin function and contribute to disease.

hiPSC derived muscle is an ideal system to study myosin variants. Studying mutant myosin in a human model system is critical, but human cardiac muscle myosin is not amenable to common recombinant protein expression methods. I have been at the forefront of developing tools and maturation protocols to study myosin and sarcomere performance at the level of isolated motor proteins and sub-cellular contractile organelles (myofibrils) from hiPSC. These approaches when combined with the state-of-the-art biochemistry approaches developed by the Kad Lab are essential to understand the molecular basis of altered function with disease-causing myosin variants.

Myosin is an emerging therapeutic target for muscle disease. Multiple myosin targeted small molecule activators and inhibitors are entering clinical care however only one has been approved. Mavacamten was recently approved as the first in class myosin targeted drug for use in patients with obstructive hypertrophic cardiomyopathy (in the EU and US). Subgroup analysis of clinical trial results showed that patients with pathogenic mutations in myofibril proteins had the most benefit, while those without a pathogenic variant showed no benefit (Olivotto et al. 2020). This demonstrates that in real world patient care it is critical to determine the patients that can best benefit from myosin targeted drugs.

The assays and tools developed by **the STEM MUSCLE project** will focus on a selection of myosin variants that impact a key aspect of myosin biochemistry: ON/OFF homeostasis. Findings from my biochemical analysis will build the scientific community's fundamental understanding of this phenomenon and will directly contribute to ongoing work in the pharmaceutical industry. The ability to select clinical trial participants based on their genetic

background, as enabled by this research, would not only improve the likelihood of successful clinical trial outcomes and drug approval but would also reduce the time and cost associated with clinical development. This endeavor directly supports the **European Commission's overarching goal of advancing personalized medicine**, which necessitates a deep understanding of how a patient's unique genetic makeup and background influence disease development. Finally, this fellowship sets the stage for **a long-term collaboration between the EU and US** a connection that will contribute to muscle research for years to come after the conclusion of the STEM MUSCLE project.

3. Implementation

3.1 Quality and effectiveness of the work plan, assessment of risks and appropriateness of the effort assigned to work packages

3.1.1 Quality and Effectiveness of The Work Plan

The work plan for STEM MUSCLE is broken into three research phases and six work packages (WPs) each with some overlap and flexibility. Note that significant overlap between research WPs will allow time for the extended differentiation and maturation of stem cell derived muscle without delaying progress. The STEM MUSCLE Gantt chart (**Figure 4-6**) illustrates the organization of each of the WPs.

Research WP1 [Months 1-12]: Addresses Objective 1 (O1) and is dedicated to: (O1a) the establishment of protocols at the University of Kent for the generation of hiPSC-SkM and (O1b) optimization of super-localization (SL) imaging for use with stem cell derived myofibrils.

Research WP2 [Months 2-18]: Will focus on O2 where technology development (O2a), and the mutant MYH cell lines (O2b) will be used to study mutant myofibrils under load to learn about ON/OFF homeostats under tension and in diseased conditions.

Research WP3 [Months 8-24]: Will pursue the ambitious objective of isolating mature myofibrils from hiPSC-CM through: (O3a) establishing protocols for the differentiation of stem cells into cardiac muscle, and (O3b) optimizing the advanced maturation of hiPSC-CM.

Dissemination WP4: Will ensure the dissemination of research results through continuously sharing results via social media, peer reviewed publications for each research package (P1, P2 & P3), presentations at four international conferences (C1-4), local seminar presentations at the University of Kent (S1-3), and international presentations at the University of Washington (S4 & S5).

Training WP5: Training will involve holding semi-annual progress meetings (PM) with my international team of collaborators. Within the first six months of the project, I will compete an ethics training (ET) on the use of human stem cells create a career development plan (CDP). After the initial six-month research program setup, I will continue my academic development by teaching two university classes related to my expertise. I will also work in lab continuously mentoring undergraduate and graduate students.

Monitoring WP6: During the first two months a data monitoring plan (DMP) will be established, and during the final two months a plan for the dissemination and exploitation of results (PDE) will be submitted. Finally, to ensure the successful advancement of the STEM MUSCLE project, progress will be regularly monitored via key research milestones which have been defined for each objective.

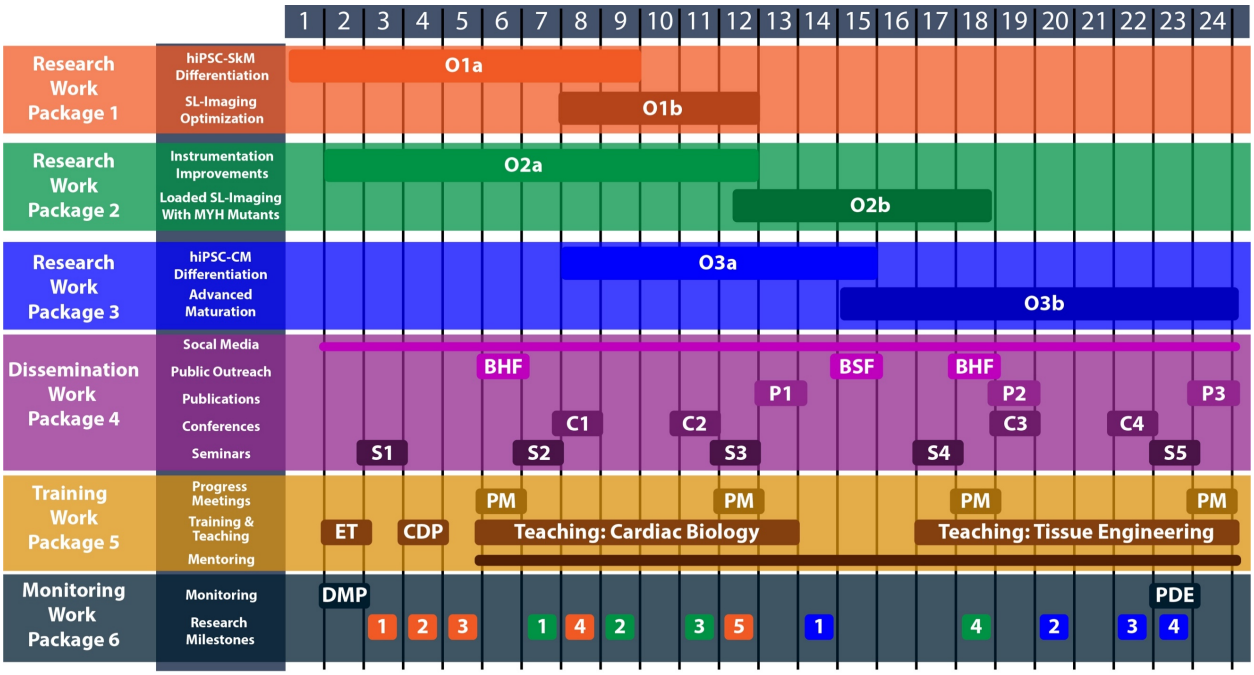

Figure 4-6: Gantt chart for the STEM MUSCLE project.

O Objective; **BHF** British Heart Foundation Fundraiser; **BSF** British Science Festival Lecture; **P** Publication; **C** Conference; **S** Seminar; **PM** Progress Meeting; **ET** Ethics Training; **CDP** Career Development Plan; **DMP** Data Monitoring Plan; **PDE** Plan for Dissemination and Exploitation. Key research milestone timepoints for each objective are color coded and listed at the bottom.

Key Research Milestones: (See color coded time points in **Figure 4-6 WP6**)

Objective 1: *Measure the spatially explicit ratio of ON to OFF myosin with super-localization molecular imaging in human stem cell derived skeletal muscle myofibrils.*

1. Primary differentiation of hiPSCs to the myoblast stage so that myoblasts can be banked (stored in liquid nitrogen) for future experimentation.
2. Secondary differentiation of myoblasts into contractile hiPSC-SkM. Autonomism contraction in the dish as well as mature myofibril morphology will indicate successful differentiation.
3. Confirm expected myosin expression (MYH3, 8, or 7) after siRNA treatment and secondary differentiation via protein isolation and myosin blot.
4. Isolation of well-formed morphometrically mature myofibrils from hiPSC-SkM.
5. Measure ON/OFF homeostasis in hiPSC-SkM derived myofibrils expressing predominantly MYH3, 8, or 7.

Objective 2: *Upgrade existing technologies for quantification of ON/OFF myosin states under conditions where mechanical tension is applied.*

1. Install instrumentation (micromanipulators) to handle isolated single myofibrils and confirm function of the system with myofibrils form adult animal tissue.
2. Integrate instrumentation with existing super-localization microscopy setup and existing microfluidic flow cell.
3. Confirm expression of expected myosin isoform (MYH3, 8, or 7) in hiPSC-SkM cells carrying MYH mutations.
4. Measure ON/OFF homeostasis in hiPSC-SkM mutant myofibrils under tension.

Objective 3: *Optimize the maturation and morphology of stem cells derived cardiac myofibrils for use with super-localization imaging.*

1. Differentiate hiPSC-CM into contractile cells showing automaticity and myofibril formation *in vitro*.
2. Patterning and long-term culture (>90 days) OR 3D-culture and pacing to mature hiPSC-CM myofibrils. Morphology will be assessed by α-actinin imaging if myofibril morphology.
3. Isolation of well-formed morphometrically mature myofibrils from hiPSC-CM.
4. Measure ON/OFF homeostasis in hiPSC-CM myofibrils carrying cardiomyopathy mutations under tension.

3.1.2 Assessment of Risks

Work with hiPSC-SkM is expected to go smoothly since the muscle tissue generated using this technique is nearly as well formed as adult muscle tissue. I expect the hiPSC-CM to be a higher risk project based on the less mature morphology seen in these tissues. However, even if hiPSC-CMs cannot be matured to a level where this assay can be run all experiments on native and mutant myosin isoforms (MYH3 & MYH7) can be run using hiPSC-SkM cells. The biochemistry of these myosin molecules is likely to be similar in both striated muscle types so even with this limitation my results would still generate meaningful data for cardiomyopathy disease. For the technological improvements proposed in objective #2 the goal is to take measurements on myofibrils derived from hiPSCs. However, if the generation of myofibrils is harder than expected or if optimization of muscle differentiation takes longer than expected all technological improvements can be validated using animal tissue.

Furthermore, every key research milestone has been designated as a go/no-go point, ensuring a deliberate and phased approach to advancing each research objective. The timeline for each objective has been carefully constructed with inherent flexibility, facilitating necessary adaptations and allowing for subsequent attempts to optimize results.

3.1.3 Appropriateness of The Effort Assigned to Work Packages

The effort assigned to the STEM MUSCLE Work Packages is highly appropriate, reflecting a well-structured research plan with clear dependencies outlined as milestones. WP1 is front-loaded to establish critical foundational differentiation, tissue isolation, and imaging

protocols within year one of the project. WP2 then builds directly on these capabilities, by establishing new tools and investigating myosin variants. WP3, the most ambitious objective, is appropriately allocated later in the project timeline, leveraging the advancements from the preceding WPs and accounting for the inherent complexity of isolating mature cardiac myofibrils. This staggered and overlapping design ensures that effort is applied efficiently as the project progresses through each research phase. Finally, dissemination as well as training and mentorship are aligned with each research phase to maximize the impact of these publications, conference meetings, and community outreach efforts.

Chapter 5 — Summary and Conclusions

This thesis embarked on an investigation into the intricate regulatory mechanisms governing myosin function, with a particular focus on its conformational dynamics and the role of myosin mutations cardiomyopathy. Through a multifaceted and multiscale approach this work utilized molecular dynamics simulations, detailed biochemical, biophysical characterization, and stem cell derived muscle models to interrogate disease pathology.

Chapter Two utilized molecular dynamics models to delve into the conformational state space occupied by myosin's critical Loop 2 structure. This work mapped the state conformational state of this flexible structure in both a native and diseased context, enabling the construction of a model how this structure regulates myosin activation and the formation of the weakly-bound state. This model posits that the extension or retraction of Loop 2 serves as a crucial regulatory axis through which force generation in the heart can be precisely modulated. By studying two specific mutations, E525K and V606M, both associated with cardiomyopathy and increased actin binding, this research directly linked the observed conformational changes of Loop 2 to disease-causing phenotypes. These findings hold substantial implications not only for understanding the mechanisms underlying various myosin mutations but also for the strategic development of myosin-targeted small molecule drugs. Given that both naturally occurring mutations and therapeutic small molecules often exert their effects by allosterically regulating myosin, it is possible that many other mutations and drugs could alter the conformational state space occupied by Loop 2, thereby impacting myosin's functional output.

Building upon the foundation laid in Chapter Two, Chapter Three specifically focused on the E525K mutation, providing a detailed characterization of its impact on myosin function. This work used stem cell derived muscle to explore the importance of mechanical load on the

regulation of myosin recruitment, activation, and cycling within the physiological context of the sarcomere. The investigations revealed several distinct changes attributable to the E525K mutation: notably, an increase in actin binding affinity, decreased force generation in both cellular and tissue environments, and observable alterations in sarcomere formation and organization. These findings collectively underscore the critical role of mechanical forces in modulating the phenotypic expression of this mutation. Equally important were the properties that remained unchanged: the overall cycling rate of E525K myosin under loaded conditions was found to be remarkably like WT. Furthermore, calcium transients, the fundamental signals for muscle contraction, were also found to be unaltered, indicating that the mutation's primary effects are intrinsic to the myosin molecule itself rather than upstream signaling pathways.

Finally, Chapter Four outlined a roadmap for future research, designed to move past some of the inherent physical limitations encountered during the present PhD work. This includes leveraging advanced techniques such as super-localization imaging and sophisticated biochemistry to comprehensively investigate the ON/OFF homeostasis of myosin in a more physiologically relevant context. As highlighted in Chapter Three, the biochemical and biophysical properties of myosin can exhibit considerable differences when the molecule is integrated into the highly organized structure of a sarcomere or subjected to the varying loaded conditions characteristic of an active muscle. Future work will therefore aim to bridge the gap between in vitro biochemical studies and in vivo mechanical function, providing a more complete picture of myosin's regulatory landscape.

In summary, this doctoral work advanced our understanding of myosin's relationship to cardiac contractility and disease. By intricately detailing the role of Loop 2 dynamics in force regulation (Chapter Two) and characterizing the specific functional consequences of the E525K mutation within loaded systems (Chapter Three), this thesis has not only provided fundamental

insights into myocardial function but also established a mechanistic link between molecular changes and cardiomyopathy. The development of a model linking Loop 2 dynamics to force regulation offers a new framework for considering myosin's allosteric regulation, with broad implications for interpreting other disease-causing mutations and guiding the rational design of small molecule therapeutics. The future directions outlined (Chapter Four), emphasizing super-localization imaging and in-sarcomere biochemical assays, are poised to overcome current experimental hurdles, promising a deeper understanding of myosin's activation states in physiological and pathological contexts. Ultimately, this research provides a crucial foundation for developing more targeted and effective interventions for cardiac diseases driven by myosin dysfunction.

Chapter 6 — Appendix

The following is an essay which has been submitted to Science's Working Life weekly publication.

Creativity in Research and Mentorship: How Juggling Made Me a Better PhD Student

If I could give myself one piece of advice when I started my graduate PhD, it would be to take up juggling. Let me explain. I worked very hard to get into graduate school, memorizing my textbooks, volunteering my time working in labs starting in my freshman year, and constantly applying for fellowships and scholarships. All that hard work paid off and I got into one of the best Bioengineering PhD programs in the world, but then something interesting happened. Suddenly I was surrounded by people who were all working just as hard as me if not even harder. People who were so dedicated to science and the pursuit of knowledge that they quite literally lost sleep over it. At the same time this was happening I also found that my usual approach to success in my studies was failing me. Working through the weekend was no longer setting me apart from the crowd and—more importantly—it also was not allowing me to generate the ideas and insight I needed to be successful as a PhD. For a mind to be creative, it cannot be exhausted. I was lacking was space for creativity.

Success in high school and college science classes had a lot to do with how dedicated I was and less to do with my creativity. There was just a lot that to learn and memorize and so spending all Sunday (or even all weekend) studying and memorizing served me well on my midterms. It has also served me well for years to come in academia—because knowing that "cervix" is Latin for neck will save you embarrassment in your anatomy class. However, there is more to being a good scientist than an ability to memorize facts and figures.

That is where my juggling balls help me. For me, juggling isn't just a break from my work it is a break from being in my mind. They are a physical activity that requires focus, and I cannot think about my research or my grant deadlines while I am juggling, or I will drop the balls. I have developed a habit of taking short juggling breaks throughout my day and they have served me well. As a side effect of pursing this PhD, I have become an excellent juggler, and I have taught three undergrads how to juggle. This is a time of uncertainty in academia, with funding cuts the future of graduate education and research in general feels insecure. As we move forward thought these times, I highly recommend juggling to keep your mind sharp and your arms limber.

The transition between undergraduate studies and graduate studies is best summed up by a transition from a focus on finding correct answers to a focus on finding good questions. The synthesis of facts into new ideas for your grant proposals, the ability to combine results from each experiment into a story—those activities take a lot of creativity. You still need to work hard to be a successful PhD student, but you also need to give your brain some time to recover so that you can have a few creative ideas. The students that I have mentored are brilliant—they come up with the most complicated and sophisticated experiments. I often find that my goal mentoring students through the transition to graduate school research is an exercise in—for want of a better word—dumbing down their approach. The best experiments in science are elegant. They are simple yes or no hypotheses that can be tested by an experiment. Being a good researcher has more to do with picking the right question than it has to do with finding the correct answer.

"It's the questions we can't answer that teach us the most. If you give a man an answer, all he gains is a little fact. But give him a question and he'll look for his own answers."

— Kvothe, The Name of The Wind

Bibliography

Ackermann, Maegen A., and Aikaterini Kontrogianni-Konstantopoulos. 2011. “Myosin Binding Protein-C: A Regulator of Actomyosin Interaction in Striated Muscle.” *Journal of Biomedicine and Biotechnology* 2011:636403. doi:10.1155/2011/636403.

Adhikari, Arjun S., Darshan V. Trivedi, Saswata S. Sarkar, Dan Song, Kristina B. Kooiker, Daniel Bernstein, James A. Spudich, and Kathleen M. Ruppel. 2019. “β-Cardiac Myosin Hypertrophic Cardiomyopathy Mutations Release Sequestered Heads and Increase Enzymatic Activity.” *Nature Communications* 10(1):2685. doi:10.1038/s41467-019-10555-9.

Ahmad, Ferhaan, J. G. Seidman, and Christine E. Seidman. 2005. “The Genetic Basis for Cardiac Remodeling.” *Annual Review of Genomics and Human Genetics* 6:185–216. doi:10.1146/annurev.genom.6.080604.162132.

Altinier, Alessandro, Alessia Paldino, Marta Gigli, Aniello Pappalardo, and Gianfranco Sinagra. 2019. “Current Management and Treatment.” in *Dilated Cardiomyopathy: From Genetics to Clinical Management*, edited by G. Sinagra, M. Merlo, and B. Pinamonti. Cham (CH): Springer.

Altis, Alexandros, Phuong H. Nguyen, Rainer Hegger, and Gerhard Stock. 2007. “Dihedral Angle Principal Component Analysis of Molecular Dynamics Simulations.” *The Journal of Chemical Physics* 126(24):244111. doi:10.1063/1.2746330.

Anandakrishnan, Ramu, Boris Aguilar, and Alexey V. Onufriev. 2012. “H++ 3.0: Automating pK Prediction and the Preparation of Biomolecular Structures for Atomistic Molecular Modeling and Simulations.” *Nucleic Acids Research* 40(Web Server issue):W537-541. doi:10.1093/nar/gks375.

Auguin, Daniel, Julien Robert-Paganin, Stéphane Réty, Carlos Kikuti, Amandine David, Gabriele Theumer, Arndt W. Schmidt, Hans-Joachim Knölker, and Anne Houdusse. 2024.

"Omecamtiv Mecarbil and Mavacamten Target the Same Myosin Pocket despite Opposite Effects in Heart Contraction." *Nature Communications* 15(1):4885. doi:10.1038/s41467-024-47587-9.

Barozet, Amélie, Pablo Chacón, and Juan Cortés. 2021. "Current Approaches to Flexible Loop Modeling." *Current Research in Structural Biology* 3:187–91. doi:10.1016/j.crstbi.2021.07.002.

Barrick, Samantha K., and Michael J. Greenberg. 2021. "Cardiac Myosin Contraction and Mechanotransduction in Health and Disease." *The Journal of Biological Chemistry* 297(5):101297. doi:10.1016/j.jbc.2021.101297.

Bartlett, Gail J., Craig T. Porter, Neera Borkakoti, and Janet M. Thornton. 2002. "Analysis of Catalytic Residues in Enzyme Active Sites." *Journal of Molecular Biology* 324(1):105–21. doi:10.1016/S0022-2836(02)01036-7.

Bello, Juan, and Mark V. Pellegrini. 2024. "Mavacamten." in *StatPearls*. Treasure Island (FL): StatPearls Publishing.

Berlow, Rebecca B., H. Jane Dyson, and Peter E. Wright. 2015. "Functional Advantages of Dynamic Protein Disorder." *FEBS Letters* 589(19, Part A):2433–40. doi:10.1016/j.febslet.2015.06.003.

Bers, Donald M. 2002. "Cardiac Excitation–Contraction Coupling." 415:8.

Bielawski, Kevin S., Andrea Leonard, Shiv Bhandari, Chuck E. Murry, and Nathan J. Sniadecki. 2016. "Real-Time Force and Frequency Analysis of Engineered Human Heart Tissue Derived from Induced Pluripotent Stem Cells Using Magnetic Sensing." *Tissue Engineering Part C: Methods* 22(10):932–40. doi:10.1089/ten.tec.2016.0257.

Blankenburg, Robert, Katarzyna Hackert, Sebastian Wurster, René Deenen, J. G. Seidman, Christine E. Seidman, Martin J. Lohse, and Joachim P. Schmitt. 2014. "β–Myosin Heavy Chain Variant V606M Causes Very Mild Hypertrophic Cardiomyopathy in Mice, but

Exacerbates HCM Phenotypes in Mice Carrying Other HCM Mutations." *Circulation Research* 115(2):227–37. doi:10.1161/CIRCRESAHA.115.303178.

Bodt, Skylar M. L., Jinghua Ge, Wen Ma, David V. Rasicci, Rohini Desetty, J. Andrew McCammon, and Christopher M. Yengo. 2024. "Dilated Cardiomyopathy Mutation in Beta-Cardiac Myosin Enhances Actin Activation of the Power Stroke and Phosphate Release." *PNAS Nexus* 3(8):pgae279. doi:10.1093/pnasnexus/pgae279.

Braunwald, Eugene, Sara Saberi, Theodore P. Abraham, Perry M. Elliott, and Iacopo Olivotto. 2023. "Mavacamten: A First-in-Class Myosin Inhibitor for Obstructive Hypertrophic Cardiomyopathy." *European Heart Journal* 44(44):4622–33. doi:10.1093/eurheartj/ehad637.

Burkett, Emily L., and Ray E. Hershberger. 2005. "Clinical and Genetic Issues in Familial Dilated Cardiomyopathy." *Journal of the American College of Cardiology* 45(7):969–81. doi:10.1016/j.jacc.2004.11.066.

Butters, Alexandra, Neal K. Lakdawala, and Jodie Ingles. 2021. "Sex Differences in Hypertrophic Cardiomyopathy: Interaction With Genetics and Environment." *Current Heart Failure Reports* 18(5):264–73. doi:10.1007/s11897-021-00526-x.

Campbell, Kenneth S., Paul M. L. Janssen, and Stuart G. Campbell. 2018. "Force-Dependent Recruitment from the Myosin Off State Contributes to Length-Dependent Activation." *Biophysical Journal* 115(3):543–53. doi:10.1016/j.bpj.2018.07.006.

Carrington, Glenn, Abbi Hau, Sarah Kosta, Hannah F. Dugdale, Francesco Muntoni, Adele D'Amico, Peter Van den Bergh, Norma B. Romero, Edoardo Malfatti, Juan Jesus Vilchez, Anders Oldfors, Sander Pajusalu, Katrin Õunap, Marta Giralt-Pujol, Edmar Zanoteli, Kenneth S. Campbell, Hiroyuki Iwamoto, Michelle Peckham, and Julien Ochala. 2023. "Human Skeletal Myopathy Myosin Mutations Disrupt Myosin Head Sequestration." *JCI Insight* 8(21):e172322. doi:10.1172/jci.insight.172322.

Case, David A., Hasan Metin Aktulga, Kellon Belfon, David S. Cerutti, G. Andrés Cisneros, Vinícius Wilian D. Cruzeiro, Negin Forouzesh, Timothy J. Giese, Andreas W. Götz, Holger Gohlke, Saeed Izadi, Koushik Kasavajhala, Mehmet C. Kaymak, Edward King, Tom Kurtzman, Tai-Sung Lee, Pengfei Li, Jian Liu, Tyler Luchko, Ray Luo, Madushanka Manathunga, Matias R. Machado, Hai Minh Nguyen, Kurt A. O'Hearn, Alexey V. Onufriev, Feng Pan, Sergio Pantano, Ruxi Qi, Ali Rahnamoun, Ali Risheh, Stephan Schott-Verdugo, Akhil Shajan, Jason Swails, Junmei Wang, Haixin Wei, Xiongwu Wu, Yongxian Wu, Shi Zhang, Shiji Zhao, Qiang Zhu, Thomas E. Cheatham, Daniel R. Roe, Adrian Roitberg, Carlos Simmerling, Darrin M. York, Maria C. Nagan, and Kenneth M. Merz. 2023. "AmberTools." *Journal of Chemical Information and Modeling* 63(20):6183–91. doi:10.1021/acs.jcim.3c01153.

Cecchini, Marco, Yuri Alexeev, and Martin Karplus. 2010. "Pi Release From Myosin: A Simulation Analysis of Possible Pathways." *Structure (London, England : 1993)* 18(4):458–70. doi:10.1016/j.str.2010.01.014.

Childers, Matthew Carter, and Valerie Daggett. 2018. "Validating Molecular Dynamics Simulations against Experimental Observables in Light of Underlying Conformational Ensembles." *The Journal of Physical Chemistry B* 122(26):6673–89. doi:10.1021/acs.jpcb.8b02144.

Childers, Matthew Carter, Michael A. Geeves, and Michael Regnier. 2024. "Interacting Myosin Head Dynamics and Their Modification by 2′-Deoxy-ADP." *Biophysical Journal* 123(22):3997–4008. doi:10.1016/j.bpj.2024.10.013.

Childers, Matthew Carter, Michael Geeves, Valerie Daggett, and Michael Regnier. 2021. "Modulation of Post-Powerstroke Dynamics in Myosin II by 2′-Deoxy-ADP." *Archives of Biochemistry and Biophysics* 699:108733. doi:10.1016/j.abb.2020.108733.

Childers, Matthew Carter, and Michael Regnier. 2024. “Atomistic Simulations of Sarcomere Proteins.” Pp. 27–41 in *Familial Cardiomyopathies: Methods and Protocols*, *Methods in Molecular Biology*, edited by M. Regnier and M. Childers. New York, NY: Springer US.

Childers, Matthew Carter, Clare-Louise Towse, and Valerie Daggett. 2016. “The Effect of Chirality and Steric Hindrance on Intrinsic Backbone Conformational Propensities: Tools for Protein Design.” *Protein Engineering, Design and Selection* 29(7):271–80. doi:10.1093/protein/gzw023.

Childers, Matthew Carter, Clare-Louise Towse, and Valerie Daggett. 2018. “Molecular Dynamics-Derived Rotamer Libraries for d-Amino Acids within Homochiral and Heterochiral Polypeptides.” *Protein Engineering, Design and Selection* 31(6):191–204. doi:10.1093/protein/gzy016.

Chin, E. R., E. N. Olson, J. A. Richardson, Q. Yang, C. Humphries, J. M. Shelton, H. Wu, W. Zhu, R. Bassel-Duby, and R. S. Williams. 1998. “A Calcineurin-Dependent Transcriptional Pathway Controls Skeletal Muscle Fiber Type.” *Genes & Development* 12(16):2499–2509. doi:10.1101/gad.12.16.2499.

Chiu, Christine, Richard D. Bagnall, Jodie Ingles, Laura Yeates, Marina Kennerson, Jennifer A. Donald, Mika Jormakka, Joanne M. Lind, and Christopher Semsarian. 2010. “Mutations in Alpha-Actinin-2 Cause Hypertrophic Cardiomyopathy: A Genome-Wide Analysis.” *Journal of the American College of Cardiology* 55(11):1127–35. doi:10.1016/j.jacc.2009.11.016.

Cieza, Alarcos, Kate Causey, Kaloyan Kamenov, Sarah Wulf Hanson, Somnath Chatterji, and Theo Vos. 2020. “Global Estimates of the Need for Rehabilitation Based on the Global Burden of Disease Study 2019: A Systematic Analysis for the Global Burden of Disease Study 2019.” *The Lancet* 396(10267):2006–17. doi:10.1016/S0140-6736(20)32340-0.

Clobes, Amy M., and William H. Guilford. 2014. “Loop 2 of Myosin Is a Force-Dependent Inhibitor of the Rigor Bond.” *Journal of Muscle Research and Cell Motility* 35(2):143–52. doi:10.1007/s10974-014-9375-z.

Daehmlow, Steffen, Jeanette Erdmann, Tanja Knueppel, Christoph Gille, Cornelius Froemmel, Manfred Hummel, Roland Hetzer, and Vera Regitz-Zagrosek. 2002. “Novel Mutations in Sarcomeric Protein Genes in Dilated Cardiomyopathy.” *Biochemical and Biophysical Research Communications* 298(1):116–20. doi:10.1016/s0006-291x(02)02374-4.

Davis, Jennifer, L. Craig Davis, Robert N. Correll, Catherine A. Makarewich, Jennifer A. Schwanekamp, Farid Moussavi-Harami, Dan Wang, Allen J. York, Haodi Wu, Steven R. Houser, Christine E. Seidman, Jonathan G. Seidman, Michael Regnier, Joseph M. Metzger, Joseph C. Wu, and Jeffery D. Molkentin. 2016. “A Tension-Based Model Distinguishes Hypertrophic versus Dilated Cardiomyopathy.” *Cell* 165(5):1147–59. doi:10.1016/j.cell.2016.04.002.

Doran, Matthew H., Michael J. Rynkiewicz, Elumalai Pavadai, Skylar M. L. Bodt, David Rasicci, Jeffrey R. Moore, Christopher M. Yengo, Esther Bullitt, and William Lehman. 2023. “Myosin Loop-4 Is Critical for Optimal Tropomyosin Repositioning on Actin during Muscle Activation and Relaxation.” *The Journal of General Physiology* 155(2):e202213274. doi:10.1085/jgp.202213274.

Doran, Matthew H., Michael J. Rynkiewicz, David Rasicci, Skylar M. L. Bodt, Meaghan E. Barry, Esther Bullitt, Christopher M. Yengo, Jeffrey R. Moore, and William Lehman. 2023. “Conformational Changes Linked to ADP Release from Human Cardiac Myosin Bound to Actin-Tropomyosin.” *The Journal of General Physiology* 155(3):e202213267. doi:10.1085/jgp.202213267.

Dorsch, Larissa M., Diederik W. D. Kuster, Jan D. H. Jongbloed, Ludolf G. Boven, Karin Y. van Spaendonck-Zwarts, Albert J. H. Suurmeijer, Aryan Vink, Gideon J. du Marchie Sarvaas, Maarten P. van den Berg, Jolanda van der Velden, Bianca J. J. M. Brundel, and Paul A.

van der Zwaag. 2021. “The Effect of Tropomyosin Variants on Cardiomyocyte Function and Structure That Underlie Different Clinical Cardiomyopathy Phenotypes.” *International Journal of Cardiology* 323:251–58. doi:10.1016/j.ijcard.2020.08.101.

Duno-Miranda, Sebastian, Shane R. Nelson, David V. Rasicci, Skylar L. M. Bodt, Joseph A. Cirilo, Duha Vang, Sivaraj Sivaramakrishnan, Christopher M. Yengo, and David M. Warshaw. 2023. “Tail Length and E525K Dilated Cardiomyopathy Mutant Alter Human β-Cardiac Myosin Super-Relaxed State.” 2023.12.07.570656.

Duno-Miranda, Sebastian, Shane R. Nelson, David V. Rasicci, Skylar M. L. Bodt, Joseph A. Cirilo Jr, Duha Vang, Sivaraj Sivaramakrishnan, Christopher M. Yengo, and David M. Warshaw. 2024. “Tail Length and E525K Dilated Cardiomyopathy Mutant Alter Human β-Cardiac Myosin Super-Relaxed State.” *Journal of General Physiology* 156(6):e202313522. doi:10.1085/jgp.202313522.

Eisner, David A., Jessica L. Caldwell, Kornél Kistamás, and Andrew W. Trafford. 2017. “Calcium and Excitation-Contraction Coupling in the Heart.” *Circulation Research* 121(2):181–95. doi:10.1161/CIRCRESAHA.117.310230.

Elfrink, Kerstin, Wanqin Liao, Uwe Pieper, Stefanie J. Oeding, and Martin Bähler. 2014. “The Loop2 Insertion of Type IX Myosin Acts as an Electrostatic Actin Tether That Permits Processive Movement.” *PLOS ONE* 9(1):e84874. doi:10.1371/journal.pone.0084874.

Eswar, Narayanan, Ben Webb, Marc A. Marti-Renom, M. S. Madhusudhan, David Eramian, Min-Yi Shen, Ursula Pieper, and Andrej Sali. 2006. “Comparative Protein Structure Modeling Using Modeller.” *Current Protocols in Bioinformatics* Chapter 5:Unit-5.6. doi:10.1002/0471250953.bi0506s15.

Feest, Erik R., F. Steven Korte, An-yue Tu, Jin Dai, Maria V. Razumova, Charles E. Murry, and Michael Regnier. 2014. “Thin Filament Incorporation of an Engineered Cardiac Troponin C Variant (L48Q) Enhances Contractility in Intact Cardiomyocytes from Healthy and

Infarcted Hearts." *Journal of Molecular and Cellular Cardiology* 72:219–27. doi:10.1016/j.yjmcc.2014.03.015.

Geeves, Michael A., and Kenneth C. Holmes. 2005. "The Molecular Mechanism of Muscle Contraction." Pp. 161–93 in *Advances in Protein Chemistry*. Vol. 71. Elsevier.

Geeves, Michael A., Sherwin S. Lehrer, and William Lehman. 2019. "The Mechanism of Thin Filament Regulation: Models in Conflict?" *Journal of General Physiology* 151(11):1265–71. doi:10.1085/jgp.201912446.

Goodson, H. V., H. M. Warrick, and J. A. Spudich. 1999. "Specialized Conservation of Surface Loops of Myosin: Evidence That Loops Are Involved in Determining Functional Characteristics." *Journal of Molecular Biology* 287(1):173–85. doi:10.1006/jmbi.1999.2565.

Gordon, A. M., E. Homsher, and M. Regnier. 2000. "Regulation of Contraction in Striated Muscle." *Physiological Reviews* 80(2):853–924. doi:10.1152/physrev.2000.80.2.853.

Gu, Yina, Da-Wei Li, and Rafael Brüschweiler. 2015. "Decoding the Mobility and Time Scales of Protein Loops." *Journal of Chemical Theory and Computation* 11(3):1308–14. doi:10.1021/ct501085y.

Hagemann, Dirk, and Rui-Ping Xiao. 2002. "Dual Site Phospholamban Phosphorylation and Its Physiological Relevance in the Heart." *Trends in Cardiovascular Medicine* 12(2):51–56. doi:10.1016/s1050-1738(01)00145-1.

Hartman, James J., Darren T. Hwee, Julien Robert-Paganin, Chihyuan Chuang, Eva R. Chin, Samantha Edell, Ken H. Lee, Roshni Madhvani, Preeti Paliwal, Julien Pernier, Saswata Sankar Sarkar, Julia Schaletzky, Kristine Schauer, Khanha D. Taheri, Jingying Wang, Eddie Wehri, Yangsong Wu, Anne Houdusse, Bradley P. Morgan, and Fady I. Malik. 2024. "Aficamten Is a Small-Molecule Cardiac Myosin Inhibitor Designed to Treat Hypertrophic Cardiomyopathy." *Nature Cardiovascular Research* 3(8):1003–16. doi:10.1038/s44161-024-00505-0.

He, Xibing, Viet H. Man, Wei Yang, Tai-Sung Lee, and Junmei Wang. 2020. “A Fast and High-Quality Charge Model for the next Generation General AMBER Force Field.” *The Journal of Chemical Physics* 153(11):114502. doi:10.1063/5.0019056.

Heidenreich, Paul A., Biykem Bozkurt, David Aguilar, Larry A. Allen, Joni J. Byun, Monica M. Colvin, Anita Deswal, Mark H. Drazner, Shannon M. Dunlay, Linda R. Evers, James C. Fang, Savitri E. Fedson, Gregg C. Fonarow, Salim S. Hayek, Adrian F. Hernandez, Prateeti Khazanie, Michelle M. Kittleson, Christopher S. Lee, Mark S. Link, Carmelo A. Milano, Lorraine C. Nnacheta, Alexander T. Sandhu, Lynne Warner Stevenson, Orly Vardeny, Amanda R. Vest, Clyde W. Yancy, and ACC/AHA Joint Committee Members. 2022. “2022 AHA/ACC/HFSA Guideline for the Management of Heart Failure: A Report of the American College of Cardiology/American Heart Association Joint Committee on Clinical Practice Guidelines.” *Circulation* 145(18):e895–1032. doi:10.1161/CIR.0000000000001063.

Herman, Daniel S., Lien Lam, Matthew R. G. Taylor, Libin Wang, Polakit Teekakirikul, Danos Christodoulou, Lauren Conner, Steven R. DePalma, Barbara McDonough, Elizabeth Sparks, Debbie Lin Teodorescu, Allison L. Cirino, Nicholas R. Banner, Dudley J. Pennell, Sharon Graw, Marco Merlo, Andrea Di Lenarda, Gianfranco Sinagra, J. Martijn Bos, Michael J. Ackerman, Richard N. Mitchell, Charles E. Murry, Neal K. Lakdawala, Carolyn Y. Ho, Paul J. R. Barton, Stuart A. Cook, Luisa Mestroni, J. G. Seidman, and Christine E. Seidman. 2012. “Truncations of Titin Causing Dilated Cardiomyopathy.” *The New England Journal of Medicine* 366(7):619–28. doi:10.1056/NEJMoa1110186.

Hernandez, Olga M., Michelle Jones, Georgianna Guzman, and Danuta Szczesna-Cordary. 2007. “Myosin Essential Light Chain in Health and Disease.” *American Journal of Physiology-Heart and Circulatory Physiology* 292(4):H1643–54. doi:10.1152/ajpheart.00931.2006.

Homburger, Julian R., Eric M. Green, Colleen Caleshu, Margaret S. Sunitha, Rebecca E. Taylor, Kathleen M. Ruppel, Raghu Prasad Rao Metpally, Steven D. Colan, Michelle Michels, Sharlene M. Day, Iacopo Olivotto, Carlos D. Bustamante, Frederick E. Dewey, Carolyn Y. Ho, James A. Spudich, and Euan A. Ashley. 2016. “Multidimensional Structure-Function Relationships in Human β-Cardiac Myosin from Population-Scale Genetic Variation.” *Proceedings of the National Academy of Sciences of the United States of America* 113(24):6701–6. doi:10.1073/pnas.1606950113.

Hooijman, Pleuni, Melanie A. Stewart, and Roger Cooke. 2011. “A New State of Cardiac Myosin with Very Slow ATP Turnover: A Potential Cardioprotective Mechanism in the Heart.” *Biophysical Journal* 100(8):1969–76. doi:10.1016/j.bpj.2011.02.061.

Iyama, Teruaki, and David M. Wilson. 2013. “DNA Repair Mechanisms in Dividing and Non-Dividing Cells.” *DNA Repair* 12(8):620–36. doi:10.1016/j.dnarep.2013.04.015.

Jorgensen, William L., Jayaraman Chandrasekhar, Jeffry D. Madura, Roger W. Impey, and Michael L. Klein. 1983. “Comparison of Simple Potential Functions for Simulating Liquid Water.” *The Journal of Chemical Physics* 79(2):926–35. doi:10.1063/1.445869.

Kao, Kerry, and Michael A. Geeves. 2024. “Protocols for Myosin and Actin-Myosin Assays Using Rapid, Stopped-Flow Kinetics.” Pp. 191–211 in *Familial Cardiomyopathies*. Vol. 2735, *Methods in Molecular Biology*, edited by M. Regnier and M. Childers. New York, NY: Springer US.

Karbassi, Elaheh, Aidan Fenix, Silvia Marchiano, Naoto Muraoka, Kenta Nakamura, Xiulan Yang, and Charles E. Murry. 2020. “Cardiomyocyte Maturation: Advances in Knowledge and Implications for Regenerative Medicine.” *Nature Reviews Cardiology* 1–19. doi:10.1038/s41569-019-0331-x.

Katz, Arnold M. 2010. *Physiology of the Heart*. Fifth edition. Philadelphia, PA: LWW.

Kiani, Farooq Ahmad, and Stefan Fischer. 2014. “Catalytic Strategy Used by the Myosin Motor to Hydrolyze ATP.” *Proceedings of the National Academy of Sciences* 111(29):E2947–56. doi:10.1073/pnas.1401862111.

Kindi, Hamood N. Al, and Magdi H. Yacoub. 2018. “Surgical Myectomy: Rationale and Personalized Technique.” *Global Cardiology Science & Practice* 2018(3):35. doi:10.21542/gcsp.2018.35.

Kinnear, Caroline, Abdelrahman Said, Guoliang Meng, Yimu Zhao, Erika Y. Wang, Naimeh Rafatian, Neha Parmar, Wei Wei, Filio Billia, Craig A. Simmons, Milica Radisic, James Ellis, and Seema Mital. 2024. “Myosin Inhibitor Reverses Hypertrophic Cardiomyopathy in Genotypically Diverse Pediatric iPSC-Cardiomyocytes to Mirror Variant Correction.” *Cell Reports Medicine* 0(0). doi:10.1016/j.xcrm.2024.101520.

Klebl, David P., Sean N. McMillan, Cristina Risi, Eva Forgacs, Betty Virok, Jennifer L. Atherton, Sarah A. Harris, Michele Stofella, Donald A. Winkelmann, Frank Sobott, Vitold E. Galkin, Peter J. Knight, Stephen P. Muench, Charlotte A. Scarff, and Howard D. White. 2025. “Swinging Lever Mechanism of Myosin Directly Shown by Time-Resolved Cryo-EM.” *Nature* 1–8. doi:10.1038/s41586-025-08876-5.

Klein, Jennifer C., Adam R. Burr, Bengt Svensson, Daniel J. Kennedy, John Allingham, Margaret A. Titus, Ivan Rayment, and David D. Thomas. 2008. “Actin-Binding Cleft Closure in Myosin II Probed by Site-Directed Spin Labeling and Pulsed EPR.” *Proceedings of the National Academy of Sciences* 105(35):12867–72. doi:10.1073/pnas.0802286105.

Kooiker, Kristina B., Saffie Mohran, Kyrah L. Turner, Weikang Ma, Amy Martinson, Galina Flint, Lin Qi, Chengqian Gao, Yahan Zheng, Timothy S. McMillen, Christian Mandrycky, Max Mahoney-Schaefer, Jeremy C. Freeman, Elijah Gabriela Costales Arenas, An-Yu Tu, Thomas C. Irving, Michael A. Geeves, Bertrand C. W. Tanner, Michael Regnier, Jennifer Davis, and Farid Moussavi-Harami. 2023. “Danicamtiv Increases Myosin Recruitment

and Alters Cross-Bridge Cycling in Cardiac Muscle." *Circulation Research* 133(5):430–43. doi:10.1161/CIRCRESAHA.123.322629.

Lakdawala, Neal K., Birgit H. Funke, Samantha Baxter, Allison L. Cirino, Amy E. Roberts, Daniel P. Judge, Nicole Johnson, Nancy J. Mendelsohn, Chantal Morel, Melanie Care, Wendy K. Chung, Carolyn Jones, Apostolos Psychogios, Elizabeth Duffy, Heidi L. Rehm, Emily White, J. G. Seidman, Christine E. Seidman, and Carolyn Y. Ho. 2012. "Genetic Testing for Dilated Cardiomyopathy in Clinical Practice." *Journal of Cardiac Failure* 18(4):296–303. doi:10.1016/j.cardfail.2012.01.013.

Lee, Kyoung Hwan, Guidenn Sulbarán, Shixin Yang, Ji Young Mun, Lorenzo Alamo, Antonio Pinto, Osamu Sato, Mitsuo Ikebe, Xiong Liu, Edward D. Korn, Floyd Sarsoza, Sanford I. Bernstein, Raúl Padrón, and Roger Craig. 2018. "Interacting-Heads Motif Has Been Conserved as a Mechanism of Myosin II Inhibition since before the Origin of Animals." *Proceedings of the National Academy of Sciences* 115(9):E1991–2000. doi:10.1073/pnas.1715247115.

Lee, Soah, Alison S. Vander Roest, Cheavar A. Blair, Kerry Kao, Samantha B. Bremner, Matthew C. Childers, Divya Pathak, Paul Heinrich, Daniel Lee, Orlando Chirikian, Saffie E. Mohran, Brock Roberts, Jacqueline E. Smith, James W. Jahng, David T. Paik, Joseph C. Wu, Ruwanthi N. Gunawardane, Kathleen M. Ruppel, David L. Mack, Beth L. Pruitt, Michael Regnier, Sean M. Wu, James A. Spudich, and Daniel Bernstein. 2024. "Incomplete-Penetrant Hypertrophic Cardiomyopathy MYH7 G256E Mutation Causes Hypercontractility and Elevated Mitochondrial Respiration." *Proceedings of the National Academy of Sciences* 121(19):e2318413121. doi:10.1073/pnas.2318413121.

Li, Lin, Arghya Chakravorty, and Emil Alexov. 2017. "DelPhiForce, a Tool for Electrostatic Force Calculations: Applications to Macromolecular Binding." *Journal of Computational Chemistry* 38(9):584–93. doi:10.1002/jcc.24715.

Li, Lin, Zhe Jia, Yunhui Peng, Arghya Chakravorty, Lexuan Sun, and Emil Alexov. 2017. "DelPhiForce Web Server: Electrostatic Forces and Energy Calculations and Visualization." *Bioinformatics* 33(22):3661–63. doi:10.1093/bioinformatics/btx495.

Li, Pengfei, and Kenneth M. Jr. Merz. 2014. "Taking into Account the Ion-Induced Dipole Interaction in the Nonbonded Model of Ions." *Journal of Chemical Theory and Computation* 10(1):289–97. doi:10.1021/ct400751u.

Li, Pengfei, Lin Frank Song, and Kenneth M. Jr. Merz. 2015a. "Parameterization of Highly Charged Metal Ions Using the 12-6-4 LJ-Type Nonbonded Model in Explicit Water." *The Journal of Physical Chemistry B* 119(3):883–95. doi:10.1021/jp505875v.

Li, Pengfei, Lin Frank Song, and Kenneth M. Jr. Merz. 2015b. "Systematic Parameterization of Monovalent Ions Employing the Nonbonded Model." *Journal of Chemical Theory and Computation* 11(4):1645–57. doi:10.1021/ct500918t.

Liao, Wanqin, Kerstin Elfrink, and Martin Bähler. 2010. "Head of Myosin IX Binds Calmodulin and Moves Processively toward the Plus-End of Actin Filaments." *The Journal of Biological Chemistry* 285(32):24933–42. doi:10.1074/jbc.M110.101105.

Lu, Qun-Wei, Xiao-Yan Wu, and Sachio Morimoto. 2013. "Inherited Cardiomyopathies Caused by Troponin Mutations." *Journal of Geriatric Cardiology : JGC* 10(1):91–101. doi:10.3969/j.issn.1671-5411.2013.01.014.

Lyon, Robert C., Fabian Zanella, Jeffrey H. Omens, and Farah Sheikh. 2015. "Mechanotransduction in Cardiac Hypertrophy and Failure." *Circulation Research* 116(8):1462–76. doi:10.1161/CIRCRESAHA.116.304937.

Ma, Weikang, Timothy S. McMillen, Matthew Carter Childers, Henry Gong, Michael Regnier, and Thomas Irving. 2023. "Structural OFF/ON Transitions of Myosin in Relaxed Porcine Myocardium Predict Calcium-Activated Force." *Proceedings of the National Academy of Sciences* 120(5):e2207615120. doi:10.1073/pnas.2207615120.

Ma, Weikang, Suman Nag, Henry Gong, Lin Qi, and Thomas C. Irving. 2022. “Cardiac Myosin Filaments Are Directly Regulated by Calcium.” *Journal of General Physiology* 154(12):e202213213. doi:10.1085/jgp.202213213.

Maier, James A., Carmenza Martinez, Koushik Kasavajhala, Lauren Wickstrom, Kevin E. Hauser, and Carlos Simmerling. 2015. “ff14SB: Improving the Accuracy of Protein Side Chain and Backbone Parameters from ff99SB.” *Journal of Chemical Theory and Computation* 11(8):3696–3713. doi:10.1021/acs.jctc.5b00255.

Malabanan, M. Merced, Tina L. Amyes, and John P. Richard. 2010. “A Role for Flexible Loops in Enzyme Catalysis.” *Current Opinion in Structural Biology* 20(6):702–10. doi:10.1016/j.sbi.2010.09.005.

Maron, Barry J., and Martin S. Maron. 2013. “Hypertrophic Cardiomyopathy.” *Lancet (London, England)* 381(9862):242–55. doi:10.1016/S0140-6736(12)60397-3.

McGurk, Kathryn A., Xiaolei Zhang, Pantazis Theotokis, Kate Thomson, Andrew Harper, Rachel J. Buchan, Erica Mazaika, Elizabeth Ormondroyd, William T. Wright, Daniela Macaya, Chee Jian Pua, Birgit Funke, Daniel G. MacArthur, Sanjay K. Prasad, Stuart A. Cook, Mona Allouba, Yasmine Aguib, Magdi H. Yacoub, Declan P. O’Regan, Paul J. R. Barton, Hugh Watkins, Leonardo Bottolo, and James S. Ware. 2023. “The Penetrance of Rare Variants in Cardiomyopathy-Associated Genes: A Cross-Sectional Approach to Estimating Penetrance for Secondary Findings.” *American Journal of Human Genetics* 110(9):1482–95. doi:10.1016/j.ajhg.2023.08.003.

McNally, Elizabeth M., Jessica R. Golbus, and Megan J. Puckelwartz. 2013. “Genetic Mutations and Mechanisms in Dilated Cardiomyopathy.” *The Journal of Clinical Investigation* 123(1):19–26. doi:10.1172/JCI62862.

Mijailovich, Srboljub M., Xiaochuan Li, R. Hugh Griffiths, and Michael A. Geeves. 2012. “The Hill Model for Binding Myosin S1 to Regulated Actin Is Not Equivalent to McKillop & Geeves Model.” *Journal of Molecular Biology* 417(1–2):112–28. doi:10.1016/j.jmb.2012.01.011.

Miyamoto, Shuichi, and Peter A. Kollman. 1992. “Settle: An Analytical Version of the SHAKE and RATTLE Algorithm for Rigid Water Models.” *Journal of Computational Chemistry* 13(8):952–62. doi:10.1002/jcc.540130805.

Mohran, Saffie, Kristina Kooiker, Max Mahoney-Schaefer, Christian Mandrycky, Kerry Kao, An-Yue Tu, Jeremy Freeman, Farid Moussavi-Harami, Michael Geeves, and Michael Regnier. 2024. “The Biochemically Defined Super Relaxed State of Myosin—A Paradox.” *Journal of Biological Chemistry* 300(1). doi:10.1016/j.jbc.2023.105565.

Mohrman, David E., and Lois Jane Heller. 2013. *Cardiovascular Physiology*. 8. Auflage edition. New York: Mcgraw-Hill Education / Medical.

Møller, Daniel Vega, Paal Skytt Andersen, Paula Hedley, Mads Kristian Ersbøll, Henning Bundgaard, Johanna Moolman-Smook, Michael Christiansen, and Lars Køber. 2009. “The Role of Sarcomere Gene Mutations in Patients with Idiopathic Dilated Cardiomyopathy.” *European Journal of Human Genetics* 17(10):1241–49. doi:10.1038/ejhg.2009.34.

Moss, Richard L., and Daniel P. Fitzsimons. 2002. “Frank-Starling Relationship.” *Circulation Research* 90(1):11–13. doi:10.1161/res.90.1.11.

Mozaffarian, Dariush, Emelia J. Benjamin, Alan S. Go, Donna K. Arnett, Michael J. Blaha, Mary Cushman, Sandeep R. Das, Sarah de Ferranti, Jean-Pierre Després, Heather J. Fullerton, Virginia J. Howard, Mark D. Huffman, Carmen R. Isasi, Monik C. Jiménez, Suzanne E. Judd, Brett M. Kissela, Judith H. Lichtman, Lynda D. Lisabeth, Simin Liu, Rachel H. Mackey, David J. Magid, Darren K. McGuire, Emile R. Mohler Iii, Claudia S. Moy, Paul Muntner, Michael E. Mussolino, Khurram Nasir, Robert W. Neumar, Graham Nichol, Latha Palaniappan, Dilip K. Pandey, Mathew J. Reeves, Carlos J. Rodriguez, Wayne Rosamond, Paul D. Sorlie, Joel Stein, Amytis Towfighi, Tanya N. Turan, Salim S. Virani, Daniel Woo, Robert W. Yeh, and Melanie B. Turner. 2016. “Heart Disease and Stroke Statistics—2016 Update.” *American Heart Association*.

Mun, Ji Young, Michael J. Previs, Hope Y. Yu, James Gulick, Larry S. Tobacman, Samantha Beck Previs, Jeffrey Robbins, David M. Warshaw, and Roger Craig. 2014. “Myosin-Binding Protein C Displaces Tropomyosin to Activate Cardiac Thin Filaments and Governs Their Speed by an Independent Mechanism.” *Proceedings of the National Academy of Sciences* 111(6):2170–75. doi:10.1073/pnas.1316001111.

Murphy, Coleen T., and James A. Spudich. 1999. “The Sequence of the Myosin 50−20K Loop Affects Myosin’s Affinity for Actin throughout the Actin−Myosin ATPase Cycle and Its Maximum ATPase Activity.” *Biochemistry* 38(12):3785–92. doi:10.1021/bi9826815.

Neese, Frank, Frank Wennmohs, Ute Becker, and Christoph Riplinger. 2020. “The ORCA Quantum Chemistry Program Package.” *The Journal of Chemical Physics* 152(22):224108. doi:10.1063/5.0004608.

Nowakowski, Sarah G., Michael Regnier, and Valerie Daggett. 2017. “Molecular Mechanisms Underlying Deoxy-ADP.Pi Activation of Pre-Powerstroke Myosin: 2-Deoxy-ADP.Pi Activation of Myosin.” *Protein Science* 26(4):749–62. doi:10.1002/pro.3121.

Olivotto, Iacopo, Artur Oreziak, Roberto Barriales-Villa, Theodore P. Abraham, Ahmad Masri, Pablo Garcia-Pavia, Sara Saberi, Neal K. Lakdawala, Matthew T. Wheeler, Anjali Owens, Milos Kubanek, Wojciech Wojakowski, Morten K. Jensen, Juan Gimeno-Blanes, Kia Afshar, Jonathan Myers, Sheila M. Hegde, Scott D. Solomon, Amy J. Sehnert, David Zhang, Wanying Li, Mondira Bhattacharya, Jay M. Edelberg, Cynthia Burstein Waldman, Steven J. Lester, Andrew Wang, Carolyn Y. Ho, Daniel Jacoby, and EXPLORER-HCM study investigators. 2020. “Mavacamten for Treatment of Symptomatic Obstructive Hypertrophic Cardiomyopathy (EXPLORER-HCM): A Randomised, Double-Blind, Placebo-Controlled, Phase 3 Trial.” *Lancet (London, England)* 396(10253):759–69. doi:10.1016/S0140-6736(20)31792-X.

Onishi, Hirofumi, Sergey V. Mikhailenko, and Manuel F. Morales. 2006. “Toward Understanding Actin Activation of Myosin ATPase: The Role of Myosin Surface Loops.” *Proceedings of the National Academy of Sciences* 103(16):6136–41. doi:10.1073/pnas.0601595103.

Palma, Juliana, and Gustavo Pierdominici-Sottile. 2023. “On the Uses of PCA to Characterise Molecular Dynamics Simulations of Biological Macromolecules: Basics and Tips for an Effective Use.” *ChemPhysChem* 24(2):e202200491. doi:10.1002/cphc.202200491.

Parker, Francine, and Michelle Peckham. 2020. “Disease Mutations in Striated Muscle Myosins.” *Biophysical Reviews* 12(4):887. doi:10.1007/s12551-020-00721-5.

Pilagov, Matvey, Laurens W. H. J. Heling, Jonathan Walklate, Michael A. Geeves, and Neil M. Kad. 2022. “Single-Molecule Imaging Reveals How Mavacamten and PKA Modulate ATP Turnover in Skeletal Muscle Myofibrils.” *Journal of General Physiology* 155(1):e202213087. doi:10.1085/jgp.202213087.

Pilagov, Matvey, Sonette Steczina, Ateeqa Naim, Michael Regnier, Michael A. Geeves, and Neil M. Kad. 2025. “Spatially Resolving How cMyBP-C Phosphorylation and Haploinsufficiency in Porcine and Human Myofibrils Affect β-Cardiac Myosin Activity.” *Journal of General Physiology* 157(5):e202413628. doi:10.1085/jgp.202413628.

Pioner, Josè Manuel, Giulia Vitale, Sonette Steczina, Marianna Langione, Francesca Margara, Lorenzo Santini, Francesco Giardini, Erica Lazzeri, Nicoletta Piroddi, Beatrice Scellini, Chiara Palandri, Maike Schuldt, Valentina Spinelli, Francesca Girolami, Francesco Mazzarotto, Jolanda van der Velden, Elisabetta Cerbai, Chiara Tesi, Iacopo Olivotto, Alfonso Bueno-Orovio, Leonardo Sacconi, Raffaele Coppini, Cecilia Ferrantini, Michael Regnier, and Corrado Poggesi. 2023. “Slower Calcium Handling Balances Faster Cross-Bridge Cycling in Human MYBPC3 HCM.” *Circulation Research* 132(5):628–44. doi:10.1161/CIRCRESAHA.122.321956.

Planelles-Herrero, Vicente J., James J. Hartman, Julien Robert-Paganin, Fady I. Malik, and Anne Houdusse. 2017. “Mechanistic and Structural Basis for Activation of Cardiac

Myosin Force Production by Omecamtiv Mecarbil." *Nature Communications* 8(1):190. doi:10.1038/s41467-017-00176-5.

Powers, Joseph D., Kristina B. Kooiker, Allison B. Mason, Abigail E. Teitgen, Galina V. Flint, Jil C. Tardiff, Steven D. Schwartz, Andrew D. McCulloch, Michael Regnier, Jennifer Davis, and Farid Moussavi-Harami. 2020. "Modulating the Tension-Time Integral of the Cardiac Twitch Prevents Dilated Cardiomyopathy in Murine Hearts." *JCI Insight* 5(20):e142446, 142446. doi:10.1172/jci.insight.142446.

Psaras, Yiangos, Francesca Margara, Marcelo Cicconet, Alexander J. Sparrow, Giuliana G. Repetti, Manuel Schmid, Violetta Steeples, Jonathan A. L. Wilcox, Alfonso Bueno-Orovio, Charles S. Redwood, Hugh C. Watkins, Paul Robinson, Blanca Rodriguez, Jonathan G. Seidman, Christine E. Seidman, and Christopher N. Toepfer. 2021. "CalTrack: High-Throughput Automated Calcium Transient Analysis in Cardiomyocytes." *Circulation Research* 129(2):326–41. doi:10.1161/CIRCRESAHA.121.318868.

Quinn, Malgorzata E., Qingnian Goh, Mitsutoshi Kurosaka, Dilani G. Gamage, Michael J. Petrany, Vikram Prasad, and Douglas P. Millay. 2017. "Myomerger Induces Fusion of Non-Fusogenic Cells and Is Required for Skeletal Muscle Development." *Nature Communications* 8(1):15665. doi:10.1038/ncomms15665.

Rasicci, David V., Prince Tiwari, Skylar ML Bodt, Rohini Desetty, Fredrik R. Sadler, Sivaraj Sivaramakrishnan, Roger Craig, and Christopher M. Yengo. 2022. "Dilated Cardiomyopathy Mutation E525K in Human Beta-Cardiac Myosin Stabilizes the Interacting-Heads Motif and Super-Relaxed State of Myosin" edited by J. R. Sellers, A. Akhmanova, and K. M. Ruppel. *eLife* 11:e77415. doi:10.7554/eLife.77415.

Regnier, M., C. Morris, and E. Homsher. 1995. "Regulation of the Cross-Bridge Transition from a Weakly to Strongly Bound State in Skinned Rabbit Muscle Fibers." *The American Journal of Physiology* 269(6 Pt 1):C1532-1539. doi:10.1152/ajpcell.1995.269.6.C1532.

Ribeiro, Alexandre J. S., Olivier Schwab, Mohammad A. Mandegar, Yen-Sin Ang, Bruce R. Conklin, Deepak Srivastava, and Beth L. Pruitt. 2017. “Multi-Imaging Method to Assay the Contractile Mechanical Output of Micropatterned Human iPSC-Derived Cardiac Myocytes.” *Circulation Research* 120(10):1572–83. doi:10.1161/CIRCRESAHA.116.310363.

Risi, Cristina, Luisa U. Schäfer, Betty Belknap, Ian Pepper, Howard D. White, Gunnar F. Schröder, and Vitold E. Galkin. 2021. “High-Resolution Cryo-EM Structure of the Cardiac Actomyosin Complex.” *Structure* 29(1):50-60.e4. doi:10.1016/j.str.2020.09.013.

Ronaldson-Bouchard, Kacey, Stephen P. Ma, Keith Yeager, Timothy Chen, LouJin Song, Dario Sirabella, Kumi Morikawa, Diogo Teles, Masayuki Yazawa, and Gordana Vunjak-Novakovic. 2018. “Advanced Maturation of Human Cardiac Tissue Grown from Pluripotent Stem Cells.” *Nature* 556(7700):239–43. doi:10.1038/s41586-018-0016-3.

Saeed, Diyar, David Feldman, Aly El Banayosy, Emma Birks, Elizabeth Blume, Jennifer Cowger, Christopher Hayward, Ulrich Jorde, Jamila Kremer, Guy MacGowan, Simon Maltais, Simon Maybaum, Mandeep Mehra, Keyur B. Shah, Paul Mohacsi, Martin Schweiger, Sarah E. Schroeder, Palak Shah, Marvin Slepian, Laurens F. Tops, Paulino Alvarez, Francisco Arabia, Saima Aslam, Louis Benson-Louis, Edo Birati, Holger W. Buchholz, Ari Cedars, Dawn Christensen, Agnieszka Ciarka, Erin Coglianese, Rebecca Cogswell, Jennifer Cook, Jack Copeland, Jose Gonzalez Costello, Stavros G. Drakos, Pirooz Eghtesady, Tonya Elliot, Jerry D. Estep, Jaime-Juergen Eulert-Grehn, De Rita Fabrizio, Jens Garbade, Jill Gelow, Maya Guglin, Jaime Hernandez-Montfort, Doug Horstmanshof, Ranjit John, Manreet Kanwar, Feras Khaliel, Gene Kim, Sachin Kumar, Jacob Lavee, Marzia Leache, Pascal Leprince, Sern Lim, Antonio Loforte, Jiri Maly, Samer Najjar, Ivan Netuka, Salpy V. Pamboukian, Snehal R. Patel, Sean Pinney, Christina Vander Pluym, Evgenij Potapov, Desiree Robson, Yogita Rochlani, Stuart Russell, Kristin Sandau, Elena Sandoval, Gabriel Sayer, Sarah Schettle, David

Schibilsky, Thomas Schlöglhofer, Jan Schmitto, Aleem Siddique, Scott Silvestry, Mark S. Slaughter, Benjamin Sun, Hiroo Takayama, Ryan Tedford, Jeffrey J. Teuteberg, Van-Khue Ton, Nir Uriel, Juliane Vierecke, Daniel Zimpfer, and David D'Alessandro. 2023. "The 2023 International Society for Heart and Lung Transplantation Guidelines for Mechanical Circulatory Support: A 10- Year Update." *The Journal of Heart and Lung Transplantation* 42(7):e1–222. doi:10.1016/j.healun.2022.12.004.

Schaaf, Sebastian, Alexandra Eder, Ingra Vollert, Andrea Stöhr, Arne Hansen, and Thomas Eschenhagen. 2014. "Generation of Strip-Format Fibrin-Based Engineered Heart Tissue (EHT)." Pp. 121–29 in *Cardiac Tissue Engineering*. Humana Press, New York, NY.

Schultheiss, Heinz-Peter, DeLisa Fairweather, Alida L. P. Caforio, Felicitas Escher, Ray E. Hershberger, Steven E. Lipshultz, Peter P. Liu, Akira Matsumori, Andrea Mazzanti, John McMurray, and Silvia G. Priori. 2019. "Dilated Cardiomyopathy." *Nature Reviews Disease Primers* 5(1):32. doi:10.1038/s41572-019-0084-1.

Shoemaker, Benjamin A., John J. Portman, and Peter G. Wolynes. 2000. "Speeding Molecular Recognition by Using the Folding Funnel: The Fly-Casting Mechanism." *Proceedings of the National Academy of Sciences* 97(16):8868–73. doi:10.1073/pnas.160259697.

Shrestha, Rijen, Tanuj Kanchan, and Kewal Krishan. 2024. "Methods of Estimation of Time Since Death." in *StatPearls*. Treasure Island (FL): StatPearls Publishing.

Smith, Quentin M., Alessio V. Inchingolo, Madalina-Daniela Mihailescu, Hongsheng Dai, and Neil M. Kad. 2021. "Single-Molecule Imaging Reveals the Concerted Release of Myosin from Regulated Thin Filaments" edited by A. Michelot, A. Akhmanova, and J. Baker. *eLife* 10:e69184. doi:10.7554/eLife.69184.

Spudich, James A. 2015. "The Myosin Mesa and a Possible Unifying Hypothesis for the Molecular Basis of Human Hypertrophic Cardiomyopathy." *Biochemical Society Transactions* 43(1):64–72. doi:10.1042/BST20140324.

Stroumpoulis, Konstantinos I., Ioannis N. Pantazopoulos, and Theodoros T. Xanthos. 2010. "Hypertrophic Cardiomyopathy and Sudden Cardiac Death." *World Journal of Cardiology* 2(9):289–98. doi:10.4330/wjc.v2.i9.289.

Sweeney, H. Lee, and Anne Houdusse. 2010. "Structural and Functional Insights into the Myosin Motor Mechanism." *Annual Review of Biophysics* 39(1):539–57. doi:10.1146/annurev.biophys.050708.133751.

Teitgen, Abigail E., Marcus T. Hock, Kimberly J. McCabe, Matthew C. Childers, Gary A. Huber, Bahador Marzban, Daniel A. Beard, J. Andrew McCammon, Michael Regnier, and Andrew D. McCulloch. 2024. "Multiscale Modeling Shows How 2'-Deoxy-ATP Rescues Ventricular Function in Heart Failure." *Proceedings of the National Academy of Sciences* 121(35):e2322077121. doi:10.1073/pnas.2322077121.

Thomas, David D., and Osha Roopnarine. 2002. "An Overview of the Actin-Myosin Interaction." *Results and Problems in Cell Differentiation* 36:1–5. doi:10.1007/978-3-540-46558-4_1.

Tobacman, L. S. 1996. "Thin Filament-Mediated Regulation of Cardiac Contraction." *Annual Review of Physiology* 58:447–81. doi:10.1146/annurev.ph.58.030196.002311.

Toepfer, Christopher N., Amanda C. Garfinkel, Gabriela Venturini, Hiroko Wakimoto, Giuliana Repetti, Lorenzo Alamo, Arun Sharma, Radhika Agarwal, Jourdan F. Ewoldt, Paige Cloonan, Justin Letendre, Mingyue Lun, Iacopo Olivotto, Steve Colan, Euan Ashley, Daniel Jacoby, Michelle Michels, Charles S. Redwood, Hugh C. Watkins, Sharlene M. Day, James F. Staples, Raúl Padrón, Anant Chopra, Carolyn Y. Ho, Christopher S. Chen, Alexandre C. Pereira, Jonathan G. Seidman, and Christine E. Seidman. 2020. "Myosin Sequestration Regulates Sarcomere Function, Cardiomyocyte Energetics, and Metabolism, Informing the Pathogenesis of Hypertrophic Cardiomyopathy." *Circulation* 141(10):828–42. doi:10.1161/CIRCULATIONAHA.119.042339.

Towel, Marcie G., Jessica Bellarby, Graeme I. Paton, Frederic Coulon, Simon J. T. Pollard, and Kirk T. Semple. 2011. "Mineralisation of Target Hydrocarbons in Three Contaminated

Soils from Former Refinery Facilities." *ENVIRONMENTAL POLLUTION* 159(2):515–23. doi:10.1016/j.envpol.2010.10.015.

Tudurachi, Bogdan-Sorin, Alexandra Zăvoi, Andreea Leonte, Laura Ţăpoi, Carina Ureche, Silviu Gabriel Bîrgoan, Traian Chiuariu, Larisa Anghel, Rodica Radu, Radu Andy Sascău, and Cristian Stătescu. 2023. "An Update on MYBPC3 Gene Mutation in Hypertrophic Cardiomyopathy." *International Journal of Molecular Sciences* 24(13):10510. doi:10.3390/ijms241310510.

Uversky, Vladimir N. 2016. "Dancing Protein Clouds: The Strange Biology and Chaotic Physics of Intrinsically Disordered Proteins *." *Journal of Biological Chemistry* 291(13):6681–88. doi:10.1074/jbc.R115.685859.

Uyeda, Taro Q. P., Kathleen M. Ruppel, and James A. Spudich. 1994. "Enzymatic Activities Correlate with Chimaeric Substitutions at the Actin-Binding Face of Myosin." *Nature* 368(6471):567–69. doi:10.1038/368567a0.

Vander Roest, Alison Schroer, Chao Liu, Makenna M. Morck, Kristina Bezold Kooiker, Gwanghyun Jung, Dan Song, Aminah Dawood, Arnav Jhingran, Gaspard Pardon, Sara Ranjbarvaziri, Giovanni Fajardo, Mingming Zhao, Kenneth S. Campbell, Beth L. Pruitt, James A. Spudich, Kathleen M. Ruppel, and Daniel Bernstein. 2021. "Hypertrophic Cardiomyopathy β-Cardiac Myosin Mutation (P710R) Leads to Hypercontractility by Disrupting Super Relaxed State." *Proceedings of the National Academy of Sciences* 118(24):e2025030118. doi:10.1073/pnas.2025030118.

Vang, Søren, Thomas J. Corydon, Anders D. Børglum, Melissa D. Scott, Judith Frydman, Jens Mogensen, Niels Gregersen, and Peter Bross. 2005. "Actin Mutations in Hypertrophic and Dilated Cardiomyopathy Cause Inefficient Protein Folding and Perturbed Filament Formation." *The FEBS Journal* 272(8):2037–49. doi:10.1111/j.1742-4658.2005.04630.x.

Vinciguerra, Claudia, Salvatore Iacono, Liliana Bevilacqua, Annamaria Landolfi, Giuseppe Piscosquito, Federica Ginanneschi, Giuseppe Schirò, Vincenzo Di Stefano, Filippo

Brighina, Paolo Barone, and Carmela Rita Balistreri. 2023. “Sex Differences in Neuromuscular Disorders.” *Mechanisms of Ageing and Development* 211:111793. doi:10.1016/j.mad.2023.111793.

Voors, Adriaan A., Jean-François Tamby, John G. Cleland, Michael Koren, Leslie B. Forgosh, Dinesh Gupta, Lars H. Lund, Albert Camacho, Ravi Karra, Henk P. Swart, Pierpaolo Pellicori, Frank Wagner, Ray E. Hershberger, Narayana Prasad, Robert Anderson, Anu Anto, Kaylyn Bell, Jay M. Edelberg, Liang Fang, Marcus Henze, Cynthia Kelly, Gregory Kurio, Wanying Li, Kate Wells, Chun Yang, Sam L. Teichman, Carlos L. Del Rio, and Scott D. Solomon. 2020. “Effects of Danicamtiv, a Novel Cardiac Myosin Activator, in Heart Failure with Reduced Ejection Fraction: Experimental Data and Clinical Results from a Phase 2a Trial.” *European Journal of Heart Failure* 22(9):1649–58. doi:10.1002/ejhf.1933.

Wagoner, Jason A., and Ken A. Dill. 2021. “Evolution of Mechanical Cooperativity among Myosin II Motors.” *Proceedings of the National Academy of Sciences* 118(20):e2101871118. doi:10.1073/pnas.2101871118.

Wales, David. 2003. *Energy Landscapes: Applications to Clusters, Biomolecules and Glasses*. Cambridge University Press.

Walklate, Jonathan, Zoltan Ujfalusi, and Michael A. Geeves. 2016. “Myosin Isoforms and the Mechanochemical Cross-Bridge Cycle” edited by S. L. Lindstedt and H. H. Hoppeler. *Journal of Experimental Biology* 219(2):168–74. doi:10.1242/jeb.124594.

Wang, Dan, Ian M. Robertson, Monica X. Li, Michelle E. McCully, Melissa L. Crane, Zhaoxiong Luo, An-Yue Tu, Valerie Daggett, Brian D. Sykes, and Michael Regnier. 2012. “Structural and Functional Consequences of the Cardiac Troponin C L48Q Ca2+-Sensitizing Mutation.” *Biochemistry* 51(22):4473–87. doi:10.1021/bi3003007.

Wang, Lin, Min Zhang, and Emil Alexov. 2016. “DelPhiPKa Web Server: Predicting pKa of Proteins, RNAs and DNAs.” *Bioinformatics* 32(4):614–15. doi:10.1093/bioinformatics/btv607.

Wang, Yanhong, Luca Fusi, Jesus G. Ovejero, Cameron Hill, Samina Juma, Flair Paradine Cullup, Andrea Ghisleni, So-Jin Park-Holohan, Weikang Ma, Thomas Irving, Theyencheri Narayanan, Malcolm Irving, and Elisabetta Brunello. 2024. “Load-Dependence of the Activation of Myosin Filaments in Heart Muscle.” *The Journal of Physiology* 602(24):6889–6907. doi:10.1113/JP287434.

van Waning, Jaap I., Kadir Caliskan, Yvonne M. Hoedemaekers, Karin Y. van Spaendonck-Zwarts, Annette F. Baas, S. Matthijs Boekholdt, Joost P. van Melle, Arco J. Teske, Folkert W. Asselbergs, Ad P. C. M. Backx, Gideon J. du Marchie Sarvaas, Michiel Dalinghaus, Johannes M. P. J. Breur, Marijke P. M. Linschoten, Laura A. Verlooij, Isabella Kardys, Dennis Dooijes, Ronald H. Lekanne Deprez, Arne S. IJpma, Maarten P. van den Berg, Robert M. W. Hofstra, Marjon A. van Slegtenhorst, Jan D. H. Jongbloed, and Danielle Majoor-Krakauer. 2018. “Genetics, Clinical Features, and Long-Term Outcome of Noncompaction Cardiomyopathy.” *Journal of the American College of Cardiology* 71(7):711–22. doi:10.1016/j.jacc.2017.12.019.

Watkins, H., W. J. McKenna, L. Thierfelder, H. J. Suk, R. Anan, A. O’Donoghue, P. Spirito, A. Matsumori, C. S. Moravec, and J. G. Seidman. 1995. “Mutations in the Genes for Cardiac Troponin T and Alpha-Tropomyosin in Hypertrophic Cardiomyopathy.” *The New England Journal of Medicine* 332(16):1058–64. doi:10.1056/NEJM199504203321603.

Watkins, Hugh, Anthony Rosenzweig, Dar-San Hwang, Tatjana Levi, William McKenna, Christine E. Seidman, and J. G. Seidman. 1992. “Characteristics and Prognostic Implications of Myosin Missense Mutations in Familial Hypertrophic Cardiomyopathy.” *New England Journal of Medicine* 326(17):1108–14. doi:10.1056/NEJM199204233261703.

Xu, Guotai, J. Ross Chapman, Inger Brandsma, Jingsong Yuan, Martin Mistrik, Peter Bouwman, Jirina Bartkova, Ewa Gogola, Daniël Warmerdam, Marco Barazas, Janneke E. Jaspers, Kenji Watanabe, Mark Pieterse, Ariena Kersbergen, Wendy Sol, Patrick H. N. Celie, Philip C. Schouten, Bram van den Broek, Ahmed Salman, Marja Nieuwland, Iris de Rink, Jorma de Ronde, Kees Jalink, Simon J. Boulton, Junjie Chen, Dik C. van Gent, Jiri Bartek, Jos Jonkers, Piet Borst, and Sven Rottenberg. 2015. “REV7 Counteracts DNA Double-Strand Break Resection and Affects PARP Inhibition.” *Nature* 521(7553):541–44. doi:10.1038/nature14328.

Yengo, Christopher M., and H. Lee Sweeney. 2004. “Functional Role of Loop 2 in Myosin V.” *Biochemistry* 43(9):2605–12. doi:10.1021/bi035510v.

Yu, Chan Jong, Yoon Ho Park, Mi Young An, Bumhan Ryu, and Hyun Suk Jung. 2024. “Insights into Actin Isoform-Specific Interactions with Myosin via Computational Analysis.” *Molecules (Basel, Switzerland)* 29(13):2992. doi:10.3390/molecules29132992.

Yu, Chan Jong, Yoon Ho Park, Bumhan Ryu, and Hyun Suk Jung. 2024. “Sequence Alignment-Based Prediction of Myosin 7A: Structural Implications and Protein Interactions.” *International Journal of Molecular Sciences* 25(6):3365. doi:10.3390/ijms25063365.

Zaleta-Rivera, Kathia, Alexandra Dainis, Alexandre J. S. Ribeiro, Pablo Cordero, Gabriel Rubio, Ching Shang, Jing Liu, Thomas Finsterbach, Victoria N. Parikh, Shirley Sutton, Kinya Seo, Nikita Sinha, Nikhil Jain, Yong Huang, Roger J. Hajjar, Mark A. Kay, Danuta Szczesna-Cordary, Beth L. Pruitt, Matthew T. Wheeler, and Euan A. Ashley. 2019. “Allele-Specific Silencing Ameliorates Restrictive Cardiomyopathy Attributable to a Human Myosin Regulatory Light Chain Mutation.” *Circulation* 140(9):765–78. doi:10.1161/CIRCULATIONAHA.118.036965.

Zinovjev, Kirill, Paul Guénon, Carlos A. Ramos-Guzmán, J. Javier Ruiz-Pernía, Damien Laage, and Iñaki Tuñón. 2024. “Activation and Friction in Enzymatic Loop Opening and Closing Dynamics.” *Nature Communications* 15(1):2490. doi:10.1038/s41467-024-46723-9.

VITA

Born and raised in Cincinnati, Ohio, Kalen Zeeh Robeson's academic journey began at The Ohio University. There, he was part of the prestigious Honors Tutorial College, earning a B.S. in Biological Sciences with a certificate in Bioinformatics in 2017. His early research experience was shaped by his time in the labs of Dr. Tomohiko Sugiyama and Dr. Molly Morris. Following his undergraduate studies, Kalen broadened his scientific horizons internationally, working in Dr. Peter Kroth's lab at the University of Konstanz in Germany until 2018. His career then led him to the University of Washington, where he was recruited into the Bioengineering Ph.D. program. Under the co-mentorship of Dr. Michael Regnier and Dr. Jennifer Davis, he successfully earned his Ph.D. in 2025.